Synthesis of Novel Triazolopyrazines as Candidate Antimalarials

Joanna Margaret Ubels

A thesis submitted in partial fulfilment of the requirements for the degree of Bachelor of Science (Honours)

The University of Sydney
School of Chemistry
November 2014

Abstract

Malaria is an infectious disease that affected 207 million people and killed 627 000 in 2012. Children under the age of five accounted for 77% of the deaths reported. Resistance to the frontline drugs, the artemisinins, is emerging in South East Asia creating an urgent need for new drugs to treat malaria. The current malaria drug pipeline contains fewer than 20 highly active compounds across all stages of clinical trials. However estimates show that less than four of these will make it to the market, highlighting the need for continued research into new compounds.

A novel series of compounds with promising anti-malarial activity, the triazolopyrazines, was placed in the public domain via the Open Source Malaria consortium in late 2013. Synthetic and characterisation data for the triazolopyrazines was limited and not published.

The synthetic route to the ether subset of the triazolopyrazines was validated, further developed and optimized in this project. The synthetic route involved an oxidative cyclization to give the heterocyclic core, and a direct substitution on that core by diverse nucleophiles. Eight novel analogues were synthesized using the validated conditions and were fully characterised. The eight compounds were assessed for their potency against *Plasmodium falciparum* and four were found to have moderate anti-malarial activity. A fluoroalkene analogue of the amide subset of the triazolopyrazines was designed and a partial synthesis towards these compounds was achieved.

Statement of Student Contribution

The initial project was designed by A/Prof. Matthew Todd. Analogues were designed by A/Prof. Matthew Todd, Dr. Alice Williamson and me. The initial idea for the fluoroalkene analogue was mine and design of the synthesis was aided by A/Prof. Matthew Todd.

Nuclear magnetic resonance data were obtained by me with the exception of 2D data and data for compound **30**. 2D NMR data were collected by Mr. Andrew Giltrap and Mr. Liam Bromhead and interpretation was aided by Dr. Ian Luck. Low resolution mass spectrometry was carried out by Mr. Marlowe Graham and Dr. Nicholas Proschogo. High resolution mass spectrometry was carried out by Dr. Nicholas Proschogo. Biological assays were carried out by GlaxoSmithKline, AstraZeneca and Syngene.

This project was performed open source, meaning all data and ideas were shared as the project progressed and the wider community was invited to contribute. Where this occurred, full credit has been given in the body of the thesis.

Proof reading was performed by A/Prof. Matthew Todd with input from Dr. Alice Williamson. A/Prof. Matthew Todd gave advice on the structure of this thesis.

I certify that this thesis is my own work except where acknowledgement has been given.

Joanna M. Ubels

Date: 3 November 2014

Acknowledgements

Firstly, thank you to Dr. Matthew Todd and Dr. Peter Rutledge for giving me the opportunity to study with you this year, for your great chemistry knowledge and guidance and support with my project. I am also thankful for your encouragement this year as I re-entered the chemistry world.

Dr. Alice Williamson, thank you for your enormous support of me this year, for helping me find my feet in the lab again and for always being prepared to answer my questions.

To Katrina Badiola, thank you for helping me to navigate the lab and for constantly challenging me in my work and to Dr. Jessica Baiget, thank you for all your help at the sticky end of the year in the lab and for encouraging me in those last few weeks.

Thank you to my honours cohort for sharing this journey with me. In particular to Elisabeth Tondl and Andrew Counsell for your wonderful friendship and for welcoming me to Sydney. I am most grateful for all the stimulating lunchtime conversations. Also to Thomas McDonald for your thought provoking conversation at the fumehood.

Thank you to Dr. Nicholas Proschogo for patiently obtaining data for my compounds and to Dr. Ian Luck for teaching me NMR.

Thank you to the University of Sydney for the provision of an Honours Scholarship, which enabled me to move to Sydney and study here.

To my family, thank you for always supporting me in my endeavours and for your love. Thank you especially to my brother Finlay for your help navigating Adobe Illustrator and Photoshop.

Finally I would like to thank my fiancé Andrew Delbridge. You have been a constant support by my side this year through all the good times and the stress and I am eternally grateful for your unwavering love and belief in me.

Table of Contents

Abstract ***(i)***

Statement of Student Contribution ***(ii)***

Acknowledgements ***(iii)***

Table of Contents ***(iv)***

List of Abbreviations ***(vi)***

1. Introduction ***(1)***

1.1 Malaria *(1)*

1.2 The lifecycle of the *Plasmodium* species *(2)*

1.3 Current therapies and associated problems *(3)*

1.4 Goals for malaria burden reduction, eradication and drug development *(5)*

1.5 The malaria drug pipeline *(7)*

1.6 The Series 4 triazolopyrazines *(10)*

1.7 Open source science/drug discovery *(11)*

2. Project Aims ***(13)***

3. Project Design ***(14)***

3.1 Analogues *(14)*

3.2 Open source methodology *(16)*

4. Results and Discussion ***(18)***

4.1 Synthesis of the ether triazolopyrazines and related analogues *(18)*

4.1.1 Synthesis of the triazolopyrazine core *(19)*

4.1.2 S_N2 displacement development and diversification *(23)*

4.1.3 Biological data for the triazolopyrazine ethers, amines and thioether *(26)*

4.1.4 Optimisation of the oxidative cyclisation and development of alternative cores *(28)*

4.1.5 Design and synthesis of round 2 ether triazolopyrazines *(32)*

4.1.6 Biological data round 2 *(35)*

4.2 Synthesis of the fluoroalkene analogues *(37)*

4.2.1 Synthesis of halopyridyl boronic acid and ester coupling partners *(39)*

4.2.2 Synthesis of the bromofluorostyrene coupling partner *(41)*

4.2.3 Suzuki coupling of bromopyridyl boronic ester and geminal alkenes *(42)*

5. Conclusions and Future Work *(44)*

6. Experimental Details *(47)*

7. References *(60)*

A Supporting NMR for Selected Compounds *(68)*

B Example UV Biotage Isolera Purification Traces *(83)*

C Experimental Biological Procedures *(85)*

List of Abbreviations

°C	degrees Celcius
18-crown-6	1,4,7,10,13,16-hexaoxacyclooctadecane
2D	two-dimensional
3D7	sensitive strain of *Plasmodium falciparum*
Å	Angstrom
ACTs	artemisinin combination therapies
app	apparent
ATPase	adenosine triphosphatase
b	broad
BC	Before Christ
calcd.	calculated
CLogP	calculated logarithm of the 1-octanol:H_2O partition coefficient
CRO	contract research organization
d	doublet
dd	doublet of doublets
DMSO	dimethyl sulfoxide
DMSO-*d6*	deuterated dimethyl sulfoxide
ELN	electronic lab notebook
ESAC	Expert Scientific Advisory Committee
G6PD	glucose-6-phosphate dehydrogenase
GMAP	Global Malaria Action Plan
GSK	GlaxoSmithKline
h	hour or hours
hERG	*human ether-a-go-go related gene*
HMBC	heteronuclear multiple bond correlation
HRMS	high resolution mass spectrometry
HSQC	heteronuclear single quantum correlation
Hz	Hertz
IC_{50}	half maximal inhibitory concentration
J	coupling constant

K	Kelvin
kg	kilograms
m	multiplet
mbar	millibar
mg	milligrams
MHz	mega-Hertz
min	minutes
mm	millimetre
mM	millimolar
MMV	Medicines for Malaria Venture
NCE	new chemical entity
NF54	sensitive strain of *Plasmodium falciparum*
nm	nanometre
nM	nanomolar
NMR	nuclear magnetic resonance
OSM	Open Source Malaria
P. berghei	*Plasmodium berghei*
PfATP4	*Plasmodium falciparum* P-type ATPase 4
P. falciparum	*Plasmodium falciparum*
pIC_{50}	log of the half maximal inhibitory concentration
PIDA	phenyliodine diacetate
PIFA	phenyliodine bis(trifluoroacetate)
P. ovale	*Plasmodium ovale*
ppm	parts per million
P. vivax	*Plasmodium vivax*
q	quartet
s	singlet
SAR	Structure Activity Relationship
SEC	Single Encounter Chemoprotection
SERCaP	Single Encounter Radical Cure and Prophylaxis
S_N2	bimolecular nucleophilic substitution
t	triplet

td	triplet of doublets
TCP	Target Candidate Profile
TEA	triethylamine
THF	tetrahydrofuran
TPP	Target Product Profile
μm	micrometre
μM	micromolar
ν_{max} (film)/cm^{-1}	transmission in wave numbers
WHO	World Health Organisation

1. Introduction

1.1 Malaria

In 2002, malaria was near untreatable. Resistance to the first line drugs chloroquine and sulfadoxone-pyrimethamine were reported to be 90% and 60% respectively in parts of East Africa.[1] Doctors were faced with the awful reality that the drugs they were prescribing would not cure their patients.[1] In 2004 the World Health Organisation (WHO) approved new artemisinin combination therapies and the burden of the disease fell dramatically.[1] However, reports of resistance to these life saving drugs has recently emerged from South-East Asia and without new effective drugs we will soon be facing the same crisis as before.[2]

Malaria is an infectious disease that is endemic in 104 countries.[3] The WHO estimates that in 2012 there were 207 million cases of malaria, causing 627 000 deaths. While this is down 42% since the year 2000[4], largely due to effective use of the combination therapies and prevention strategies such as insecticides and treated mosquito nets,[5] the burden of malaria is still too high. The disease disproportionally affects some of the world's poorest nations; Africa has the highest burden, accounting for 80% of cases and 90% of deaths.[3] Children are also unequally affected: 77% of malaria-related deaths in 2012 were children under the age of 5.

The oldest known mention of the symptoms of malaria dates back to ancient Chinese texts in 2700 BC.[6] The first symptoms of infection, fever, headache, chills and vomiting, occur 10–15 days after a mosquito bite and are not easily recognizable as malaria.[4] Left untreated, the disease can become life threatening in as little as 24 hours, causing severe anaemia, cerebral malarial, coma and death.[4] Malaria is caused by protozoan parasites of the genus *Plasmodium*, transmitted by female mosquitoes of the *Anopheles* species.[7] There are four species that are known to infect humans: *Plasmodium falciparum, Plasmodium vivax, Plasmodium ovale* and *Plasmodium malariae.* Of these, *P. vivax* is the most widespread while *P. falciparum* causes the highest number of deaths.[7] There are also several species that infect only animals: *Plasmodium knowlesi* infects primates and *Plasmodium berghei* infects mice. These species are frequently used as animal models of the disease.

1.2 The lifecycle of the *Plasmodium* species

The lifecycle of the *Plasmodium* species is complex and occurs in both mosquitoes and humans. An understanding of this lifecycle can aid drug discovery, by identifying weaknesses that would be ideal drug targets. There are two stages in the *Plasmodium* lifecycle, the sexual or reproductive stage in the mosquito, and the asexual or non-reproductive stage, which occurs in the liver and blood of humans (Figure 1.1).

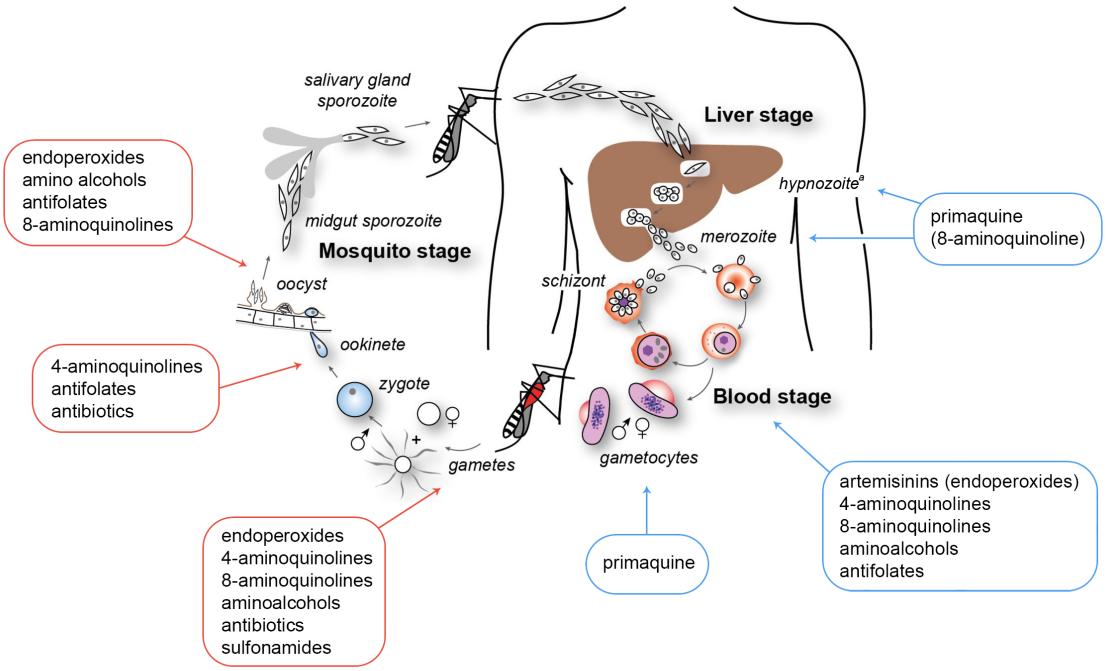

Figure 1.1: The lifecycle of the *Plasmodium* species and the drug classes that target different stages. Red boxes indicate drug classes that have been shown to target the mosquito stage forms of the parasite *in vitro*. Blue boxes indicate drug classes that target the liver and blood stages of the parasite *in vivo*. (Adapted from Cowman *et al.*, 2012.)[8]

The sexual stage of *Plasmodium* begins when an *Anopheles* mosquito ingests male and female *Plasmodium* gametocytes in its blood meal (Figure 1.1).[9] Upon entering the gut of the mosquito the gametocytes develop into gametes, fertilization occurs and the zygote is formed.[9] The zygote transforms into an ookinete, which passes through the gut epithelia and forms an oocyst on the midgut wall.[9] In each oocyst, thousands of sporozoites are produced, which burst out and migrate to the salivary glands where they stay until the mosquitoes next feed.[9]

The sporozoites are deposited into a person's skin when the mosquito feeds (Figure 1.1).[10] From there they quickly find blood vessels and migrate to the liver where they infect the liver cells, beginning the asexual liver stage of the lifecycle.[10] In the liver they develop into merozoites, each one replicating thousands of times.[10] In *P. ovale* and *P. vivax* a few of the invading sporozoites will develop into dormant hypnozoites which can reactivate into merozoites weeks to months later and cause a relapse of malaria.[10]

Symptoms of malaria begin when merozoites enter the blood stream and invade red blood cells developing into schizonts, commencing the blood stage of the disease (Figure 1.1).[8, 10] Schizonts are packed full of new merozoites that burst out into the blood stream and invade more red blood cells. Some merozoites do not invade red blood cells but instead develop into gametocytes, which circulate in the blood until a mosquito feeds, restarting the lifecycle.

The blood stage merozoites are the targets of the artemisinin based drugs, the 4-aminoquinolines such as chloroquine, the 8-aminoquinolines, the aminoalcohols and the antifolate anti-malarial drug classes (blue boxes, Figure 1.1).[11] Primaquine is the only drug on the market that can kill gametocytes, merozoites in the liver and the dormant hypnozoites in *P. vivax* and *P. ovale*.[11-12] By killing the gametocytes, primaquine can block transmission back to the mosquito, which stops malaria from spreading.[12] There are also anti-malarial drugs that can kill the mosquito stages of *Plasmodium* (red boxes, Figure 1.1), however these have only been evaluated *in vitro* and it is not feasible to drug mosquitoes in the field.[13]

1.3 Current therapies and associated problems

Malaria is a very treatable disease; with unlimited resources malaria would be curable in almost every case.[14] The main treatments used are primaquine, for *P. vivax* infections, and artemisinin combination therapies (ACTs) for *P. falciparum* infections (Figure 1.2).[7] ACTs contain one of the fast acting artemisinin drugs, and a longer lasting partner drug. Primaquine and the ACTs are highly effective therapies although there are several major issues with them that need to be addressed in the development of new drugs.

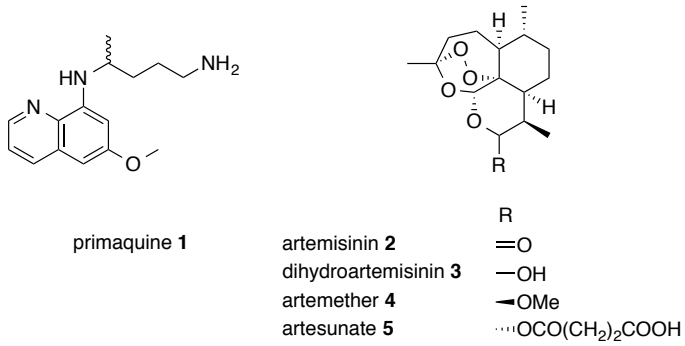

Figure 1.2: Primaquine (**1**) and the artemisinins. Dihydroartemisinin (**3**), artemether (**4**) and artesunate (**5**) are semisynthetic derivatives of artemisinin.[15]

The first issue is that resistance to the artemisinins in *P. falciparum* has emerged on both the Thai-Cambodia[16-17] and Thai-Myanmar[18] borders. The first well-documented study into artemisinin resistance on the Thai-Cambodia border was published in 2008[2, 16] and was confirmed by the WHO in May 2009.[2] Resistance in this instance is defined as a delayed clearance of the parasite, taking three or more days to clear instead of two with adequate blood levels of artemisinin.[16-18] With careful management and use of combination therapies, patients are still able to fully recover.[2] However the artemisinins are the last fast acting drugs available to treat *P. falciparum* infections.[2] If resistance worsens then without new drugs malaria will again become incurable and a huge increase in mortality will ensue as when chloroquine resistance emerged in Africa in the 1980's.[19]

Additionally, there are several issues with primaquine. This drug cannot be given to people with a glucose-6-phosphate dehydrogenase (G6PD) deficiency, a genetic disease affecting around 5–10% of the population in sub-saharan Africa.[20] In G6PD deficient people, primaquine treatment causes life-threatening haemolytic anaemia, however without primaquine, they are left extremely vulnerable to relapse from the dormant liver stages of *P. vivax* which cannot be cleared by other drugs.[21] Primaquine also has a short half-life in the blood so must be taken daily for 14 days to achieve a full cure.[22] The long treatment time is a problem for patient compliance: many do not finish the full treatment course leaving them susceptible to future relapses and parasite resistance.[22]

The problems with primaquine and the artemisinins highlight the pressing need to develop new anti-malarial drugs.[2, 11, 23] This is compounded by the lack of a vaccine for malaria; the most recent candidate to reach phase III clinical trials has an efficacy of only 30%.[24] Even if the vaccine does make it to the market, its low efficacy means that drugs will still be needed as the frontline treatment.

1.4 Goals for malaria burden reduction, eradication and drug development

At the 2008 Millennium Development Goals Malaria Summit, the global malaria community approved a bold plan to eradicate malaria, the Global Malaria Action Plan (GMAP).[25] The GMAP outlines specific goals and targets for reducing malaria cases and deaths to the point where the disease can be eliminated (zero new cases of infection in a country or region) and eradicated (global, permanent elimination).[25-26] The GMAP strategy is to control and reduce the number of infections in each country or region to the point where elimination strategies can be put in place.[25-26] Alongside this work will be research into new tools to assist these efforts, such as drugs, vaccines and insecticides.[25-26]

Antimalarial drugs will be a crucial part of the elimination and eradication effort, although it is widely acknowledged amongst the global malaria community that new drugs must enter the market.[23] To assist researchers in developing new antimalarials, the Medicines for Malaria Venture (MMV) developed two Target Product Profiles (TPPs; Table 1.1) describing attributes of the ideal drugs for achieving eradication; SERCaP, Single Encounter Radical Cure and Prophylaxis, and SEC, Single Encounter Chemoprotection.[5, 23] Single encounter describes a compound that can clear the parasite in one dose. Radical cure is defined as completely eliminating all stages of the parasite from the body including dormant liver stages. Prophylaxis and chemoprotection describe compounds that have long half-lives in the blood, preventing against re-infection. Finding a drug that encompasses SERCaP and/or SEC will be difficult, perhaps impossible.[5] In recognition of this MMV has also developed target candidate profiles (TCPs; Table 1.1) that describe the critical and desirable attributes for a new chemical entity (NCE) entering into preclinical trials.[5] The target candidate profiles

under SERCaP are fast parasite clearance, preferably achieved in a single dose, long duration in the blood to provide prophylaxis and transmission blocking/relapse prevention of new and recurring infections.[5, 23] Chemoprotection is the only target candidate profile under SEC.[5] The ideal drug or combination for SEC also needs to be effective in a single dose and must have a different mode of action to drugs used for SERCaP to prevent resistance developing.[5]

Table 1.1: Target product and candidate profiles of new drugs to treat malaria. (Adapted from Burrows *et al.*, 2013).[5]

Target Product Profiles (TPPs)	Single Encounter Radical Cure and Prophylaxis (SERCaP)			Single Encounter Chemoprotection (SEC)
Target Candidate Profile (TCPs)	Fast Parasite Clearance	Long Duration	Transmission blocking/relapse prevention	Chemoprotection
Essential Characteristics	• Minimum 99.9% parasite clearance over 24 h • >6 log total parasite reduction	• >80% clinical efficacy as a monotherapy • >95% clinical efficacy when combined with a fast clearing drug	• Kills gametocytes • Kills hypnozoites • Safe in patients with G6PD	• Kills liver schizonts • Slow onset of action (>48 h) against asexual blood stages • High safety in all patients* • One dose per month
Desirable Characteristics	• Kills gametocytes • Kills hypnozoites	• Kills gametocytes • Kills hypnozoites	• Vector stage activity	• Kills gametocytes • Vector stage activity • Different mode of action or target to SERCaP compounds
Current Gold Standard	Artemisinins e.g. artemisinin (**2**) 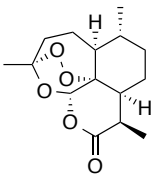	4-aminoquinolines, e.g. amodiaquine (**6**) 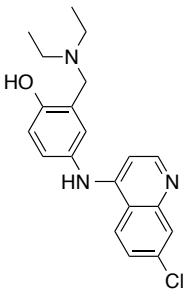	Primaquine (**1**) 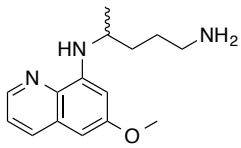	Mefloquine (**7**) 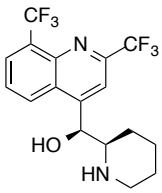

*Including children, pregnant women, and patients with G6PD, HIV/AIDS and tuberculosis.

1.5 The malaria drug pipeline

The malaria drug pipeline is a diverse set of fewer than twenty new chemical entities (NCEs) in preclinical and clinical trials.[7, 27] Many other drug discovery projects are being conducted that have not yet entered compounds into preclinical trials.[27] The compounds in the pipeline have a range of structures, therapeutic activities and new and existing targets, although not all the targets and modes of action are known.[7] The development of compounds with novel targets is important for reducing the likelihood of the parasite developing drug resistance.[28] Four of the compounds in the malaria drug pipeline are of particular interest (Figure 1.3), MMV390048 (**8**) is able to cure infected mice in a single dose, KAE609 (**9**) has a novel target within the parasite and the development of OZ277 (**10**) and OZ439 (**11**) highlights the difficulty in getting a drug from design stage to the market.

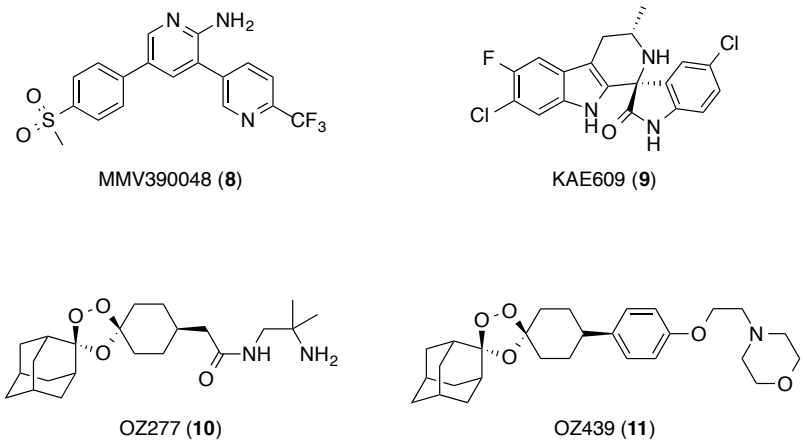

Figure 1.3: The structures of MMV390048, KAE609, OZ227 and OZ439; a representative selection of four drugs at different stages of preclinical and clinical testing.[7, 29]

MMV390048 belongs to the novel class of antimalarial compounds called the 3,5-diaryl-2-aminopyridines.[7, 30] The compound was discovered through a combination of high throughput blood stage screens and hit to lead optimisation.[30] The first hit from the initial screen was an analogue of MMV390048, possessing near identical structures with the exception of a 2-methoxyphenyl group in place of the trifluoromethylpyridine group. Preliminary studies showed good potency but only moderate metabolic stability, which was attributed to the presence of the 2-methoxyphenyl group. Replacement of this group with the methoxypyridyl substituent gave a compound with the same potency and improved metabolic stability. Subsequent optimisation gave MMV390048, which

outperformed its precursors and both chloroquine and artesunate in antiplasmodial and pharmacokinetic tests. MMV390048 also cured mice infected with *P. berghei* with a single oral dose of 30 mg/kg.[30] The target of MMV390048 is still unknown, although kinases have been suggested as the target of the 2-aminopyridines drug class.[31] Despite this, the potency, stability and oral bioavailability of MMV390048 are such that it has progressed quickly into preclinical trials.[7]

KAE609 is from another novel class of antimalarials, the spiroindolones.[7] Having just completed phase IIa clinical trials,[32] KAE609 has the ability to cure patients infected with *P. falciparum* and *P. vivax* in three days with a dose of 30 mg/day[32] as well blocking transmission *in vitro*.[33] KAE609 was developed from the precursor **12a** of which there is four possible stereoisomers, only one of which is highly potent (Figure 1.4).[34]

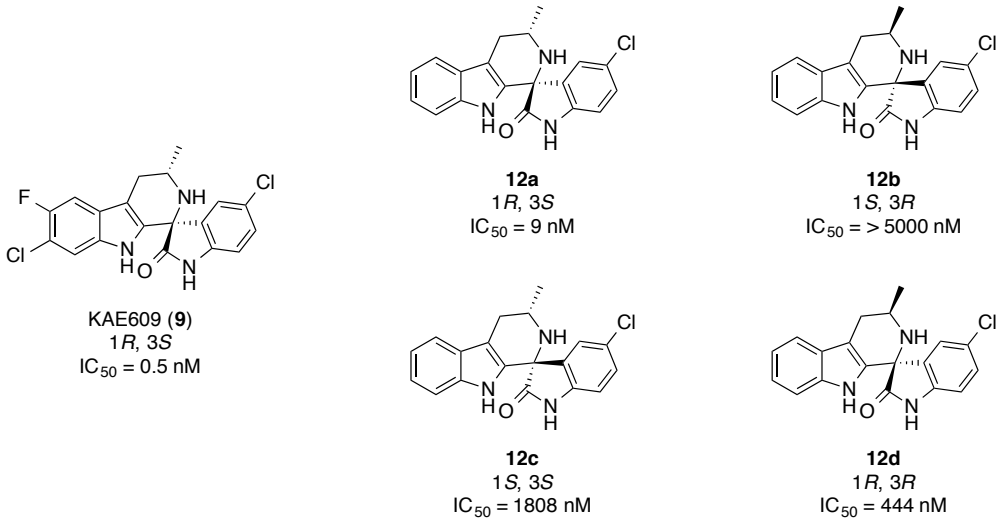

Figure 1.4: KAE609 (**9**) and its precursor stereoisomers **12a-d**.[33-34] Compounds were tested against *P. falciparum* strain NF54. IC_{50} is defined as half maximal inhibitory concentration.

The spiroindolone class of drugs that includes KAE609 targets *Plasmodium falciparum* P-type ATPase 4 (PfATP4), which is a sodium/hydrogen exchanger on the outer membrane of the parasite (Figure 1.5).[33, 35] PfATP4 is responsible for pumping sodium ions out of the parasite against the sodium gradient thus maintaining a low intraparasitic concentration relative to the surrounding environment.[35] Inhibition of this pump by the spiroindolones causes an increase in the intraparasitic sodium concentration and subsequent alkalinisation that kills the parasite.[35-36]

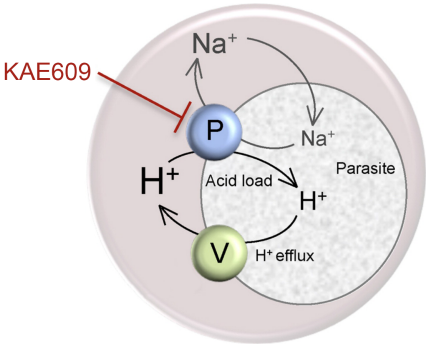

Figure 1.5: *Plasmodium falciparum* P-type ATPase 4 (PfATP4) is a sodium/hydrogen exchanger located on the outer membrane of the parasite. Inhibition of PfATP4 by KAE609 causes an increase in the intracellular concentration of sodium, and a subsequent decrease in the concentration of protons through the V-type ATPase H^+ pump causing the intracellular environment to become alkaline.[36] (Adapted from Lehane, A. M. *et al.*, 2014.)[36]

OZ277 is a synthetic ozonide,[7] developed as a drug that would overcome problems with the artemisinin drug class at a time when artemisinin resistance was still unknown.[29] The endoperoxide bridge, the active functional group of the artemisinins, was kept while the surrounding scaffold was significantly modified.[29] The compound has the same mode of action as the artemisinins but exhibits greatly improved plasma stability (arising from the bulky adamantane ring) and oral bioavailability, and is less expensive to synthesise. OZ277 also has improved antimalarial activity, curing mice infected with *P. berghei* after three 10 mg/kg doses.[29] Unfortunately when OZ277 underwent phase IIa clinical trials it was cleared too quickly from the blood to continue through as a viable monotherapy.[11, 28, 37] The Indian company Ranbaxy that conducted the trials have shown that OZ277 is much more effective in combination therapies with piperaquine.[28] The resulting therapy, named Synriam, has recently gone on the market in India.[7, 11]

A second-generation synthetic ozonide, OZ439, has now been developed showing significant improvements on OZ277.[37] Currently in phase IIa clinical trials,[7] OZ439 cures blood stage mouse *P. berghei* infections in one oral 30 mg/kg dose, is a prophylactic and prevents transmission.[7] The improvements were made after it was discovered that the mechanism behind the rapid clearance of OZ277 was probably Fe (II) mediated degradation.[37] OZ439 possesses a *cis*-8'-phenyl substituent in place of OZ277's *cis*-8'-alkyl group and this confers 50-fold greater stability against Fe (II)

mediated degradation. OZ439 appears to be a promising candidate, however as it has the same mode of action as the artemisinins and only targets blood stage parasites, it may not be a viable answer for the emerging artemisinin resistance in South East Asia.[7]

The malaria drug pipeline contains many promising potent compounds with new targets and modes of action. Despite this, few pass the rigorous testing and make it to the market because of deficiencies, as was the case for OZ277, or because they are no better than current options already on the market. Due to the high attrition rates of drugs in clinical trails, MMV estimates that for every combination therapy of two compounds that enters the market, 7–10 new compounds must enter phase I trials.[28] Thus for the current existing pipeline of less than 20 candidates, only two combination therapies can be expected. This highlights the need to continue to develop NCEs that are potent, have promising pharmacokinetic profiles and have new mechanisms of action.

1.6 The Series 4 triazolopyrazines

In September 2013, the Open Source Malaria (OSM) Consortium was given data on a set of compounds with promising anti-malarial activity, the triazolopyrazines.[38] The series was initially discovered by Pfizer in collaboration with MMV in a high throughput screen of 160,000 compounds for *P. falciparum*. Optimisation of the series was carried out by Pfizer and then TCG Lifesciences (henceforth known as the contract research organisation [CRO]) before being placed in the public domain through OSM.

MMV has partnered with OSM since 2011. This is the fourth series of compounds on which the consortium has worked. Series 1–3 all arose from data that GlaxoSmithKline (GSK) put into the public domain in 2010.[39] Series 1 was parked because a key functional group in the lead compound was metabolically unstable and could not be replaced. Series 2 was parked because another (closed) group was researching it. Investigation into Series 3 is ongoing, however analogs of the lead compound synthesised so far have not improved pharmacokinetic properties.

When OSM inherited the data on series 4, there were 118 novel compounds, each of which had at least an IC_{50} value for *P. falciparum*. The compounds can be split into two subsets based on the linkage to the pyrazine: the ethers and the amides (Figure 1.6).

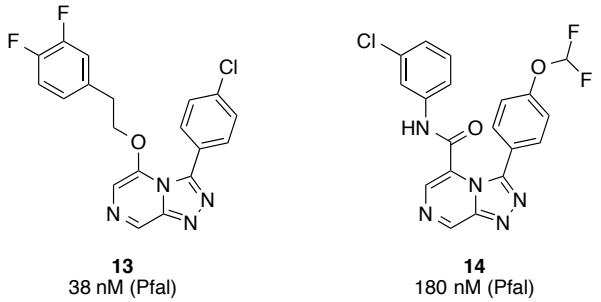

Figure 1.6: A representation of each subset of series 4: the ethers and the amides.

Along with potency data, the OSM team were also given a document describing the synthetic route to one of the ether compounds with limited ^{1}H NMR data for some of the intermediates.[23] No other characterisation data were given. The triazolopyrazine compounds in this series are all novel, and currently no data on them has been formally published. Work by the OSM team on Series 4 began in October 2013.

1.7 Open source science/drug discovery

The aims of open source science are simple: to accelerate research by bringing together previously unknown experts or able people resulting in a reduction of duplication of work and constant peer review, arguably making for better research.[40-41] There are six laws governing the OSM consortium:[41]

1. All data are open and all ideas are shared
2. Anyone can take part at any level of the project
3. There will be no patents
4. Suggestions are the best form of criticism
5. Public discussion is much more valuable than private email
6. The project is bigger than, and is not owned by, any given lab.

The project platform has recently been published and describes the practical aspects of undertaking an open source project.[41] In practice open science means that each scientist keeps an electronic lab notebook (ELN) rather than a traditional paper one, and the ELN is publicly viewable. OSM use Labtrove, developed using open source principles at the University of Southampton. GitHub is used as a virtual to do list, keeping track of tasks that are happening and problems that the consortium needs to solve; it can also be a place for posing problems and starting discussion. The OSM wiki is a more formal write up of the project as a whole. Twitter and Google+ are used to promote the project, while also sparking discussion and being platforms for posing questions and seeking help.

2. Project aims

The aims of this project were:

1. To validate and develop the synthetic route to the ether triazolopyrazines.
2. To improve the pharmacokinetic properties of Series 4 by exploring new functionality in the ether triazolopyrazines.
3. To design and develop a synthetic route towards fluoroalkene triazolopyrazine analogs as a novel isosteric subset of the series.

The strategic planning underpinning these aims will be described in the following section.

3. Project Design

3.1 Analogues

The ether subset of Series 4 and is the most extensively investigated. Several ether compounds were found to possess excellent potency, making them promising anti-malarial drug candidates (Figure 3.1).[42]

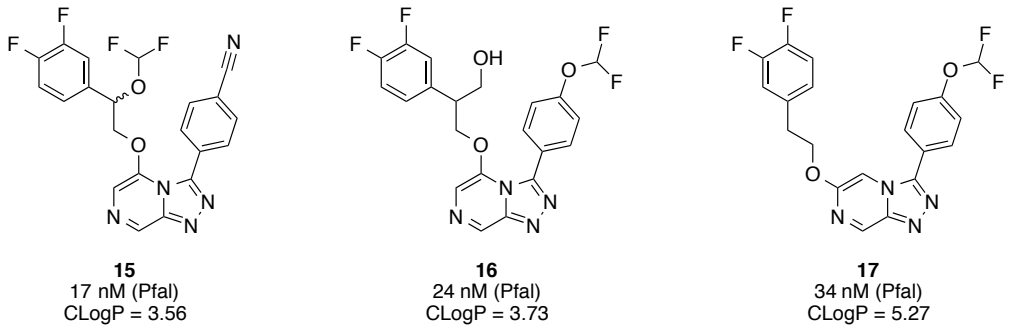

Figure 3.1: The three most potent compounds against *P. falciparum* in the Series 4 ether subset from prior work.[42] CLogP is the calculated logarithm of the 1-octanol:H_2O partition coefficient. The lower the CLogP the more hydrophilic the compound is.

However, despite their excellent potencies, the ether compounds were found to suffer from poor solubility and metabolic stability, thus limiting progression into preclinical trials without resolution of these issues. Attempts to improve these properties without negatively affecting potency had been made prior to the OSM teams work (Figure 3.2).[42]

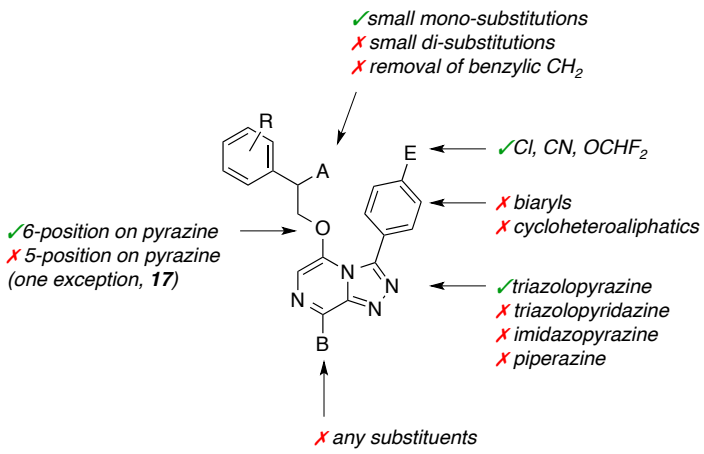

Figure 3.2: Structure Activity Relationship (SAR) of the ether triazolopyrazines.

The triazolopyrazine core was thought to be a site of metabolic weakness and a significant amount of work has been carried out by the CRO to try to improve this.[42] Alterations to the triazolopyrazine structure and the addition of functional groups in the three position of the pyrazine were detrimental to potency and did not improve the metabolic stability. Shifting the ether substituent from the six position to the five position on the pyrazine also lost potency with one exception (**17**, Figure 3.1). Modifications to the triazolo substituent were also not tolerated. The benzylic position on the ether substituent was thought to be a point of metabolism. Removal of the benzylic carbon by creating phenolic ethers resulted in loss of potency. Mono-substitution in this position retained potency however di-substitution did not.

There has been little exploration of analogues of the ether and amide subsets. A small number of aliphatics and cyclic amines have been synthesised as analogues of the ether subset although generally showed no improvement on potency and stability.[42] There are few examples of linear amine analogues of the ether and no compounds containing the thioether functional group in the previous work. A search of PubChem for similar compounds by OSM member Dr Chris Southan[43] found a compound with similarities to ours containing the thioether group and which was potent against *P. falciparum* at 2.9 nM;[44] hence the decision to explore this functionality. There has also been no exploration of analogues of the amides. It was proposed that a fluoroalkene isostere would be interesting replacement to investigate (Figure 3.3).

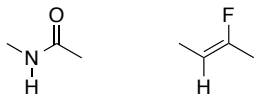

Figure 3.3: A peptide bond and the fluoroalkene mimetic.

Fluoroalkenes are well established as isosteres for amide bonds in peptides[45-48] and are increasingly incorporated into compounds of medicinal interest.[49-50] The fluoroalkene functional group has a similar size and shape to the amide and is a reasonable mimic of the charge separation in a peptide bond.[51] Computational analysis also suggests that the fluorine may be able to act as a hydrogen-bond acceptor, although this is likely to change the structure relative to the native peptide.[51] Conversely the C-H bond is not able to act as a hydrogen-bond donor like its N-H counterpart.[51] Therefore fluoroalkene

has enough similarity to the amide bond to be an interesting analogue of the amide subset of Series 4 to explore.

In July 2014 the OSM team was given recommendations for the design of new compounds in Series 4 by the MMV Expert Scientific Advisory Committee (ESAC).[52] These are as follows:

- Lower CLogP
- De-planarise the structure of Series 4 compounds by the introduction of new stereocentres and non-aromatic groups
- Introduce more heteroaryl groups

These criteria all aim to increase the solubility and metabolic stability of Series 4.

Design of the compounds in this project was therefore based upon exploring new functionality in the ether and amide subsets, and extending knowledge on existing functionality in the ether subset while addressing some of the issues identified with these compounds.

3.2 Open Source Methodology

The project structure followed an open source approach (Figure 3.4). Input from the scientific community was continually sought throughout the project on all aspects of chemistry, compound design and interpretation of biological data.

The project began with evaluation of the existing potency and synthetic data. Suggestions for improvement to the route were placed on GitHub and the ELN and feedback was sought. The initial compounds for synthesis were chosen with the intention of evaluating the synthetic route and were placed on the GitHub to do list. A small library was created and was submitted for biological evaluation of potency. Following consultation with the OSM team and wider scientific community, metabolic assessment of the most promising compounds was undertaken. A period of community consultation ensued, including input from the MMV ESAC, on the outcomes of the biological testing and the next targets of interest. The community and committee input

aided design of the next small library of molecules that was synthesised and submitted for biological testing.

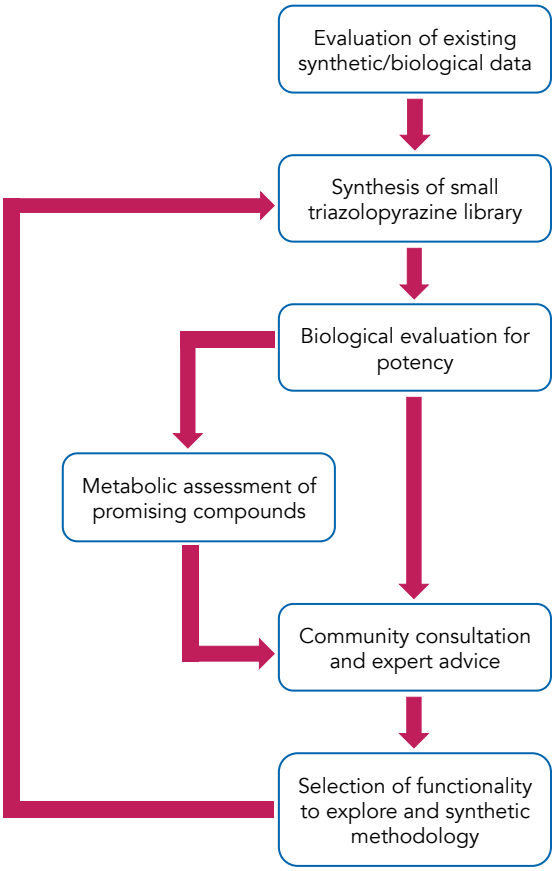

Figure 3.4: Project structure and methodology. Each stage of the project was documented online in the ELN and GitHub and input and feedback were continually sought.

4. Results and Discussion

4.1 Synthesis of the ether triazolopyrazines and related analogues

The ether subset of Series 4 is an attractive set of compounds, with several members showing excellent potency against *P. falciparum* (Figure 3.1). The compounds in the subset have not yet been fully explored and optimised for their pharmacokinetic properties. The molecular target of Series 4 is thought to be the PfATP4 ion exchanger. Currently there are no drugs on the market that target PfATP4 although there are three compounds in the malaria drug pipeline, KAE609 (**9**),[35] dihydroisoquinolones[53] and aminopyrazoles[54] (Figure 4.1). These inhibitors all have distinct structures, indicating different sites of action on PfATP4. The distinct structures of the PfATP4 inhibitors means that the ether subset is still worthy of further study as it is unlikely that all of these compounds will make it to the market.

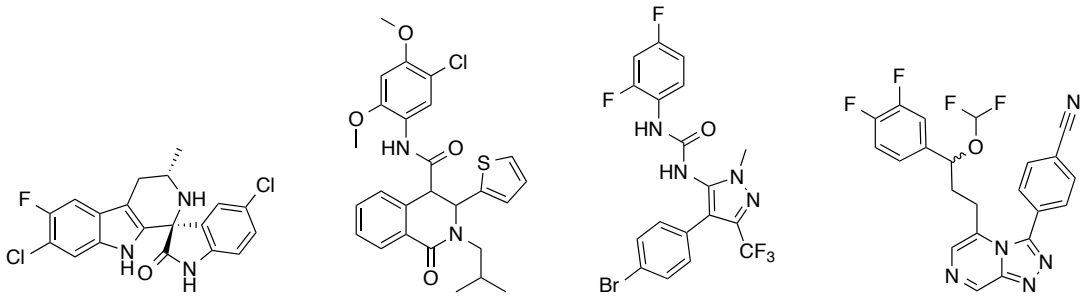

9
KAE609
Spiroindolones

18
Dihydroisoquinolones

19
Aminopyrazoles

15
Triazolopyrazines

Figure 4.1: The four inhibitors of the PfATP4 ion exchanger on the outer membrane of *P. falciparum*. These are representative compounds from each compound class.

The synthesis and characterisation data given to the OSM team from the CRO for the ether subset of Series 4 was incomplete and unpublished.[23] The first task was to validate the route given to these compounds by exploring the chemistry outlined in the CRO document (Scheme 4.1), starting with the triazolopyrazine core followed by the attachment of the ether. Optimisation of the chemistry could then be attempted in order to demonstrate the wider viability of this route.

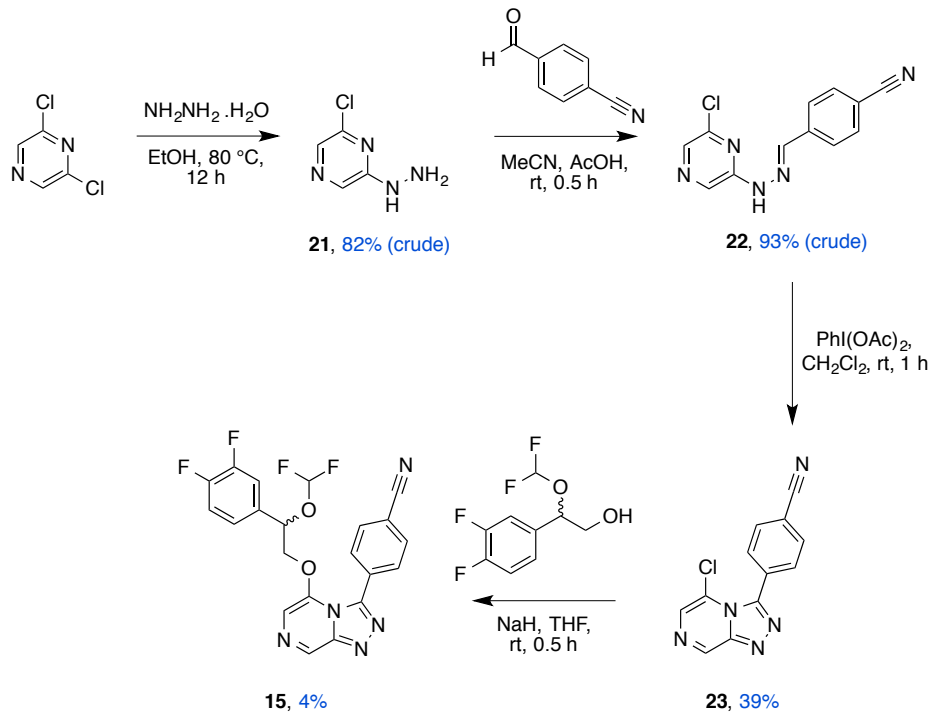

Scheme 4.1: Example synthesis of the ether triazolopyrazines by the CRO. Synthesis begins with the displacement of chlorine on 2,6-dichloropyrazine (**20**) with hydrazine. The hydrazinyl pyrazine product (**21**) is carried through without purification into an acid catalysed condensation with an aromatic aldehyde to give the hydrazone (**22**). The hydrazone is carried through crude into an oxidative cyclisation using phenyliodine diacetate (PIDA) as the oxidant to give the triazolopyrazine core (**23**). An S_N2 displacement of the pyrazine chlorine with an alcohol to form an ether triazolopyrazine (**15**) is the final step.

4.1.1 Synthesis of the triazolopyrazine core

The starting point for the synthesis of the triazolopyrazine core was the displacement of chlorine on commercially available 2,6-dichloropyrazine (**20**) with hydrazine hydrate to form **21** (Scheme 4.2). This procedure has previously been reported in the literature with yields of 69% (pure).[55] The yield reported by the CRO was 82% (crude) and the reaction initially proceeded as expected to give similar yields of >85% (crude) over five attempts.

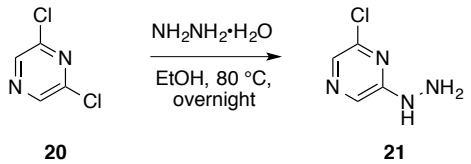

Scheme 4.2: Synthesis of compound **21** from 2,6-dichloropyrazine (**20**) using conditions reported by the CRO.[23]

A more recent attempt to synthesise **21** resulted in the formation of an alternative product and the absence of **21**. The two signals arising from what were presumed to be the pyrazine protons of a mono-substituted product were shifted notably downfield from 8.04 and 7.72 ppm (for the desired product) to 8.34 and 7.96 ppm respectively (circled, Figure 4.1). Three new peaks at 10.10, 1.98 and 1.93 ppm appeared and the signals expected from the protons attached to the nitrogens in the hydrazine were no longer present. This data and the *m/z* of 185 (APCI, MH^+, 100%) indicated the compound was a condensation product between **21** and residual acetone in the reaction flask forming the hydrazone **24** (blue, Figure 4.1). This result indicates that the condensation reaction (Step 2) is surprisingly easy and suggests that development of a one-pot displacement condensation reaction for the formation of the hydrazone is feasible.

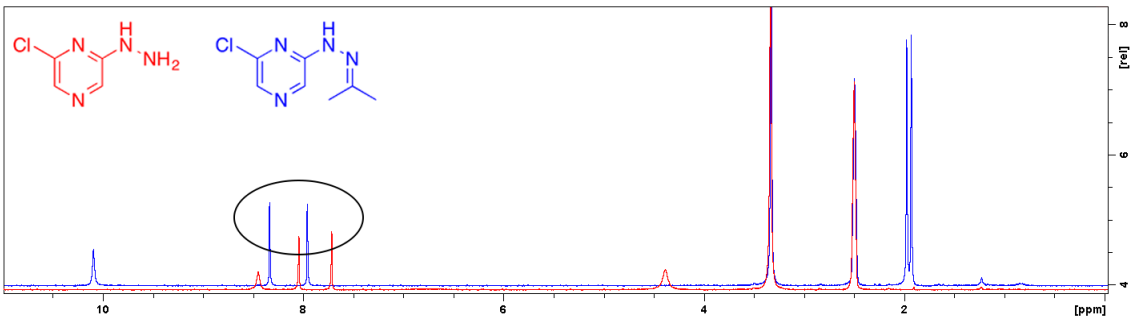

Figure 4.1: A comparison of the ^{1}H NMR spectra for **21** (red) and **24** (blue). The pyrazine protons in **24** are shifted downfield relative to the pyrazine protons in **21** (circled) indicating a more electron deficient environment. The peak in the spectrum of **21** at 8.45 ppm is residual starting material **20**.

The second step towards the triazolopyrazine core was an acid catalysed condensation reaction between **21** and an aromatic aldehyde (Scheme 4.3). *Para*-formylbenzonitrile was used initially as a direct comparison with the synthesis and potency data obtained.[23, 42] The known SAR data for Series 4 suggested a nitrile group in the *para* position could provide potency but there were few examples of compounds containing this functionality. The reaction proceeded as expected giving an approximately quantitative crude yield of **22**, comparable to the result from the CRO. Purification was not attempted at this stage, as the procedure suggested it was not necessary for the subsequent step. The core could be trivially diversified at this step by modification of the

aldehyde. Compound **25** was also synthesised by this method using *para*-chlorobenzaldehyde as starting material in an approximately quantitative crude yield (Scheme 4.3). Compounds containing a *para*-chloro group were also underexplored in the original dataset but what examples there were showed good potency.[23]

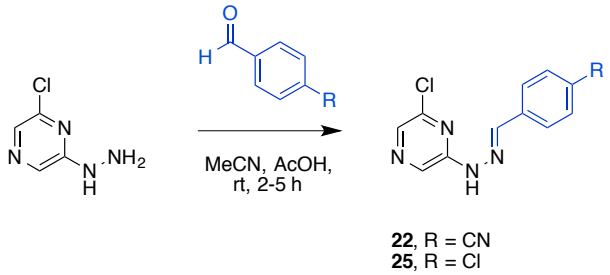

Scheme 4.3: Acid catalysed condensation of the **21** with an aromatic aldehyde to form the two hydrazones, **22** and **25**.

A ^{1}H NMR spectrum of crude **22** showed the expected number of peaks, however one proton was shifted far downfield at 11.86 ppm (A, Figure 4.2). The literature for similar compounds containing an aromatic hydrazone reports this peak as the NH proton although the shifts vary between ~9.0 ppm[56] and 11.56 ppm.[57] ^{1}H-^{13}C Heteronuclear Single Quantum Correlation (HSQC) and ^{1}H-^{13}C Heteronuclear Multiple Bond Correlation (HMBC) spectroscopy were used to confirm the identity of the proton giving rise to this signal as full characterisation had never been reported for this compound. HSQC (blue, Figure 4.2) confirmed that the proton at 11.86 ppm was not directly bound to a carbon. Long-range coupling (2–3 bonds) was seen in the HMBC spectrum (red, Figure 4.2) between this proton and three carbons (B, C, D). Carbon C was the imine proton because of its coupling to the benzene ring, while B was determined to be one of the pyrazine protons. D was found to be a quarternary carbon. Proton A therefore must be the NH proton to be in the close proximity to these three environments. The ^{1}H NMR spectrum of the chloro analogue **25** contained similar shifts to **22**, again with a far downfield NH proton at 11.63 ppm. The hydrazones were pale orange powders and stable under ambient conditions.

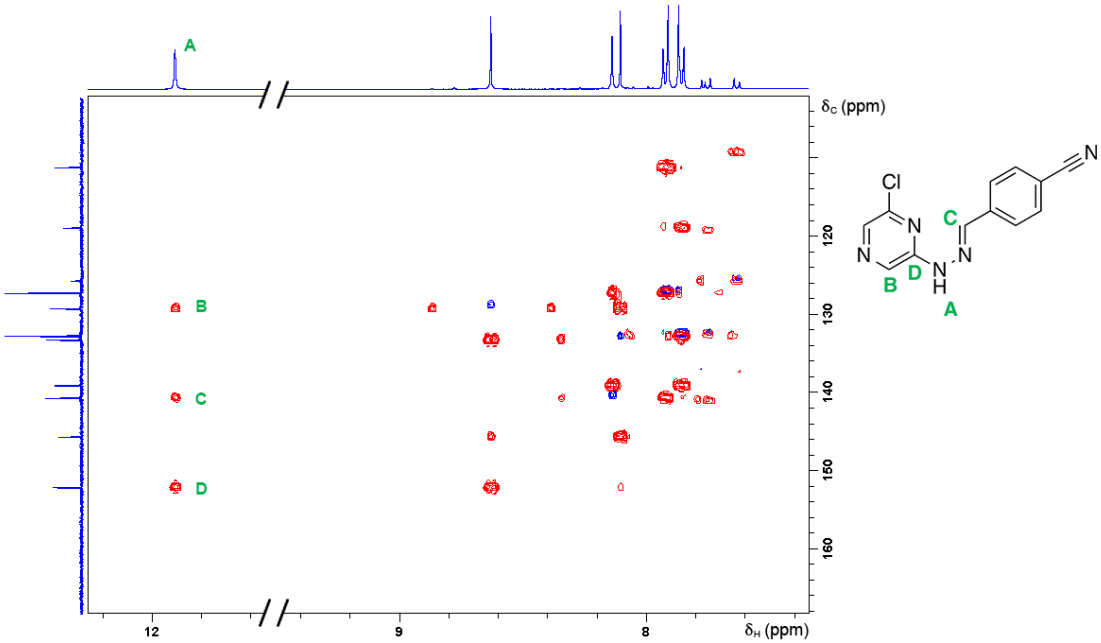

Figure 4.2: HSQC (blue) and HMBC (red) experiments of **22** (crude). Only aromatic regions are shown, for full spectra see Appendix X. HSQC shows the proton at 11.86 ppm (A) is not directly bound to a carbon. HMBC shows that this same proton is coupled to three carbons (B-D).

The final step in the synthesis of the triazolopyrazine core was an oxidative cyclisation of the hydrazone. The CRO reported using PIDA as the oxidant to achieve this transformation (Scheme 4.4) with a yield of 39%.[23] Previous attempts at this reaction in the OSM group were performed at the concentration given (1.4 mM) and were found to give only trace amounts of the desired product **23**. The poor yield was initially attributed to the partial solubility of **22** in the solvent employed, dichloromethane. Previous attempts to change the solvent to acetonitrile and 2–methyl THF did not increase solubility or yield.

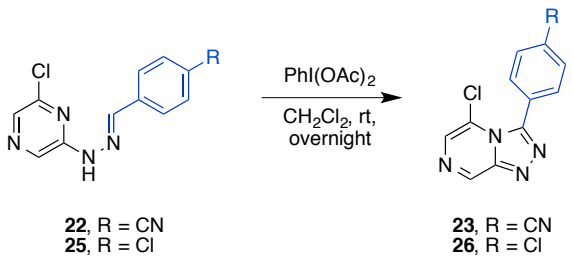

Scheme 4.4: Oxidative cyclisation of the hydrazones **22** and **25** to form the triazolopyrazine core compounds **23** and **26** respectively.

In this work, dilution of the reaction mixture to 0.02 mM gave an increased yield of ~17% of **23** in two attempts, consistent with literature on a similar reaction.[58] In the aqueous workup of **23**, significant amounts of insoluble material were present between the aqueous and organic phases in the separating funnel. Three extractions of this material with dichloromethane saw little decrease in the quantity of insoluble material and gave yields of <20% of pure **23** over two attempts at the reaction. The number of extractions with dichloromethane was doubled to six, resulting in the almost complete solubilisation of the insoluble material and an increased yield of 43%. Low yields in this reaction can therefore be partially attributed to low solubility of the product. **25** was cyclised with PIDA to form **26** in a 42% yield using the improved dilution (Scheme 4.4). **26** was found to have greater solubility than **23**; less insoluble material was present between the phases in the separating funnel and therefore only three extractions instead of six were required.

The overall yield of the oxidative cyclisation to form the triazolopyrazine core was reliably 40–45%, giving enough product to begin developing the S_N2 displacement for formation of the ether triazolopyrazine. The oxidative cyclisation was revisited after the development of the S_N2 displacement (Section 4.1.4)

4.1.2 S_N2 displacement development and diversification

The final step in the synthesis of the ether triazolopyrazines was an S_N2 displacement of the chlorine of **23**. The CRO reported the use of an alcohol with sodium hydride in THF to achieve this displacement with a yield of only 4% (Scheme 4.1). Early attempts within the group to replicate this reaction with an analogous alcohol were unsuccessful. Development of a new process for this displacement reaction was therefore necessary.

A search of the literature for similar displacements of pyridyl or pyrazinyl chlorines by alcohols found several sets of relevant reaction conditions which were compiled on the OSM blog.[59] The most promising conditions employed KOH and 18-crown-6 in toluene at reflux to achieve a displacement on 2-chloropyridine with a benzyl alcohol with excellent yields of 90–96%.[60] These conditions were first tested on 2,6-dichloropyrazine (**20**) and phenethyl alcohol proceeding with the displacement of both chlorines to give a

yield of 68% of the **27** (B), (Scheme 4.5). The single displacement product (A) was not observed (Scheme 4.6). The triazolopyrazine core (**23**) intended for this reaction contains only one pyrazine chlorine and so the double displacement would not be a complicating factor in the Series 4 ether synthesis, but clearly these conditions were capable of effecting the desired displacement reaction.

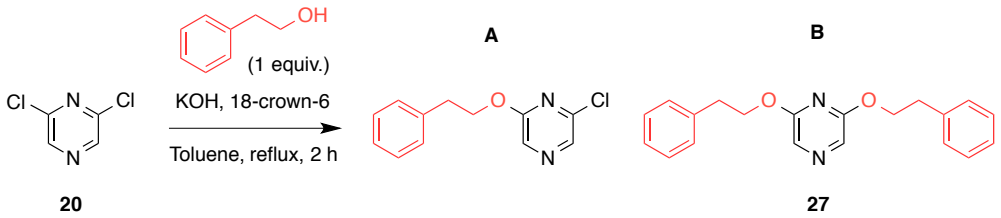

Scheme 4.5: Synthesis of **27** using KOH and 18-crown-6. The single displacement product (A) was not observed. **27** (B) was the only product isolated.

The conditions were then validated on **23** with phenethyl alcohol (Scheme 4.7). A procedure employing reflux in toluene with 3 equivalents of KOH was found to be too harsh and resulted in decomposition of triazolopyrazine core **23** (characteristic peaks absent in the crude ^{1}H NMR spectrum) with recovery of the phenethyl alcohol (A, Scheme 4.7). Adjustment of the temperature to 40 °C resulted in the formation of the desired product **28** in 26% yield (B, Scheme 4.7).

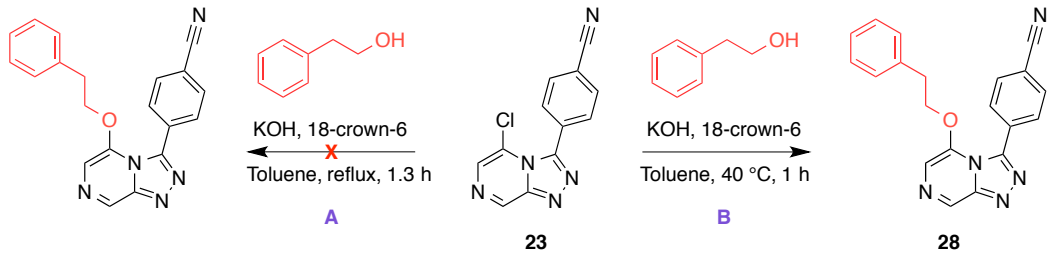

Scheme 4.6 Conditions for the synthesis of compound **28**. The conditions used for **27** (A) resulted in decomposition of the triazolopyrazine core **23**. Lowering the temperature to 40 °C (B) produced the desired compound **28**.

As previously mentioned in section 3.1, there were few examples of amines analogues and no examples of thioethers in the previous work. This presented an opportunity to explore the S_N2 displacement with other nucleophiles and thereby contribute further to the SAR data of Series 4. Four compounds were synthesised using the conditions as developed for **28**, one ether (**29**), one thioether (**30**) and two amines (**31** and **32**) (Figure 4.3) all in moderate yields.

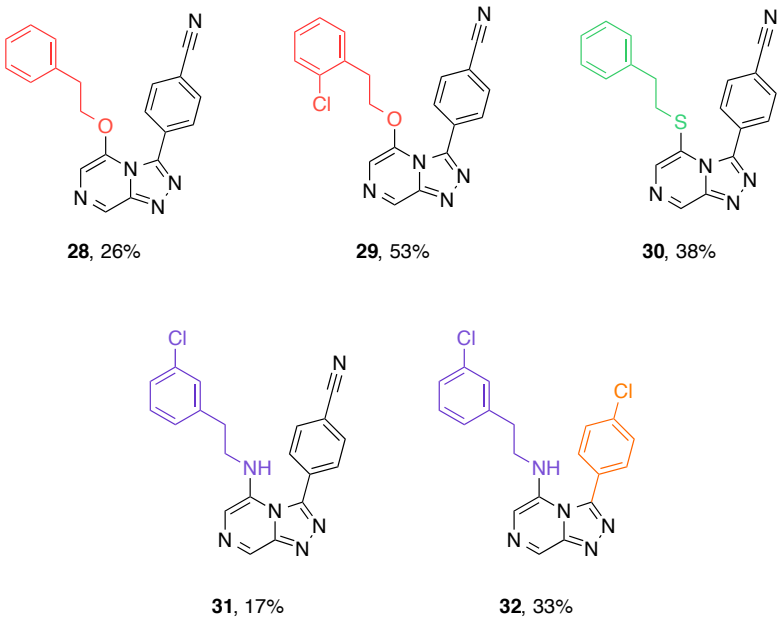

Figure 4.3: The first five triazolopyrazine compounds **28**–**32** synthesised by S_N2 displacement on the pyrazine with alcohol, amine or thiol nucleophiles. Percentage yields for the final displacement step are indicated.

Synthesis of these five compounds proceeded with little difficulty. **31** was an exception, proving difficult to separate out from impurities resulting in the loss of a small amount of the product. These yields have room for improvement however due to time constraints optimisation was not attempted and these initial attempts provided sufficient material for biological evaluation. Increasing the strength of the base may be one way to improve this reaction. Potassium *tert*-butoxide has been used successfully in reactions between benzyl and phenethyl alcohols and chloropyridines with yields ranging from 58–98%.[61] Sodium hydride has also been used successfully as a base in analogous reactions with solvents such as dioxane[62] and dimethoxyethane[63] in yields of 83% and 94% respectively; this obviously stands in contrast to the low yield of 4% reported by the CRO. The reaction using NaH in dimethoxyethane was performed at 45 °C[63] which should be compatible with the triazolopyrazine core. The disadvantage of the NaH/dioxane and KO^{t}Bu reactions are their temperatures of 100 °C,[61-62] however as for the lower temperature adapted for **28** (Scheme 4.7), these literature temperatures may also be similarly lowered.

4.1.3 Biological data for the triazolopyrazine ethers, amines and thioether

The five triazolopyrazine analogues (compounds **28–32**, Figure 4.3) and the two triazolopyrazine cores (compounds **23** and **26**, Scheme 4.4) were evaluated for their anti-malarial activity against the senstitive *P. falciparum* strain 3D7 in an asexual blood stage assay. The experiments were conducted by Ms Laura Maria Sanz-Alonso at GlaxoSmithKline (GSK) in Spain.

The anti-malarial activity of compounds **28–32** was initially evaluated in a single shot potency assay of whole cell *P. falciparum* strain 3D7 at 2 μM (Table 4.1). Two of the compounds, **28** and **29** had potencies of >99% at 2 μM (entry 3 and 5, Table 4.1) and were sent for additional testing. The remaining five, including the two cores, were not potent with inhibition at <22%. Thioethers and amines were not viable analogues of the ethers. The two compounds **28** and **30** only differ in their attachment of the phenethyl group; **28** is an ether while **30** is a thioether, the change completely destroying potency. There is no information on how these compounds may bind to the putative target PfATP4. This makes drawing conclusions difficult about why the thioether replacement is so detrimental to activity, but this will be an important data point in any future studies that attempt to deduce the pharmacophore for this series. In an analogous change, replacing the ether with an amine also destroys potency. In this case the CLogPs of the two amine compounds **31** and **32** were much higher than for the ethers synthesized which may account for their lack of potency.

Table 4.1: Single shot potencies and CLogP of compounds **23, 26** and **28–32** evaluated against *P. falciparum* strain 3D7 by GSK in a whole cell asexual blood stage assay.

Entry	Compound	CLogP	% Inhibition
1	23	1.7	22
2	26	2.9	6
3	28	3.6	100
4	29	4.3	99
5	30	3.9	22
6	31	4.6	18
7	32	5.9	9

Compounds **28** and **29** were evaluated in a whole cell *P. falciparum* assay (strain 3D7) to determine their IC_{50} values (Table 4.2). Both **28** and **29** were potent in the nanomolar range however did not compare with the most potent ether triazolopyrazine of Series 4 so far, **15**, with an IC_{50} of 17 nm (Figure 3.1).

Table 4.2: IC_{50} values (μM) for compounds **28** and **29** evaluated against *P. falciparum* strain 3D7 by GSK. [a]Pyrimethamine was used as a control.

Entry	Compound	CLogP	IC_{50} (μM)
1	28	3.6	0.534
2	29	4.3	0.309
3	Pyrimethamine[a]	3.0	0.041

A group of compounds from the series synthesised so far were selected for hERG ion channel cross-reactivity. The *human ether-a-go-go related gene* (hERG) encodes a potassium ion channel that is expressed in a number of tissues including the heart.[64] Blockage of the hERG ion channel by a drug significantly increases the chance of developing life-threatening cardiac arrhythmias which can result in sudden death. A growing number of drugs have been found to block this channel as a side effect in recent years and have been withdrawn from the market. Therefore testing for hERG cross-reactivity in the early stages of drug development is critical. Compound **29** was tested for hERG cross-reactivity by AstraZeneca. The pIC_{50} (log of the IC_{50}) for **29** was >4.48, indicating no cross-reactivity with the hERG ion channel. This is an improvement on the amide compounds, which generally showed high levels of cross-reactivity with hERG, for example **33** with a pIC_{50} of 5.60 (Figure 4.5). This could suggest an issue with the amide functional group or the difluoromethoxy group within the compound.

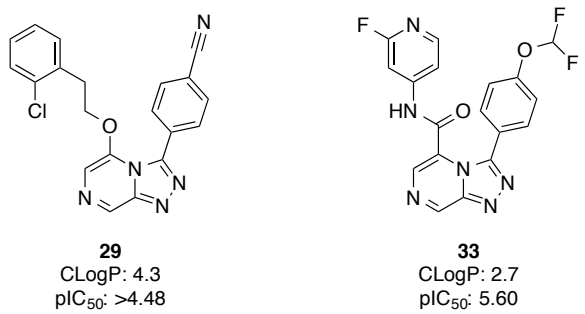

Figure 4.5: 29, and **33** with pIC_{50} data for hERG ion channel cross-reactivity.

With the validation and development of the chemistry to synthesise the final ether analogues complete, and promising new biological data for these analogues, attention could be turned to optimization of specific steps within this synthesis before completing a second set of analogues for biological testing.

4.1.4 Optimisation of the oxidative cyclisation and development of alternative cores

The yield for the synthesis of the triazolopyrazine core is moderate, and further improvements could be made since this is an important intermediate in the synthesis of the biologically active ether compounds. Three oxidants were chosen to test initially (Figure 4.6).

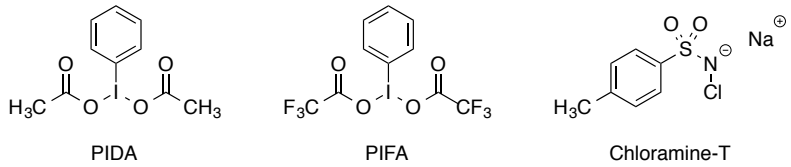

Figure 4.6: Oxidants PIDA, PIFA and Chloramine-T tested in the formation of the triazolopyrazine core.

PIDA was used as a control for comparison. Phenyliodine bis(trifluoroacetate) (PIFA) was chosen as it was shown to be highly effective in similar cyclisations.[58] Chloramine-T in 2-methyl THF was the third oxidant, having been suggested by an OSM member[65] from the United States as an option because of the good yield of 75% reported on a similar starting material lacking both chlorine groups;[66] and excellent yields of 75-90% were reported on pyridine analogues of **22** and **25**.

The test reactions were all carried out on **25** (pure) because of its greater solubility than **22**. Cyclisation with PIDA yielded 83% of **26**, PIFA yielded only 39%, while cyclisation with chloramine-T yielded 53% (Table 4.3). Minimal starting material was isolated from the three reactions. The doubling of the yield with PIDA by changing from crude to pure **25** (entry 1 and 2, Table 4.3) indicates the presence of a significant impurity in the crude material, or an unreactive isomer. However the crude ^{1}H NMR spectrum does not indicate the presence of a second isomer, and impurities other than small amounts of starting material were not able to be isolated.

Table 4.3: Optimisation of the oxidative cyclisation reaction to form the triazolopyrazine core. All reactions were carried out at room temperature except entry 3 which was carried out at 60 °C. Reactions were monitored by TLC until completion. [a]Phenyliodine diacetate; [b]Phenyliodine bis(trifluoroacetate); [c]2-Methyl tetrahydrofuran.

Entry	SM Purity	Oxidant	Solvent	Yield
1	Impure	PIDA[a]	CH_2Cl_2	42%
2	Pure	PIDA[a]	CH_2Cl_2	83%
3	Pure	Chloramine-T	2-MeTHF[c]	53%
4	Pure	PIFA[b]	CH_2Cl_2	39%

The significant decrease in yield of **26** between PIDA and PIFA was surprising, given the similarities of these two oxidants and the yields of ~90% for similar cyclisations with PIFA reported in the literature.[58] The yield of **26** from the cyclisation with chloramine-T was significantly lower than that reported for the analogous pyrazine and pyridine compounds.[66] Cyclisations of pyridine analogues with both electron-donating and withdrawing substituents were reported with excellent yields, however only one pyrazine analogue was tested under these conditions.[50] This may mean that pyrazines are less amenable to oxidative cyclisation. The overall yield between entries 1 and 2 (Table 4.3) was found to be the same. Purification of the hydrazone **25** resulted in the loss of 51% of the crude mass, which results in a 41% overall yield of the triazolopyrazine **26**. This is comparable to the yield of 42% from the impure starting material and means that identification of the insoluble by products may be needed for further improvement of this reaction.

Two cores were developed with an alternative pendant aromatic group, **35** and **37** from their respective hydrazone intermediates **34** and **36** (Scheme 4.8). Compound **35** was synthesised from pure **34** (75% yield), whereas **36** was carried straight through crude to synthesise **37** (42% yield).

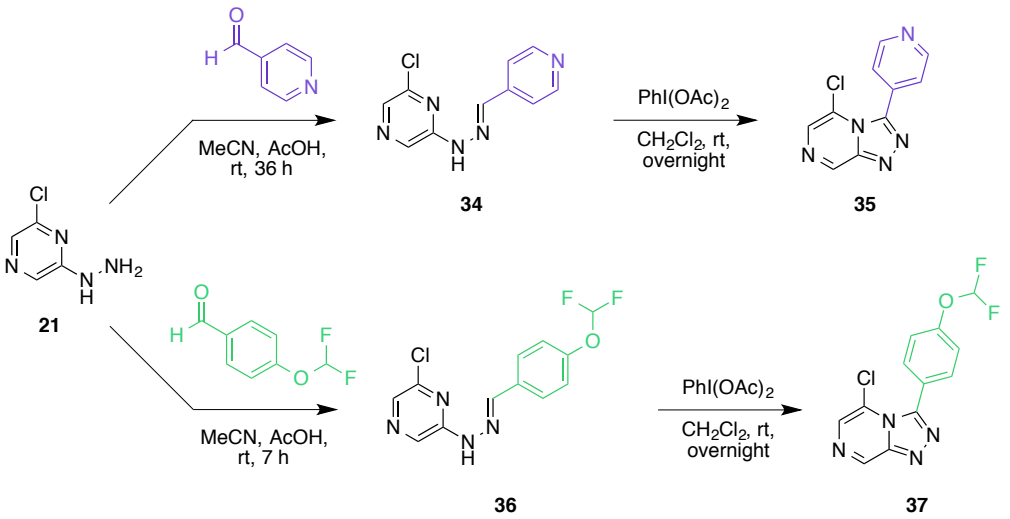

Scheme 4.8: Synthesis of hydrazones **34** and **36** followed by cyclisation with PIDA to form the corresponding triazolopyrazine cores, **35** and **37**.

The CLogP of **34** is 1.63, much lower than that of hydrazones **22** (2.37), **25** (3.65) and **36** (3.60). The reaction time for the formation of **34** was considerably lengthened, from 2.5–7 h for **22**, **25** and **36** to approximately 36 h for **34**. The comparatively electron rich 4-pyridyl ring may decrease the electrophilicity of the carbonyl carbon resulting in a longer reaction time. This is also reflected in the yield, only 23% of pure **34** was obtained.

The mechanism for the oxidative cyclisation of hydrazones to triazolopyrazines with PIDA has not been experimentally determined, but has been proposed in the literature for compounds similar to **22** (Figure 4.6).[56, 67]

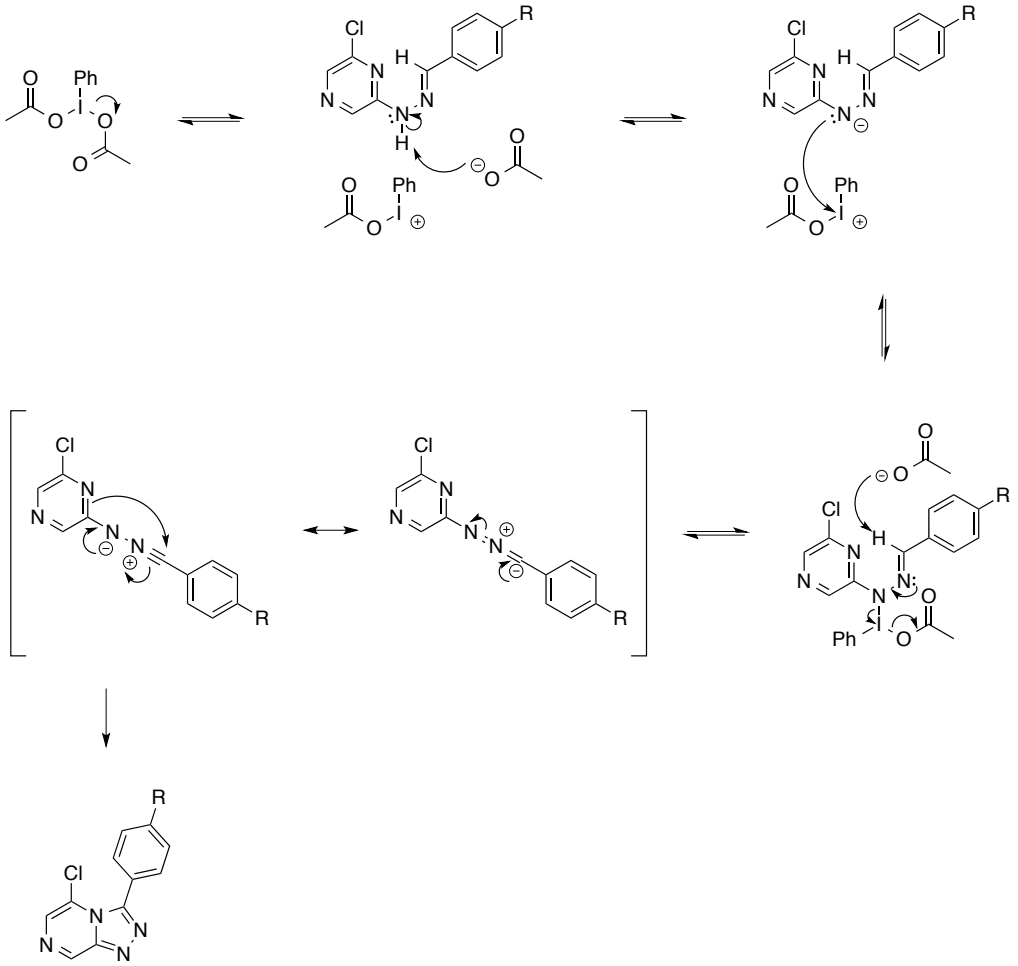

Figure 4.6: Proposed mechanism in the literature for the oxidative cyclisation of hydrazones to triazolopyrazines with PIDA via a nitrile imine ylid.

The mechanism begins with removal of the amine proton by acetate and formation of a nitrogen-iodine bond. Phenyl iodine then leaves along with an acetate anion to form a nitrile imine ylid intermediate species. The benzylic carbon is then subject to nucleophilic attack by the pyrazine ring forming the triazolopyrazine. The ylid intermediate has two resonance forms, both of which would be likely to have linear geometry for the N-N-C bonds. This mechanism does not seem to allow the benzylic carbon to be close enough to the pyrazine nucleophile for cyclisation. An alternative mechanism without the nitrile imine ylide intermediate is therefore proposed here (Figure 4.7).

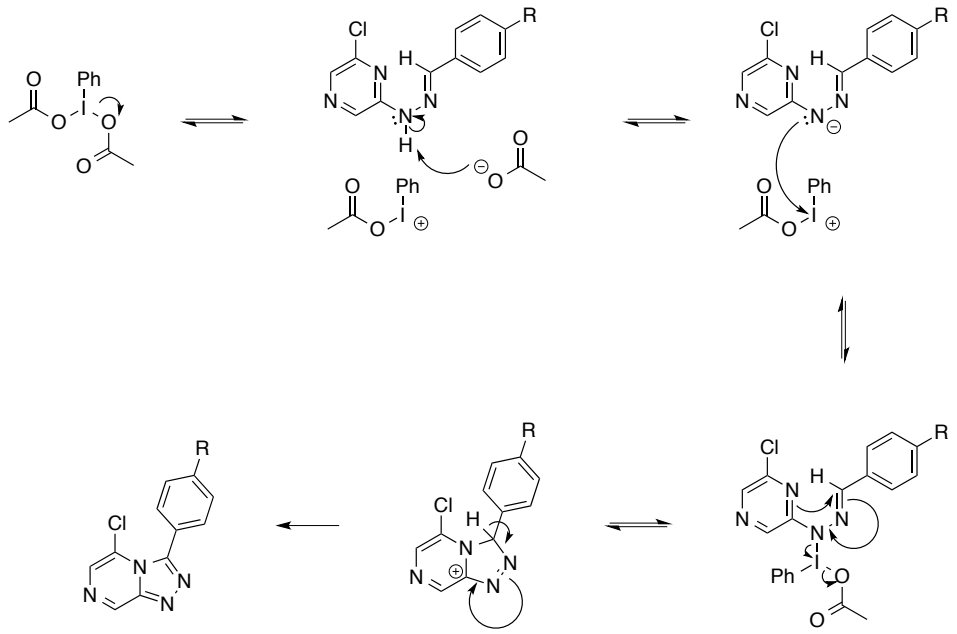

Figure 4.7: Alternate proposed mechanism for the oxidative cyclisation of hydrazones to form the triazolopyrazine core with PIDA.

The alternative mechanism begins in the same way with acetate from PIDA removing the amine proton and formation of the nitrogen iodine bond. Intramolecular cyclisation then occurs without formation of the nitrile imine ylid intermediate, kicking off phenyliodine and the acetate anion in the process. Removal of the benzylic proton by the free acetate anion then results in aromatization of the triazolopyrazine, completing the reaction. This alternate mechanism does not include the linear nitrite imine ylid, thereby allowing the nitrite to be closer to the pyrazine for nucleophilic attack and cyclisation. The true mechanism could be experimentally determined by following the reaction by ^{1}H NMR and monitoring the change in shift of imine proton and the pyrazine protons for the point at which cyclisation occurs.

4.1.5 Design and synthesis of round 2 ether triazolopyrazines

Evaluation of the biological data obtained from GSK and AstraZeneca confirmed that the ether triazolopyrazines were worth exploring further, but that the thioether and amine analogues were not. The potency data from the CRO was re-evaluated along with the new data and from this two targets were chosen for synthesis, compounds **38** and **39** (Figure 4.8).

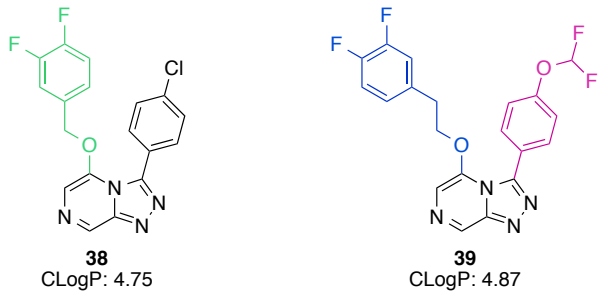

Figure 4.8: Ether triazolopyrazines **38** and **39** were chosen as desirable synthetic targets for the second round of biological testing.

There were only two benzylic ethers tested in the inherited CRO data, with low potencies of 1.46 and 1.67 μM.[42] The benzylic ether **38** was chosen because it is analogous to the phenethyl ether compound **13** (Figure 1.6) which exhibited an excellent potency of 0.038 μM, allowing for a direct comparison of chain length on potency. Compound **39** contains the two most commonly used functional groups in the CRO data, the 3,4-difluorophenethoxy group (blue, Figure 4.8) and the difluoromethoxy phenyl group (pink). While these two groups have been extensively tested separately, there is no data for them in the same compound with this attachment pattern. An analogous compound **17** with the ether in the 5 position has an excellent potency of 0.034 μM (Figure 3.1) but with low stability measured in rat liver microsomes.

A third and fourth target were designed based on two of the suggestions from the MMV Expert Scientific Advisory Committee (ESAC) after the first round of testing.[52] The suggestions were to bring the CLogP between 1.5 and 3.5 and to de-planarise the molecules by, for example, introducing stereocentres. With that in mind, compounds **40** and **41** were designed (Figure 4.9).

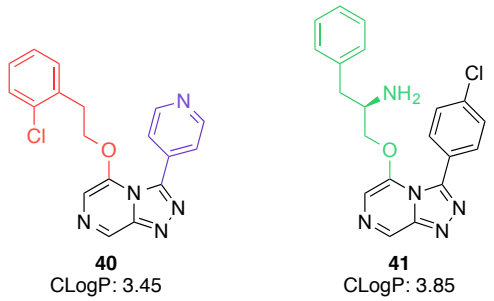

Figure 4.9: Ether triazolopyrazines **40** and **41** (R) were chosen as targets for the second round of biological testing.

Compound **40** has a CLogP of 3.45 which satisfies the criteria; the 4-pyridyl group is responsible for this improvement. The compound also contains the 2-chlorophenethoxy group from compound **29** (Figure 4.3) for direct comparison of the effect of the 4-pyridyl group to the benzonitrile group on potency. Compound **41** has a new stereocentre in the ether chain, and an extra CH_2 group to investigate de-planarisation and the effect of the elongated ether chain on potency. There are no examples of propanolic ethers in the CRO data. Given that it had been found that both amines and alcohols could displace the pyrazine chlorine on the core, it was anticipated that, if an aminoalcohol was used in the synthesis, an amine could also be formed instead of or as well as the desired ether. The amine would be interesting to evaluate if it were formed, however, as a comparison to the data obtained in Round 1. The compound is also analogous to **42**, which is a phenethyl ether with a reasonable IC_{50} of 0.279 μM (Figure 4.10).

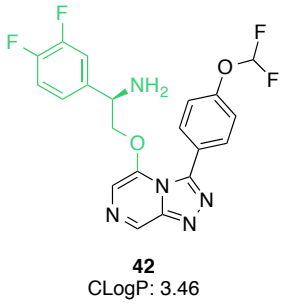

Figure 4.10: Compound **42** is analogous to **41** with an IC_{50} of 0.279 μM.

Compounds **38**, **39** and **40** were synthesised according to the procedure developed in section 4.2.2 with yields of 38%, 19% and 12% respectively (Scheme 4.8). The low yields of <20% for **39** and **40** were likely in part due to the difficulty in purifying these

compounds and the number of purifications attempted for each before a pure sample was obtained for biological evaluation. **40** was particularly difficult to handle because of its low solubility.

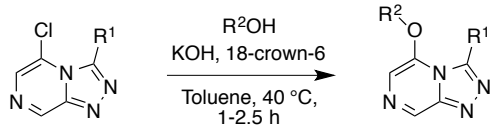

Entry	Compound	R^1	R^2
1	38	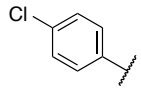	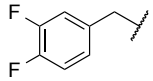
2	39	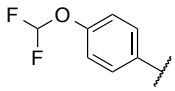	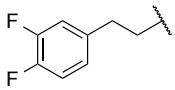
3	40	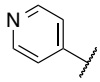	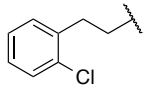

Scheme 4.8: Synthesis of the triazolopyrazines **38**, **39** and **40**.

The synthesis of **41** was also attempted through this method, however neither of the two possible products were isolated (Scheme 4.9). Synthesis of **41** was not reattempted due to time constraints.

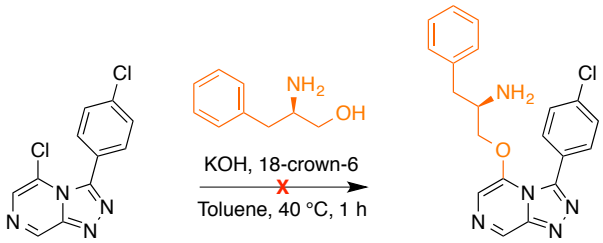

26 **41**

Scheme 4.9: Synthesis of **41** was not achieved.

4.1.6 Biological data round 2

Compounds **38**, **39** and **40** were evaluated for their anti-malarial activity against *P. falciparum*. The experiments were conducted by at Syngene in India. The IC_{50} of each compound was determined in a whole cell erythrocyte assay on *P. falciparum* NF54 sensitive strain (Table 4.4).

Table 4.4: IC_{50} values (μM) for compounds **38**, **39** and **40** evaluated against *P. falciparum* NFS4 by Syngene.

Entry	Compound	CLogP	IC_{50} (μM)
1	38	4.75	0.452
2	39	4.87	0.281
3	40	3.45	>10

The replacement of the 4-nitrile group in **29** to a 4-pyridyl group in **40** destroyed the potency of this compound (entry 3, Table 4.4). Like the changes from an ether to a thioether in the first set of compounds, a small change has had a large impact on the effectiveness of the compound. This result is surprising as **33** (Figure 4.5) contains a 4-pyridyl on the pyrazine substituent. Shortening the length of the ether chain from two CH_2 groups in **13** to one in **38** decreased the potency of this compound from 0.038 μM to 0.452 μM. This adds to the SAR data for the Series 4 and suggests that the phenethyl ether linkage is more favourable. The phenethyl ether linkage has been explored more than the benzylic ether linkage in this series.

Lastly, adding together the two typical side groups into one molecule, compound **39**, does not confer the high level of potency one might expect, with an IC_{50} of 0.281 μM. The analogous compound, **17** that differs in the point of attachment of the ether onto the pyrazine ring only, has a potency of 0.034 μM. The trend for the compounds in the series data is that this alternative point of attachment generally lowers potency and negatively affects pharmacokinetic properties,[42] however for potency at least, the reverse is seen here. The CLogP of **39** is 4.87, which could mean that it is too lipophilic. It is also possible that differences in the assays used, and in the strains employed, could be responsible for the differences in data, and there may here be a justification for re-testing **17**.

There are many more ether analogues to be made and tested, exploring the effects of lower ClogP, de-planarising the molecules and investigating heteroaryls on metabolic stability and hERG cross-reactivity. Although there is more work to be done in this area, it was decided to attempt a more radical alteration to the compound structure. A new set of analogues based on the amide subset of Series 4 was designed, broadening the available functionality that could be attached to the triazolopyrazine core.

4.2 Synthesis of the fluoroalkene analogues

Fluoroalkenes are an established isostere for peptide bonds and are proposed as an analogue of the amide subset of Series 4 (Figure 4.11). The fluoroalkene is a reasonable mimic of the amide bond however its rigidity and limited ability be a hydrogen bond donor means that it will give new functionality to the triazolopyrazines.[51] The results of the hERG cross-reactivity assay showed that the amides block the hERG ion channel (Section 4.1.3). Previous work has also shown that, like the ethers, the amides suffer from poor metabolic stability.[42] Therefore exploration of new analogues of the amide subset may help to ameliorate the hERG cross-reactivity and metabolic stability issues while aiding in the understanding of the SAR of Series 4.

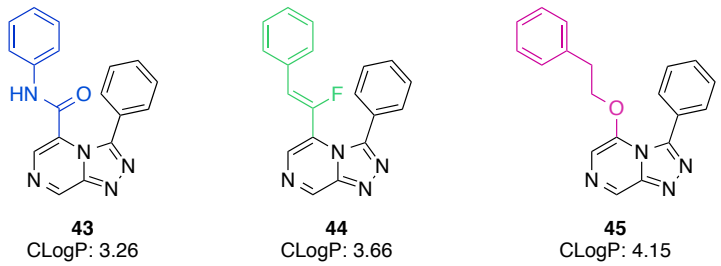

Figure 4.11: A comparison of the CLogP of a basic amide (**43**), fluoroalkene (**44**) and ether (**45**). The fluoroalkene is predicted to be more hydrophilic than the ether but less than the amide.

The fluoroalkene functional group increases the CLogP of compounds relative to amides and ethers (Figure 4.11). This replacement seems counterproductive since lowering CLogP is one of the design criteria for new compounds in Series 4. However, once the synthetic route towards the fluoroalkenes has been established, introducing more hydrophilic groups onto the triazolo ring, or into the fluorobromostyrene coupling partner could lower the ClogP.

Fluoroalkenes can be synthesised by a range of methods in small molecules including olefination reactions, the Shapiro reaction and metal-catalysed coupling reactions with stannanes, silanes and boronic acids.[49] These reactions do not typically give good diastereoselectivity with the exception of the Shapiro reaction.[49] Initially the Shapiro reaction was chosen as the method for synthesising the fluoroalkene because of its reported diastereoselectivity (dr >5.5:1). However, no straightforward and short routes to install the required 3-phenylpropanone group onto pyridine or pyrazine were found. It was then decided that pursuing high diastereoselectivity was less important than a short synthetic route as diastereoisomers could hopefully be separated and it would in any case be instructive to compare their biological activities. A new route was chosen to create the fluoroalkene using a Suzuki coupling between a halopyridyl boronic acid or ester and bromofluorostyrene (Scheme 4.10).

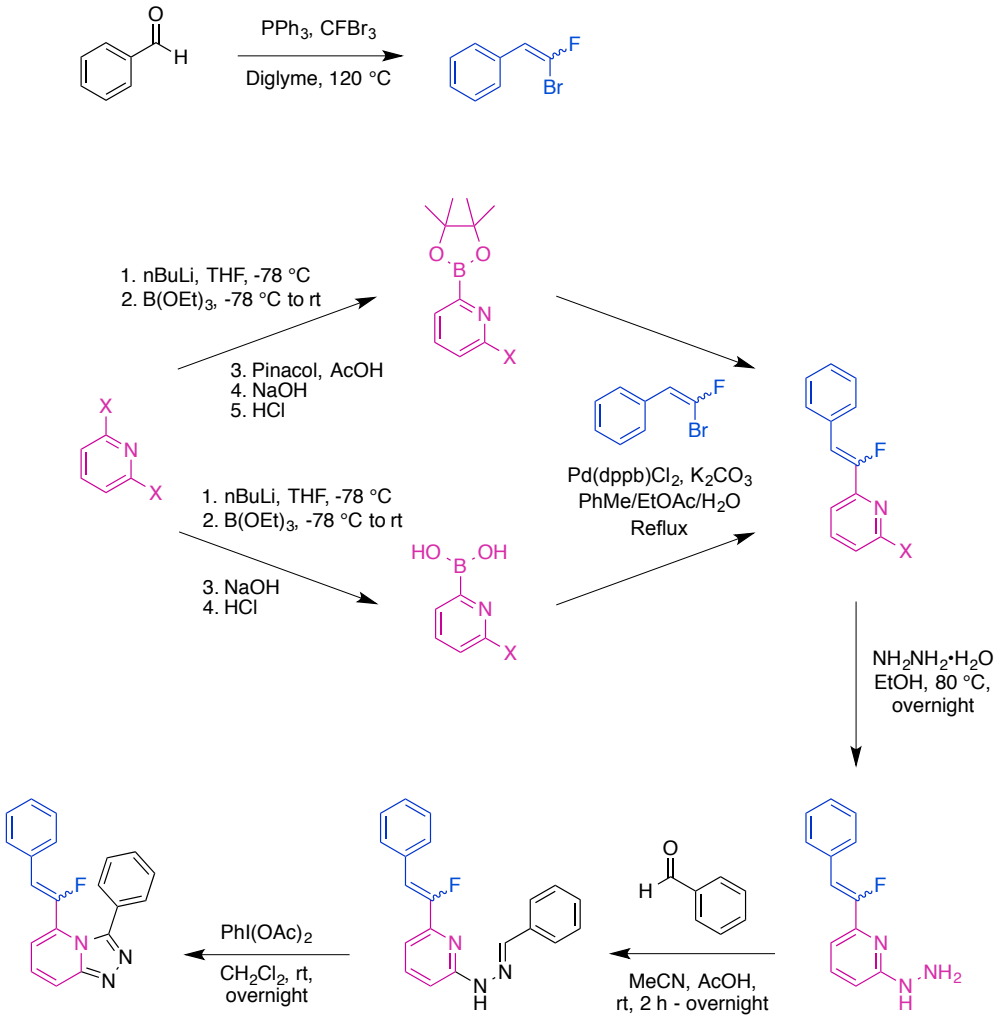

Scheme 4.10: Proposed synthetic route towards the fluoroalkene triazolopyrazine **44**.

This method was selected because it is only two steps longer than the synthesis of the ether compounds, providing a reasonably short route. The synthesis of the fluoroalkene triazolopyrazine begins with the formation of bromofluorostyrene (blue, Scheme 4.10). The procedure is well established and gram scale preparations are known and have been achieved.[68] In parallel to the formation of bromofluorostyrene is the synthesis of the halopyridyl boronic acid and ester. Both the acid and the ester can be used in the subsequent Suzuki coupling reaction. Synthesis of the halopyridyl boronic acid and ester have previously been reported, although yields were ~50%.[69] Despite this boronic acids and esters are less toxic than organostannanes and are therefore a preferable coupling partner. If the syntheses of halopyridyl boronic acids or esters were successful then creation of pyrazinyl and triazolopyrazinyl boronic acids or esters would be attempted. Introduction of the fluoroalkene group onto the triazolopyrazine in the last step would be ideal as large quantities of different triazolopyrazine cores could be produced and diversified in the final step. The third step in the synthesis of the fluoroalkene is the Suzuki coupling between the halopyridyl boronic acid or ester and fluorobromostyrene. This exact reaction is not known however there are many similar.[50, 69] The final three steps are all common to the ether triazolopyrazine synthesis beginning with nucleophilic substitution with hydrazine, acid catalysed condensation with an aromatic aldehyde and lastly cyclisation with PIDA.

4.2.1 Synthesis of halopyridyl boronic acid and ester coupling partners

The first step in the creation of the fluoroalkene was to synthesise the halopyridyl boronic acid or ester coupling partner for the Suzuki coupling. Synthesis of the halopyridyl boronic acid was attempted first, using both 2,6-dichloropyridine (**46**) and 2,6-dibromopyridine (**47**) in separate attempts (Scheme 4.11).

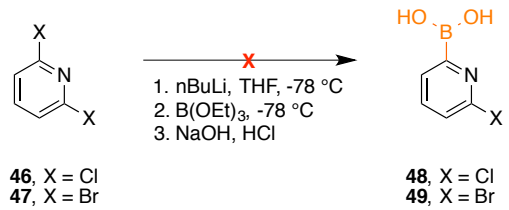

Scheme 4.11: The synthesis of the halopyridyl boronic acids **48** and **49** was unsuccessful.

The synthesis of **49** was unsuccessful despite a reported yield of 55%.[69] Synthesis of **48** from **46** was also unsuccessful but has not been reported under these conditions. Starting materials were not recovered from these reactions. Bromine is known to exchange preferentially over chlorine when 2-bromo-6-chloropyridine is used which could mean that chlorine does not exchange under these conditions. The ^{1}H NMR spectrum of the crude material for **48** and **49** showed a number of peaks in the aromatic region that did not correspond to those reported for the products, nor those determined for the two starting materials. Attempts at purification of the two crude materials by recrystallization from ether were also unsuccessful, the material was a sticky substance that did not dissolve. A possible explanation for the absence of **48** and **49** was given on one of the OSM websites by Dr Andrew Leach from Liverpool John Moores University.[70] His (unpublished) computational analysis of related compounds suggests that two pyridyl boronic acids form a cyclic complex with the pyridine nitrogen acting as a Lewis base, which is then subject to attack by water or free boronic acids. The computational data indicated that the barrier to protodeboronation was the lowest for 2-pyridyl boronic acids.[71] A halogen in the 2 or 6 position on the pyridine can increase the barrier to protodeboronation although not enough to prevent it from occurring.[71] To overcome this it was suggested that the corresponding pyridyl boronic ester should be made which may be more stable and resistant to protodeboronation.[70]

Synthesis of the bromopyridyl boronic ester (**50**) was successful using **47** with a yield of 36% (crude), less than the reported yield of 56% (pure, Scheme 4.12).[69] Purification was attempted according to the literature[69] by washing with acetonitrile however the both the product and impurities dissolved and so the material was used crude in the subsequent Suzuki coupling reaction due to time constraints. The lower yield can be attributed to the use of triethylborate instead of triisopropyl borate; the latter is suggested to form a more stable intermediate.[69]

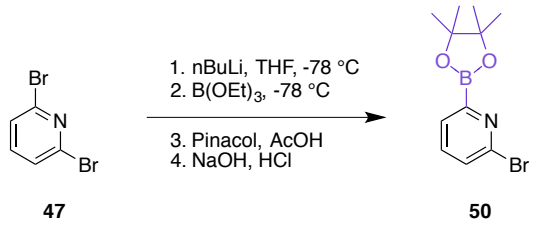

Scheme 4.12: Synthesis of the bromopyridyl boronic ester **50** from **47** proceeded as expected.

Synthesis of the corresponding chloropyridyl boronic ester from **46** was also attempted, however no evidence of this product could be found in the ^{1}H NMR spectrum of the crude product.

4.2.2 Synthesis of the bromofluorostyrene coupling partner

Bromofluorostyrene (**51**) is the second coupling partner for the synthesis of the fluoroalkene. Synthesis of **51** was *via* the creation of a Wittig reagent with triphenylphosphine and tribromofluoromethane followed by addition of the carbene to benzaldehyde (Scheme 4.13).[68]

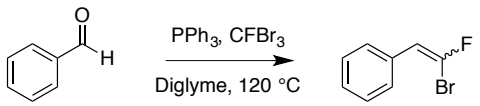

51

Scheme 4.13: Synthesis of the bromofluorostyrene **51** in a Wittig reaction.

The reaction proceeded to give a 2% yield (crude) of a mixture of the (*E*)- and (*Z*)-isomers of **51**. The vinylic proton adjacent to fluorine appears as a doublet and this proton provides a peak in the ^{1}H NMR spectrum with a different chemical shift and hydrogen-fluorine coupling constant: the proton in the (*E*)-isomer gave a peak at 5.98 ppm with a coupling constant of J_{HF} = 32.8 Hz, while the (*Z*)-isomer appeared further downfield at 6.67 ppm with a coupling constant of J_{HF} = 15.2 Hz which is in excellent agreement with the literature for both isomers.[68, 72] The reported yield for the standard preparation of **51** is 75% (mixture of (*E*)- and (*Z*)-isomers)[68] significantly higher than the 2% crude yield obtained. Purification of the product was attempted by vacuum distillation according to the literature[68] as well as by flash column chromatography, however pure compound was not obtained as during the distillation procedure the product was unintentionally lost into the Schlenk line and was contaminated with grease. Loss of product in the purification was not the cause of the low yield as determined by ^{1}H NMR spectroscopy. The low yield could be attributed to hydrolysis of the (fluorodibromomethyl)triphenylphosphonium bromide intermediate in the Wittig formation with water still present in the solvent or atmosphere.[73-74] Hydrolysis would

destroy the ylid, forming dibromofluoromethane instead of reacting with benzaldehyde to form **51**.[74]

4.2.3 Suzuki coupling of bromopyridyl boronic ester and geminal alkenes

The Suzuki cross coupling reaction is a common, facile method for forming new carbon-carbon bonds. Both **51** and halopyridyl boronic esters have been used as coupling partners successfully under Suzuki conditions,[50, 69] although there are no reports of their being coupled to each other in the literature. Halopyridyl boronic acids and esters have been coupled to aryl halides using tertrakis(triphenylphosphine)palladium (0)[69] and halopyridines have been coupled to phenyl boronic acids with 1,4-bis(diphenylphosphino)butane-palladium (II) chloride.[75]

A model coupling reaction was carried out first between the readily available starting material β-bromostyrene (**52**, mixture of (*E*)- and (*Z*)-isomers) and the **49** using Pd(dppb)Cl_2 to form **53** (Scheme 4.14).

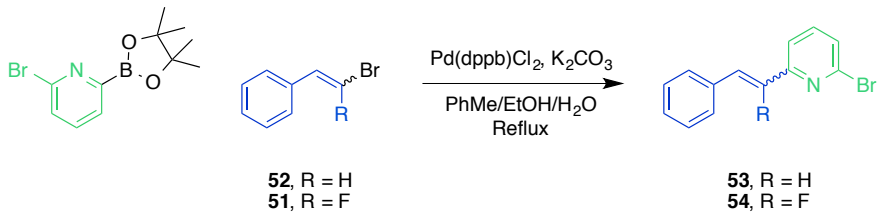

Scheme 4.14: Suzuki coupling between **49** and β-bromostyrene (**52**) or bromofluorostyrene (**51**) to form **53** and **54**.

The reaction proceeded to give a yield of 22% of **53** (crude, mixture of isomers) after purification by flash chromatography. Analysis of the crude material by HRMS gave the mass corresponding to **53**, indicating that formation of the product was successful.

Following the confirmation of the formation of **53** by HRMS, synthesis of the fluoroalkene **54** was attempted with the **49** and **51** (Scheme 4.14). The reaction proceeded to give a yield of ~30% (crude, mixture of isomers) after purification by flash chromatography. HRMS analysis of **54** indicated the formation of the desired product. Analysis of the ^{1}H NMR spectrum also indicated that the product had been formed: the signals for the vinylic protons for what were assumed to be the (*E*)- and (*Z*)-isomers had

shifted downfield compared to **51**, and the hydrogen-fluorine coupling constants had increased slightly. The (*Z*)-isomer appeared at 7.12 ppm with a coupling constant of J_{HF} = 39.5 Hz, while the (*E*)-isomer could be one of two doublets at 6.73 ppm with a coupling constant of J_{HF} = 23.0 Hz or at 6.70 ppm with a coupling constant of J_{HF} = 22.5 Hz. These are close to those reported for analogues of β-fluorostilbene.[50]

The next step towards the synthesis of the fluoroalkene **44** would be to attempt the Suzuki coupling of **49** to **51** and **52** on a larger scale following improvements to the syntheses of these two coupling partners. This would allow for the purification and full characterisation of **53** and **54** and demonstrate the viability of the synthetic route. The Suzuki coupling should also be undertaken using $Pd(PPh_3)_4$ as the catalyst to compare yields with those obtained using $Pd(dppb)Cl_2$ as suggested in the literature.[69] Following the validation of the route towards **54**, an attempt to build the triazolopyrazine core onto this compound can be made. The first step is displacement of the bromine with hydrazine[76] followed by acid catalysed condensation with an aromatic aldehyde and oxidative cyclisation to form the final fluoroalkene triazolopyrazine (**44**).

5. Conclusions and Future Work

This work reports the synthesis of a new set of substituted triazolopyrazines, and their biological activity against *P. falciparum*. The triazolopyrazines have not been published in the literature before and limited unpublished data were inherited at the start of the project.

The synthetic route towards the ether triazolopyrazines was validated, further developed and optimised. That the chemistry is now reproducible and robust greatly helps the future development of this series by the wider community. In particular the final step in the synthesis, the S_N2 displacement, was extensively developed and gave moderate yields for a range of substrates and nucleophiles. The compounds and their intermediates were fully characterised providing a full set of data for these compounds. Future studies could include the development of a one pot reaction to form the hydrazone intermediate from the 2,6-dichloropyrazine (**20**) starting material to shorten the synthetic route. The S_N2 displacement could also be optimised to improve yields of the final ether triazolopyrazine products and expanded to include new functional groups such as secondary amines. An NMR assay could be designed to follow the displacement reaction and determine the influence of nucleophilicity on the rate of reaction.

A small library of ether triazolopyrazines and close analogues was synthesised using the validated route. The potencies of these compounds were determined against *P. falciparum* and one of the more promising compounds, **29**, was sent for evaluation against the hERG ion channel. The compounds displayed activities ranging from inactive to 0.281 μM and the data increases our understanding of the SAR of the series. Future work should continue to address the poor solubility and metabolic stability issues of the series. The metabolic weakness in the triazolopyrazines is still unknown; results from an aldehyde oxidase assay (an enzyme thought to be metabolizing the compounds[77]) are needed before new analogs to address the issues can be designed. The solubility of the series could be improved by modifications such as the addition of acidic groups in the side chains (**55**), incorporating amines on the aromatic rings (**56**) or by re-attempting synthesis of compound **41** (Figure 5.1).

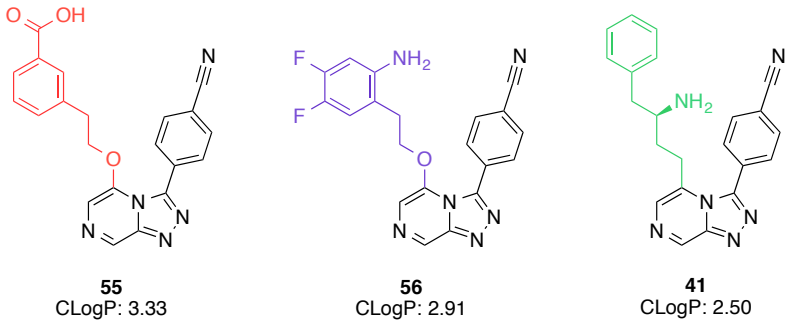

Figure 5.1: Three example compounds to address solubility issues within Series 4. The benzonitrile substituent on the triazole ring is for easy comparison of the three compounds.

A new analogue for the amide triazolopyrazines was designed; the fluoroalkene triazolopyrazine. A synthetic route was designed for the fluoroalkenes and partially validated with results suggesting that the installation of the fluoroalkene functional group onto a pyridyl boronic ester using Suzuki coupling conditions was feasible. Further experimental studies should begin by optimising the chemistry demonstrated so far to validate the route and obtain enough material to synthesise the final fluoroalkene triazolopyrazine (**44**) for biological testing. Analogues of these compounds could then be explored. The introduction of alternate aromatic aldehydes into the synthesis of the bromofluorostyrene could be attempted such as a pyridyl (**57**) or chloro group (**58**), or by using a phenylacetaldehyde (**59**) to lengthen the chain (Figure 5.2). The triazolo substituent could also be altered using the validated chemistry in the synthesis of the triazolopyrazine core.

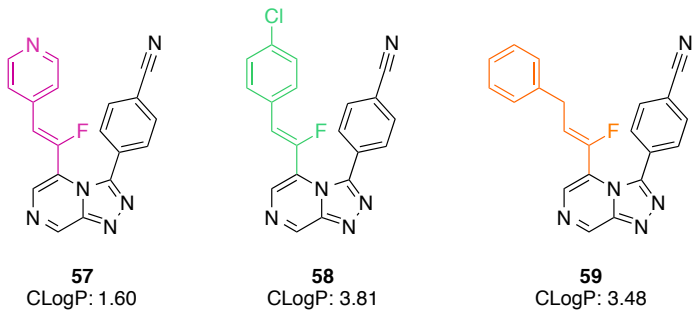

Figure 5.2: Three example compounds to diversify the fluoroalkene analogues.

The triazolopyrazines are an exciting new set of compounds with promising anti-malarial activity against *P. falciparum*. With the validation of their synthetic route, new compounds to optimise the potency and pharmacokinetic properties of the series can now be made with relative ease. New anti-malarial compounds with novel mechanisms of action are needed now more than ever, so the continued exploration of the triazolopyrazines is of utmost importance.

6. Experimental Details

The ELN is online at **http://malaria.ourexperiment.org/triazolopyrazine_se**. It will be archived following examination of this thesis in the University of Sydney repository to ensure preservation of all data.

6.1 General experimental details

Reagents were purchased from Sigma-Aldrich, Alfa Aesar, Merck, Apollo Scientific and AK Scientific. Reagents were used without further purification. Anhydrous reactions were performed in oven-dried glassware (>130 °C, overnight) that was cooled under high vacuum and flushed with nitrogen or argon gas. Anhydrous solvents were dried using an Innovative technology Pure Solv or over 3 Å molecular sieves (1.5–2.5 mm) activated by microwave. High temperature reactions were performed in a silicone oil bath and controlled by a temperature probe in the bath. Reactions at -78 °C were performed in a dry ice/acetone bath. Reduced pressure refers to rotary evaporation at 40 °C from 900–20 mbar and *in vacuo* refers to ~1 mbar on a schlenk line. Nitrogen gas was dried over calcium chloride. Argon gas was used Thin layer chromatography (TLC) was performed on Silica gel 60 F_{254} aluminium plates and visualised under UV light (254 nm) or by staining with anisaldehyde, vanillin or permanganate. Flash chromatography was performed on Davisil Grace Davison 40–63 µm (230–400 mesh) silica gel or on a Biotage Isolera One.

6.2 General analytical and preparative instrumentation and notation

Melting points were determined using a Stanford Research Systems OptiMelt at 1 °C min^{-1}. Infrared spectroscopy was performed on a Bruker Alpha-E. Samples were analysed as films prepared by dissolving in acetone and evaporating the solvent. Spectra were processed using OPUS 7 software. Nuclear magnetic resonance spectroscopy was performed on Bruker spectrometers at 300 K. Spectrometers used were an AVANCE 200 (^{1}H at 200 MHz), AVANCE 300 (^{1}H at 300 MHz, ^{13}C at 75 MHz), AVANCE III 400 with 5 mm broadband observe nitrogen cooled cryo probe (^{1}H at 400 MHz, ^{13}C at 101 MHz) and AVANCE III 500 (^{1}H at 500 MHz, ^{13}C at 126 MHz). Deuterated solvents ($CDCl_3$, DMSO-*d6*) were purchased from the Cambridge Isotope Laboratories. Spectra

were processed using MestReNova-LITE or Bruker Topspin software. Calibration of the spectra was to residual solvent peaks (^{1}H: $CHCl_3$ 7.26 ppm, DMSO 2.50 ppm; ^{13}C: $CHCl_3$ 77.23 ppm, DMSO 39.51 ppm) and chemical shifts are reported with respect to these values. The multiplicity of ^{1}H signals were reported as: s = singlet, d = doublet, t = triplet, q = quartet, dd = doublet of doublets, td = triplet of doublets, m = multiplet, app = apparent. Broad signals were reported as b = broad.

6.3 Procedures and characterisation for anti-malarial ether analogues

6.3.1 2-Chloro-6-hydrazinylpyrazine 21

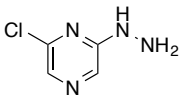

This procedure was adapted from the CRO method.[23] To a stirred solution of 2,6-dichloropyrazine (**20**, 1.0 g, 6.7 mmol) in ethanol (10 mL) was added hydrazine hydrate (0.35 mL, 360 mg, 7.2 mmol) dropwise. The reaction mixture was heated at reflux (oil bath temperature 80 °C) overnight. The crude material was concentrated under reduced pressure and dried *in vacuo* to yield pale yellow fluffy needles (1.19 g, 122%) which were used in subsequent reactions without further purification; mp 130–131 °C; ν_{max} (film)/cm^{-1} 3210, 3075, 1566, 1544; δ_H (200 MHz; DMSO-*d6*) 8.04 (s, 1 H), 7.72 (s, 1 H), 6.74 (b, 1 H), 4.39 (b, 2 H); *m/z* (APCI) 145 (MH^+, 100%). The data was consistent with the literature.[55]

6.3.2 2-Chloro-6-phenethoxypyrazine 27

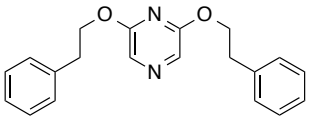

This procedure was adapted from the literature.[60] To a stirred solution of phenethyl alcohol (100 mg, 0.8 mmol, 1.0 equiv.) and 2,6-dichloropyrazine (**20**, 140 mg, 0.9 mmol, 1.1 equiv.) in toluene (1.6 mL) was added potassium hydroxide (170 mg, 3.0 mmol, 3.7 equiv.) and 18-crown-6 (10 mg, 0.04 mmol, 0.050 equiv.). The reaction mixture was heated at reflux (oil bath temperature 110 °C) for 4.5 h and allowed to cool. The mixture was diluted with water (4 mL) and the aqueous fraction was extracted with ethyl acetate (4 × 3 mL). The combined organic fractions were washed with water until neutral followed by brine (3 mL). The organic fractions were dried (Na_2SO_4), concentrated under reduced pressure and dried *in vacuo*. The crude material was a pale yellow oil and was purified by flash chromatography (50–100% ethyl acetate/hexanes) to yield the title compound as a pale yellow oil (85 mg, 68%); ν_{max} (film)/cm^{-1} 3062, 3028, 2954, 1581, 1421, 1182; δ_H

(200 MHz; $CDCl_3$) 7.75 (s, 2 H), 7.30–7.23 (m, 10 H), 4.48 (t, J = 7.2 Hz, 4 H), 3.08 (t, J = 7.2 Hz, 4 H); δ_C (101 MHz; $CDCl_3$) 158.8, 138.0, 129.2, 128.8, 126.8, 124.4, 67.2, 35.6; *m/z* (APCI) 321 (MH^+, 100%); HRMS (APCI) 321.15975 ($[M+H]^+$), calcd. for $C_{20}H_{21}N_2O_2^+$ 321.15975.

6.3.3 General Synthetic Procedure A: Hydrazone Formation

This procedure was adapted from the CRO method.[23] Compounds **22**, **25**, **34** and **37** (part 1) were prepared using this procedure. To a stirred solution of **21** (crude, 1 equiv.) and acetic acid (glacial, 1 equiv.) in acetonitrile (to 0.60 M of **21**) was added the appropriate aldehyde (1 equiv.). The reaction mixture was stirred at rt for 2.5–36 h until complete by TLC (30% ethyl acetate/hexanes). The reaction was concentrated under reduced pressure and dried *in vacuo* to give the crude material and used as crude in the subsequent reaction or subjected to the stated purification by flash chromatography over silica.

6.3.4 4-((2-(6-Chloropyrazin-2-yl)hydrazono)methyl)benzonitrile 22

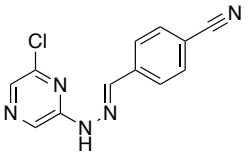

21 (crude, 1.68 g, ~12.0 mmol, 1 equiv.) and 4-formylbenzonitrile (1.52 g, 11.6 mmol, 1 equiv.) were reacted according to General Synthetic Procedure A. The crude material was a pale orange powder (3.04 g, 102%) and was used in subsequent steps without purification; mp 191–193 °C; ν_{max} (film)/cm^{-1} x; δ_H (200 MHz; DMSO-*d6*) 11.91 (s, 1 H), 8.64 (s, 1 H), 8.12 (s, 1 H), 8.11 (s, 1 H), 7.96–7.84 (m, 4 H); δ_C (101 MHz; DMSO-*d6*) 152.0, 145.5, 140.6, 139.0, 133.1, 132.6, 129.1, 127.1, 118.8, 111.1; *m/z* (APCI) 258 (MH^+, 100%); HRMS (ESI) 258.05406 ($[M+H]^+$), calcd. for $C_{12}H_9N_5Cl^+$ 258.05410.

6.3.5 2-Chloro-6-(2-(4-chlorobenzylidene)hydrazinyl)pyrazine 25

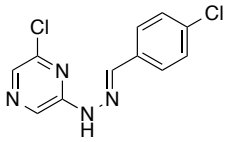

21 (crude, 2.51 g, ~17.0 mmol, 1.0 equiv.) and 4-chlorobenzaldehyde (1.95 g, 13.9 mmol, 0.8 equiv.) were reacted according to General Synthetic Procedure A to give the crude material as a pale yellow powder (3.89 mg, 105%); mp 224–226 °C; ν_{max} (film)/cm^{-1} 3026, 1582; δ_H (300 MHz; DMSO-*d6*) 11.63 (s, 1 H), 8.58 (s, 1 H), 8.06 (s, 1 H), 8.05 (s, 1 H), 7.77 (d, *J* = 8.7, 2 H), 7.48 (d, *J* = 8.4, 2 H); δ_C (75 MHz; DMSO-*d6*) 152.2, 145.5, 141.3, 133.8, 133.4, 132.6, 131.0, 128.8, 128.2; HRMS (ESI) 267.01999 ([M+H]$^+$), calcd. for $C_{11}H_9Cl_2N_4^+$ 267.01988.

6.3.6 2-Chloro-6-(2-(pyridin-4-ylmethylene)hydrazinyl)pyrazine 34

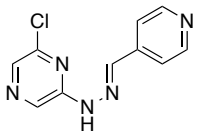

21 (crude, 1.0 g, ~7.0 mmol, 1.0 equiv.) and 4-pyridinecarboxaldehyde (0.65 mL, 740 mg, 6.9 mmol, 1.0 equiv.) were reacted according to General Synthetic Procedure A. The crude material was a bright yellow powder (1.97 g, 122%) and was purified by flash chromatography (Biotage isolera, 40-90% ethyl acetate/hexanes/1% TEA) to give the title compound as a pale yellow powder (377 mg, 23%); mp 254–256 °C; ν_{max} (film)/cm^{-1} 3188, 3035, 2971, 1586, 1561, 1417; δ_H (200 MHz; DMSO-*d6*) 11.89 (b, 1 H), 8.66 (s, 1 H), 8.62–8.59 (m, 2 H), 8.13 (s, 1 H), 8.03 (s, 1 H) 7.71–7.68 (m, 2 H); δ_C (75 MHz; DMSO-*d6*) 153.0, 151.1, 146.5, 142.5, 140.8, 134.3, 130.1, 121.5; *m/z* (APCI) 234 (MH$^+$, 100%); HRMS (ESI) 234.05414 ([M+H]$^+$), calcd. for $C_{10}H_9ClN_5^+$ 234.05410.

6.3.7 General Synthetic Procedure B: Oxidative Cyclisation of Hydrazones

This procedure was adapted from the CRO method.[23] Compounds **23**, **26**, **35** and **37** were prepared using this procedure. To a stirred solution of a hydrazone (crude or pure, 1 equiv.) in dichloromethane (to 60 mM of hydrazone) was added phenyliodine diacetate (1 equiv.). The reaction mixture was stirred at room temperature for 2–36 h until complete by TLC (30% ethyl acetate/hexanes). The reaction was stopped and the organic layer washed with a solution of saturated $NaHCO_3$. The inorganic layer was extracted with dichloromethane (3–6 times). The organic fractions were dried ($MgSO_4$), concentrated under reduced pressure and *in vacuo*. The crude material subjected to the stated purification by flash chromatography over silica

6.3.8 4-(5-Chloro-[1,2,4]triazolo[4,3-a]pyrazin-3-yl)benzonitrile 23

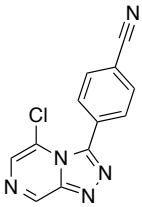

22 (crude, 2.0 g, ~8 mmol) was reacted according to General Synthetic Procedure B. Purification (Biotage isolera, 50–100% ethyl acetate/hexanes) gave the title compound as an orange powder (1.14 g, 56%); mp 226–227 °C; ν_{max} (film)/cm^{-1} 3089, 2228, 1597; δ_H (200 MHz; DMSO-*d6*) 9.53 (s, 1 H), 8.14 (s, 1 H), 8.08–7.93 (m, 4 H); δ_C (75 MHz; DMSO-*d6*) 147.1, 146.1, 142.7, 132.3, 132.0, 131.6, 129.4, 121.9, 118.4, 113.1; *m/z* (APCI) 256 (MH$^+$, 100%); HRMS (ESI) 256.03845 ([M+H]$^+$), calcd. for $C_{12}H_7N_5Cl^+$ 256.03845.

6.3.9 5-Chloro-3-(4-chlorophenyl)-[1,2,4]triazolo[4,3-a]pyrazine 26

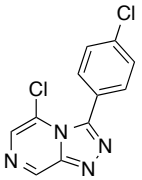

25 (pure, 250 mg, 0.94 mmol) was reacted according to General Synthetic Procedure B. Purification (Biotage isolera, 7–85% ethyl acetate/hexanes) gave the title compound as pale yellow crystals (207 mg, 83%); mp 172–173 °C; ν_{max} (film)/cm^{-1} 3089, 1601, 1465; δ_H (200 MHz; $CDCl_3$) 9.35 (s, 1 H), 7.89 (s, 1 H), 7.56–7.49 (m, 4 H); δ_C (101 MHz; DMSO-*d6*) 147.1, 146.5, 142.7, 135.5, 133.2, 129.3, 127.9, 126.2, 121.9; *m/z* (APCI) 265 (MH$^+$, 100%); HRMS (ESI) 265.00440 ([M+H]$^+$), calcd. for $C_{11}H_7Cl_2N_4^+$ 265.00423.

6.3.10 5-Chloro-3-(pyridin-4-yl)-[1,2,4]triazolo[4,3-a]pyrazine 35

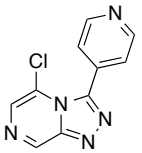

34 (550 mg, 2.4 mmol) was reacted according to General Synthetic Procedure B. Purification (Biotage isolera, 60–100% ethyl acetate/hexanes) gave the title compound as a pale yellow powder (406 mg, 75%); mp 165–167 °C; ν_{max} (film)/cm^{-1} 3036, 3003, 1593; δ_H (200 MHz; DMSO-*d6*) 9.54 (s, 1 H), 8.81–8.78 (m, 2 H), 8.16 (s, 1 H), 7.79–7.76 (m, 2 H); δ_C (101 MHz; DMSO-*d6*) 149.1, 147.2, 145.4, 142.7, 135.3, 129.5, 125.8, 121.9; *m/z* (APCI) 232 (MH$^+$, 100%); HRMS (APCI) 232.03834 ([M+H]$^+$), calcd. for $C_{10}H_7ClN_5^+$ 232.03845.

6.3.11 5-Chloro-3-(4-(difluoromethoxy)phenyl)-[1,2,4]triazolo[4,3-a]pyrazine 37

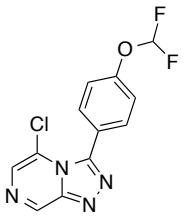

Prepared according to General Synthetic Procedures A and B. **21** (crude, 1.0 g, ~7.0 mmol, 1.0 equiv.) and 4-(difluoromethoxy)benzaldehyde (0.9 mL, 1.2 g, 7.0 mmol, 1.0 equiv.) were used to synthesise the hydrazone intermediate, **36**. The identity of the major product in the crude material (2.2 g, ~7 mmol, 104%) was verified by ^{1}H NMR spectroscopy (DMSO-*d6*) before carrying through to the next step without purification. **36** (crude, 2.01 g, ~7 mmol) was used in part B. Purification (30–100% ethyl acetate/hexanes) gave the title compound as brown plates (829 mg, 40%); mp 122–123 °C; ν_{max} (film)/cm^{-1} 3086, 1612, 1467, 1235, 1122, 1045; δ_H (400 MHz; DMSO-*d6*) 9.49 (s, 1 H), 8.09 (s, 1 H), 7.81–7.77 (m, 2 H), 7.41 (t, J_{HF} = 73.6 Hz, 1 H), 7.37–7.33 (m, 2 H); δ_C (101 MHz; DMSO-*d6*) 152.6, 147.1, 146.7, 142.8, 133.4, 129.2, 124.0, 121.9, 117.4, 116.2 (t, J_{CF} = 259 Hz); *m/z* (APCI) 297 (MH$^+$, 100%); HRMS (APCI) 297.03484 ([M+H]$^+$), calcd. for $C_{12}H_8ClF_2N_4O^+$ 297.03492.

6.3.12 General Synthetic Procedure C: S_N2 Displacement

This procedure was adapted from the literature.[60] Compounds **28**–**32** and **38**–**40** were prepared using this procedure. To a stirred solution of the appropriate alcohol, amine or thiol (1.0–1.2 equiv.) and the appropriate triazolopyrazine (1.0 equiv.) in toluene (to 0.40 M of triazolopyrazine) was added potassium hydroxide (3.3 equiv.) and 18-crown-6 (0.050 equiv.). The reaction mixture was heated at 40 °C (bath temperature) for 1–2 h and allowed to cool to rt. The mixture was diluted with water and the aqueous fraction was extracted with ethyl acetate. The combined organic fractions were washed with water until neutral (pH 10 for the amines) followed by brine. The organic fractions were dried (Na_2SO_4), concentrated under reduced pressure and dried *in vacuo*. The crude material was purified by flash chromatography over silica to yield the title compounds.

6.3.13 4-(5-Phenethoxy-[1,2,4]triazolo[4,3-a]pyrazin-3-yl)benzonitrile 28

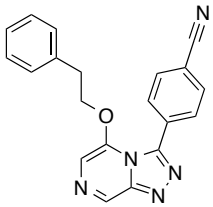

Phenethyl alcohol (60 µL, 60 mg, 0.5 mmol, 1.2 equiv.) and **23** (96 mg, 0.4 mmol, 1.0 equiv.) were reacted according to General Synthetic Procedure C. Purification (manual, 50–100% ethyl acetate/hexanes) gave the title compound as pale brown needles (33 mg, 26%); mp 142–143 °C; ν_{max} (film)/cm^{-1} 3063, 2228, 1610, 1507, 1297; δ_H (400 MHz; DMSO-*d6*) 9.09 (s, 1 H), 7.94–7.89 (m, 4 H), 7.67 (s, 1 H), 7.19–7.18 (m, 3 H), 6.92–6.90 (m, 2 H), 4.54 (t, 2 H, *J* = 6.4 Hz), 2.89 (t, 2 H, *J* = 6.4 Hz); δ_C (101 MHz; DMSO-*d6*) 147.6, 144.9, 143.9, 137.2, 134.9, 132.4, 131.5, 131.5, 128.7, 128.2, 126.4, 118.6, 112.2, 109.3, 71.1, 33.7; *m/z* (APCI) 342 (MH$^+$, 100%); HRMS (ESI) 342.13477 ([M+H]$^+$), calcd. for $C_{20}H_{16}N_5O^+$ 342.13494.

6.3.14 4-(5-(2-Chlorophenethoxy)-[1,2,4]triazolo[4,3-a]pyrazin-3-yl)benzonitrile 29

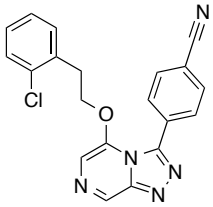

2-Chlorophenethyl alcohol (60 µL, 60 mg, 0.4 mmol, 1 equiv.) and **23** (107 mg, 0.4 mmol, 1 equiv.) were reacted according to General Synthetic Procedure C. Purification (manual, 50–100% ethyl acetate/hexanes) gave the title compound as pearlescent cream needles (78 mg, 53%); mp 183–185 °C; ν_{max} (film)/cm^{-1} 2229, 1611, 1507, 1369, 1298; δ_H (400 MHz; DMSO-*d6*) 9.10 (s, 1 H), 7.87–7.81 (m, 4 H), 7.72 (s, 1 H), 7.40 (dd, *J* = 8.0, 1.2 Hz, 1 H), 7.24 (td$_{app}$, *J* = 7.7, 1.7 Hz, 1 H), 7.13 (td$_{app}$, *J* = 7.5, 1.3 Hz, 1 H), 6.90 (dd, *J* = 7.7, 1.6 Hz, 1 H), 4.58 (t, *J* = 6.4 Hz, 2 H), 2.99 (t, *J* = 6.4 Hz, 2 H); δ_C (101 MHz; DMSO-*d6*) 147.6, 144.9, 143.8, 135.1, 134.4, 133.1, 132.4, 131.4, 131.3, 130.3, 129.2, 128.5, 127.1, 118.5, 112.2, 109.3, 68.9, 31.3; *m/z* (APCI) 376 (MH$^+$, 100%); HRMS (ESI) 376.09585 ([M+H]$^+$), calcd. for $C_{20}H_{15}ClN_5O^+$ 376.09596.

6.3.15 4-(5-(Phenethylthio)-[1,2,4]triazolo[4,3-a]pyrazin-3-yl)benzonitrile 30

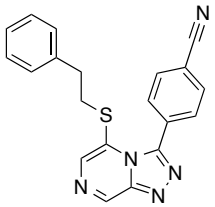

Phenylethyl mercaptan (60 µL, 60 mg, 0.4 mmol, 1 equiv.) and **23** (103 mg, 0.4 mmol, 1 equiv.) were reacted according to General Synthetic Procedure C. Purification (manual, 50–100% ethyl acetate/hexanes) gave the title compound as pearlescent cream stars (55 mg, 38%); mp 237–238 °C; ν_{max} (film)/cm^{-1} 2324, 1450, 1273; δ_H (500 MHz; DMSO-*d6*) 8.43 (d, *J* = 5.0 Hz, 1 H), 8.16–8.10 (m, 4 H), 7.89 (d, *J* = 5.0 Hz, 1 H), 7.34–7.23 (m, 5 H), 3.61 (t_{app}, *J* = 8.0, 7.5 Hz, 2 H), 3.06 (t, *J* = 7.5 Hz, 2 H); δ_C (126 MHz; DMSO-*d6*) 153.1, 146.4, 144.1, 139.9, 133.2, 130.1, 129.9, 129.0, 128.6, 128.4, 126.4, 118.3, 113.5, 112.8, 54.9, 34.4; *m/z* (APCI) 358 (MH^+, 100%); HRMS (ESI) 358.11199 ($[M+H]^+$), calcd. for $C_{20}H_{16}N_5S^+$ 358.11209.

6.3.16 4-(5-((3-Chlorophenethyl)amino)-[1,2,4]triazolo[4,3-a]pyrazin-3-yl)benzonitrile 31

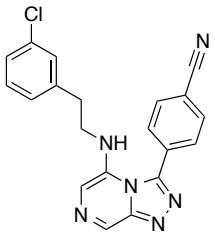

2-(3-Chlorophenyl)ethylamine (0.06 µL, 67 mg, 0.43 mmol, 1.1 equiv) and **23** (101 mg, 0.39 mmol, 1.0 equiv) were reacted together according to General Synthetic Procedure C. Purification (Biotage isolera, 17–100% ethyl acetate/hexanes) gave the title compound as a cream powder (25 mg, 17%); mp 246–248 °C; ν_{max} (film)/cm^{-1} 3250, 2923, 2227, 1573; δ_H (400 MHz; DMSO-*d6*) 8.40 (t, *J* = 5.6 Hz, 1 H), 8.14–8.08 (m, 4 H), 7.85 (d, *J* = 4.8 Hz, 1 H), 7.41 (d, *J* = 4.8 Hz, 1 H), 7.37–7.23 (m, 4 H), 3.75 (q_{app}, *J* = 6.8, 6.4 Hz, 2 H), 2.99 (t, *J* = 7.6 Hz, 2 H); δ_C (101 MHz; DMSO-*d6*) 161.1, 147.9, 146.5, 142.2, 141.9, 139.9, 133.2, 132.9, 130.7, 130.6, 130.2, 128.7, 128.6 127.5, 126.1, 118.4, 112.5, 106.3; *m/z* (APCI) 375 (MH^+, 100%); HRMS (ESI) 375.11174 ($[M+H]^+$), calcd. for $C_{20}H_{16}ClN_6^+$ 375.11195.

6.3.17 N-(3-chlorophenethyl)-3-(4-chlorophenyl)-[1,2,4]triazolo[4,3-a]pyrazin-5-amine 32

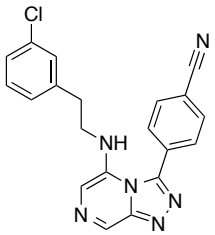

2-(3-Chlorophenyl)ethylamine (50 µL, 56 mg, 0.36 mmol, 1.0 equiv.) and **26** (103 mg, 0.39 mmol, 1.1 equiv.) were reacted together according to General Synthetic Procedure C. Purification (Biotage isolera, 12–100% ethyl acetate/hexanes) gave the title compound as a cream powder (46 mg, 33% yield); mp 191–193 °C; ν_{max} (film)/cm^{-1} 3248, 3111, 2917, 2034, 1975, 1613, 1582; δ_H (400 MHz; DMSO-*d6*) 8.35 (t, *J* = 5.6 Hz, 1 H), 7.94–7.91 (m, 2 H), 7.77 (d, *J* = 4.8 Hz, 1 H), 7.71–7.67 (m, 2 H), 7.37–7.23 (m, 5 H), 3.75 (m, 2 H), 2.99 (t, *J* = 7.1 Hz, 2 H); δ_C (101 MHz; DMSO-*d6*) 147.9, 146.8, 142.2, 139.7, 135.0, 132.9, 130.3, 130.2, 129.9, 129.4, 128.6, 127.5, 126.1, 125.1, 106.1, 41.2, 33.9; *m/z* (APCI) 384 (MH^+, 100%); HRMS (ESI) 384.07772 ($[M+H]^+$), calcd. for $C_{19}H_{16}ClN_5^+$ 384.07773.

6.3.18 3-(4-Chlorophenyl)-5-((3,4-difluorobenzyl)oxy)-[1,2,4]triazolo[4,3-a]pyrazine 38

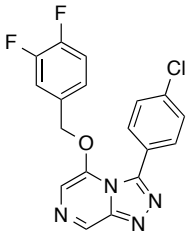

Part 1 of this procedure was adapted from a procedure developed by Ms Katrina Badiola.[78] To a dry flask was added 3,4-difluorobenzaldehyde (0.4 mL, 520 mg, 3.7 mmol, 1.0 equiv.) and tetrahydrofuran (10 mL). The mixture was cooled in an ice bath (0 °C) under argon. Sodium borohydride (500 mg, 13.0 mmol, 3.5 equiv.) was added carefully in portions. The reaction mixture was stirred for 15 min on ice before warming to room temperature and stirring for a further 25 min. The solution was adjusted to pH 7 with hydrochloric acid (1 M) and extracted with dichloromethane (3 × 15 mL). The combined organic fractions were dried ($MgSO_4$) and concentrated under reduced pressure and dried *in vacuo* to give the crude material ((3,4-difluorophenyl)methanol) as a pale yellow oil (620 mg, 116%). The identity of the crude material was verified by ^{1}H NMR ($CDCl_3$) and carried through to the next step without purification. (3,4-difluorophenyl)methanol (80 µL, 100 mg, 0.7 mmol, 1.2 equiv) and **26** (154 mg, 0.6 mmol, 1.0 equiv) were reacted together according to General Synthetic Procedure C. Purification (Biotage isolera, 30–100% ethyl acetate/hexanes) gave the title compound as fluffy white needles (86 mg, 38%); mp 181–182 °C; ν_{max} (film)/cm^{-1} 3070,

1612, 1509, 1303; δ_H (500 MHz; DMSO-*d6*) 9.11 (s, 1 H), 7.67 (s, 1 H), 7.66–7.64 (m, 2 H), 7.36–7.33 (m, 2 H), 7.13–7.05 (m, 3 H), 5.29 (s, 2 H); δ_C (126 MHz; DMSO-*d6*) 147.4, 145.4, 143.8, 135.4, 134.6, 132.4, 127.4, 126.7, 131.7 (2C), 125.4 (2C), 117.4, 117.3, 109.2, 70.9; *m/z* (APCI) 373 (MH^+, 100%), 345 (52%) 318 (23%); HRMS (APCI) 373.06609 ($[M+H]^+$), calcd. for $C_{18}H_{12}ClF_2N_4O^+$ 373.06622.

6.3.19 3-(4-(Difluoromethoxy)phenyl)-5-(3,4-difluorophenethoxy)-[1,2,4]triazolo[4,3-a]pyrazine 39

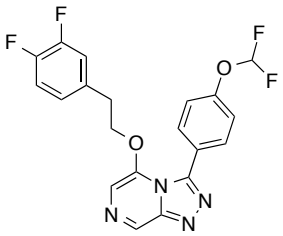

2-(3,4-Difluorophenyl)ethan-1-ol (98 mg, 0.62 mmol, 1.1 equiv.) and **37** (159 mg, 0.54 mmol, 1.0 equiv.) were reacted together according to General Synthetic Procedure C. Purification (Biotage isolera, 50–100% ethyl acetate/hexanes) did not yield pure product. The product was purified a second time by flash chromatography over silica (20% ethanol/hexanes) before recrystallisation from ethyl acetate (washed with cold methanol) to give the title compound as white needles (43 mg, 19%); mp 111–112 °C; ν_{max} (film)/cm^{-1} 3074, 2956, 1612, 1508, 1118, 1046; δ_H (200 MHz; DMSO-*d6*) 9.05 (s, 1 H), 7.79–7.73 (m, 2 H), 7.60 (s, 1 H), 7.36 (t, J_{HF} = 73.6 Hz, 1 H), 7.30–6.69 (m, 5 H), 4.51 (t, *J* = 6.2, 2 H), 2.90 (t, *J* = 6.2, 6.0 Hz, 2 H); δ_C (75 MHz; DMSO-*d6*) 151.9, 147.4, 146.4, 145.4, 143.8, 135.1, 132.5, 125.3 (2C), 124.7, 117.5, 117.3, 117.0, 116.9, 116.1 (t, J_{CF} = 256.7 Hz), 108.8, 70.6, 32.8; *m/z* (APCI) 419 (MH^+, 100%); HRMS (APCI) 419.11215 ($[M+H]^+$), calcd. for $C_{20}H_{15}F_4N_4O^+$ 419.11256.

6.3.20 5-(2-Chlorophenethoxy)-3-(pyridin-4-yl)-[1,2,4]triazolo[4,3-a]pyrazine 40

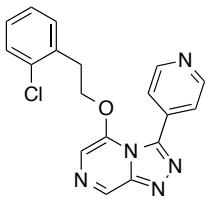

2-Chlorophenethyl alcohol (0.18 mL, 210 mg, 1.3 mmol, 1.0 equiv.) and **35** (300 mg, 1.3 mmol, 1.0 equiv.) were reacted together according to General Synthetic Procedure C. Purification (Biotage isolera, 15–80% ethanol/hexanes/1% TEA) gave the title compound as light brown plates (56 mg, 12%); mp 132–134 °C; ν_{max} (film)/cm^{-1} 2959, 2926, 1602, 1507, 1465, 1359, 1239, 824; δ_H (200 MHz; DMSO-*d6*) 9.11 (s, 1 H), 8.67–8.64 (m, 2 H), 7.75 (s, 1 H), 7.71–7.68 (m, 2 H), 7.41 (dd, *J* = 7.8, 7.6, 1.2, 1.0 Hz, 1 H), 7.24 (td_{app}, *J* = 7.8, 7.6, 7.4, 1.8, 1.6 Hz, 1 H) 7.14 (td_{app}, *J* = 7.4, 7.2, 1.2 Hz, 1 H) 6.90 (dd, *J* = 7.4, 1.6 Hz, 1 H), 4.58 (t, *J* = 6.6, 6.4 Hz, 2 H), 3.03 (t, *J* = 6.6, 6.4 Hz, 2 H); δ_C (75 MHz; DMSO-*d6*)

148.9, 147.7, 144.2, 143.6, 135.5, 135.0, 134.3, 133.1, 130.7, 129.3, 128.6, 127.2, 124.9, 109.5, 69.3, 31.4; *m/z* (APCI) 352 (MH^+, 100%) 324 (25%); HRMS (APCI) 352.09599 ($[M+H]^+$), calcd. for $C_{18}H_{15}ClN_5O^+$ 352.09596.

6.4 Procedures and characterisation for fluoroalkene synthesis

6.4.1 2-Bromo-6-(4,4,5,5-tetramethyl-1,3,2-dioxaborolan-2-yl)pyridine 50

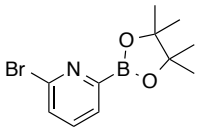

This procedure was adapted from the literature.[69] To a solution of ~1.7 M solution of *n*-BuLi (2.9 mL, ~5.0 mmol, ~1.2 equiv.) in freshly distilled tetrahydrofuran (40 mL) under argon, cooled to -78 °C, was added a solution of **47** (1.0 g, 4.2 mmol, 1.0 equiv.) in THF (20 mL). The reaction was stirred at -78 °C for 45 min. A solution of triethylborate (730 mg, 0.85 mL, 5.0 mmol, 1.2 equiv.) in THF (8 mL) was added and the dark mixture stirred at rt for 3 h. A solution of pinacol (670 mg, 5.7 mmol, 1.35 equiv) in THF (8 mL) was added, followed by glacial acetic acid (0.25 mL, 265 mg, 4.4 mmol, 1.05 equiv) after 5 min. The mixture was filtered through Celite™ and quenched by slow addition of 2.5% aqueous NaOH solution (100 mL). The aqueous layer was separated and acidified down to pH 6 by careful addition of 3M HCl, keeping the internal temperature below 5 °C. The solution was extracted with ethyl acetate (3 × 50 mL), dried ($MgSO_4$), concentrated under reduced pressure and dried *in vacuo*. The crude material was an orange solid (370 mg, 36%); mp 103-106 °C; ν_{max} (film)/cm^{-1} 2978, 2929, 1547, 1390, 1347, 1318, 1143, 1125, 1105; δ_H (500 MHz; DMSO-*d6*) 7.73–7.67 (m, 3 H), 1.31 (s, 12 H); *m/z* (GC-EI) 157 (MH^+-$BO_2C_6H_{12}$, 32%) 159 (MH^+-$BO_2C_6H_{12}$, 32%). This data was consistent with the literature.[69]

6.4.2 (2-Bromo-2-fluorovinyl)benzene 51

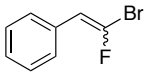

This procedure was adapted from the literature.[68] A dry 250 mL three neck flask fitted with a reflux condenser was flushed with nitrogen before adding triphenylphosphine (20.4 g, 78 mmol, 2.5 equiv.) and anhydrous diglyme (120 mL, dried over molecular sieves). The reaction mixture was heated to 70 °C before injecting tribromofluoromethane (8.4 g, 3.05 mL, 31 mmol, 1.0 equiv.). The solution turned yellow and a precipitate formed. At 90 °C benzaldehyde (3.29 g, 31 mmol, 1.0 equiv.) was added and the reaction was stirred at 120 °C for 3 h. The reaction was stopped and cooled to room temperature before transferring to a clean 500 mL flask. The product and diglyme were co-distilled with water (125 mL) at 90–102 °C (temperature at connection). The crude material was a pale yellow oil and was washed with water to remove the diglyme. The crude material was extracted with ether, dried ($MgSO_4$), concentrated under reduced pressure and dried *in vacuo*. It was distilled under vacuum (~0–1 mbar) at 40–46 °C (temperature at connection) to remove impurities. Purified was further attempted by flash chromatography (Biotage isolera, 100% hexanes) to obtain a mixture of isomers as a crude colourless oil (110 mg, 2%) in a 6:1 ratio of isomers; ν_{max} (film)/cm^{-1} 3211, 3092, 3063, 2954, 2924, 2854, 1719, 1648, 1495, 1449, 1044, 747, 691; δ_H (400 MHz; $CDCl_3$) 7.42–7.26 (m, 6 H), 6.67 (d, J_{HFcis} = 15.2 Hz, 0.16 H), 5.98 (d, $J_{HFtrans}$ = 32.8 Hz, 1 H); *m/z* (GC-EI) 200 (MH^+, 62%). This data was consistent with the literature.[68, 72]

6.4.3 2-Bromo-6-styrylpyridine 53

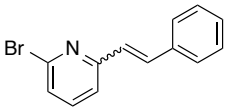

This procedure was adapted from the literature.[50] **52** (100 mg, 0.55 mmol, 1 equiv.), **50** (200 mg, 0.7 mmol, 1.3 equiv.), potassium carbonate (228 mg, 1.65 mmol, 3 equiv.) were stirred into toluene (7.5 mL), ethanol (1.5 mL) and water (1.5 mL). Argon was bubbled through to remove oxygen. 1,4-Bis(diphenylphosphino)butane-palladium(II) chloride (18 mg, 0.03 mmol, 0.05 equiv.) was added and the mixture heated at reflux overnight. The mixture was filtered through Celite™ (washed with ethyl acetate), dried ($MgSO_4$), and dried *in vacuo*. Clean product was not obtained following an initial purification by flash chromatography over silica (Biotage isolera, 20% ethyl acetate/hexanes). The crude material was bright yellow crystals (32 mg, 22%) as a 7:1 mixture of isomers. The following data was obtained and indicates the formation of the desired product: δ_H (500 MHz; $CDCl_3$) 7.67–7.27 (m, 11 H), 7.07 (d, J = 16.0 Hz, 1 H) 6.87 (d, J = 12.5 Hz, 0.14H); *m/z* (APCI) 260 (MH^+, 100%); HRMS (APCI) 260.00707 ($[M+H]^+$), calcd. for $C_{13}H_{11}BrN^+$ 260.00694.

6.4.4 2-Bromo-6-(1-fluoro-2-phenylvinyl)pyridine 54

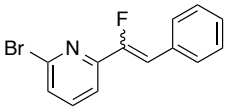

This procedure was adapted from the literature.[50] **51** (~20–30 mg, flask was washed out, ~0.1–0.15 mmol, 1 equiv.), **50** (85 mg, 0.3 mmol, 2 equiv), potassium carbonate (104 mg, 0.75 mmol, 6 equiv.) were stirred into toluene (3.75 mL), ethanol (0.75 mL) and water (0.75 mL). Argon was bubbled through to remove oxygen. 1,4-Bis(diphenylphosphino)butane-palladium(II) chloride (12 mg, 0.02 mmol, 0.2 equiv) was added and the mixture heated at reflux overnight. The mixture was filtered through Celite™ (washed with ethyl acetate), dried ($MgSO_4$), and dried *in vacuo*. Clean product was not obtained following an initial purification by flash column chromatography over silica (Biotage isolera, 20% ethyl acetate/hexanes). The crude material was bright yellow crystals (8 mg, 30%) as a 5:1 mixture of isomers. The following data was obtained and indicates the formation of the desired product: δ_H (500 MHz; $CDCl_3$) 7.76–7.31 (m, 15 H), 7.12 (d, J_{HF} = 39.5 Hz, 1 H), 6.73 (d, J_{HF} = 23.0 Hz, 0.2 H); *m/z* (APCI) 278 (MH^+, 68%); HRMS (APCI) 277.99759 ($[M+H^+]$), calcd. for $C_{13}H_{10}BrFN^+$ 277.99752.

7. References

1. Aspinall, A.; Diap, G.; Jagoe, G.; Kiechel, J. R.; Poll, E., From famine to feast: the transformation of the ACT malaria treatment landscape since 2004. *Africa Health* **2014,** *36*, 29–31.
2. Barrette, A.; Ringwald, P. *Global report on antimalarial drug efficacy and drug resistance: 2000–2010*; World Health Organisation: Switzerland, **2010**.
3. World Health Organisation, *World Malaria Report 2013*; France, **2013**. http://www.who.int/malaria/publications/world_malaria_report_2013/en/ (accessed 07/06/2014).
4. World Health Organisation. *Malaria*. http://www.who.int/mediacentre/factsheets/fs094/en/ (accessed 07/06/2014).
5. Burrows, J. N.; van Huijsduijnen, R. H.; Mohrle, J. J.; Oeuvray, C.; Wells, T. N. C., Designing the next generation of medicines for malaria control and eradication. *Malar. J.* **2013,** *12*, 20. DOI: 10.1186/1475-2875-12-187
6. Cox, F. E. G., History of the discovery of the malaria parasites and their vectors. *Parasites Vectors* **2010,** *3*, 9. DOI: 10.1186/1756-3305-3-5
7. Flannery, E. L.; Chatterjee, A. K.; Winzeler, E. A., Antimalarial drug discovery - approaches and progress towards new medicines. *Nat. Rev. Microbiol.* **2013,** *11*, 849–862. DOI: 10.1038/nrmicro3138
8. Cowman, A. F.; Berry, D.; Baum, J., The cellular and molecular basis for malaria parasite invasion of the human red blood cell. *J. Cell Biol.* **2012,** *198*, 961–971. DOI: 10.1083/jcb.201206112
9. Aly, A. S. I.; Vaughan, A. M.; Kappe, S. H. I., Malaria parasite development in the mosquito and infection of the mammalian host. In *Annual Review of Microbiology*, Annual Reviews: Palo Alto, **2009**; Vol. 63, pp 195–221.
10. Prudencio, M.; Rodriguez, A.; Mota, M. M., The silent path to thousands of merozoites: the Plasmodium liver stage. *Nat. Rev. Microbiol.* **2006,** *4*, 849–856. DOI: 10.1038/nrmicro1529
11. Burrows, J. N.; Burlot, E.; Campo, B.; Cherbuin, S.; Jeanneret, S.; Leroy, D.; Spangenberg, T.; Waterson, D.; Wells, T. N. C.; Willis, P., Antimalarial drug discovery - the path towards eradication. *Parasitology* **2014,** *141*, 128–139.

12. Rodrigues, T.; Prudencio, M.; Moreira, R.; Mota, M. M.; Lopes, F., Targeting the liver stage of malaria parasites: A yet unmet goal. *J. Med. Chem.* **2012,** *55*, 995–1012. DOI: 10.1021/jm201095h
13. Delves, M.; Plouffe, D.; Scheurer, C.; Meister, S.; Wittlin, S.; Winzeler, E. A.; Sinden, R. E.; Leroy, D., The activities of current antimalarial drugs on the life cycle stages of Plasmodium: A comparative study with human and rodent parasites. *PLos Med.* **2012,** *9*, 14. DOI: 10.1371/journal.pmed.1001169
14. World Health Organisation. Malaria Treatment. http://www.who.int/malaria/areas/treatment/en/ (accessed 22/06/2014).
15. White, N. J., Qinghaosu (artemisinin): The price of success. *Science* **2008,** *320*, 330–334. DOI: 10.1126/science.1155165
16. Noedl, H.; Se, Y.; Schaecher, K.; Smith, B. L.; Socheat, D.; Fukuda, M. M., Evidence of artemisinin-resistant malaria in western Cambodia. *N. Engl. J. Med.* **2008,** *359*, 2619–2620. DOI:10.1056/NEJMc0805011
17. Dondorp, A. M.; Nosten, F.; Yi, P.; Das, D.; Phyo, A. P.; Tarning, J.; Lwin, K. M.; Ariey, F.; Hanpithakpong, W.; Lee, S. J.; Ringwald, P. *et al.*, Artemisinin resistance in Plasmodium falciparum malaria. *N. Engl. J. Med.* **2009,** *361*, 455–467. DOI: 10.1056/NEJMoa0808859
18. Phyo, A. P.; Nkhoma, S.; Stepniewska, K.; Ashley, E. A.; Nair, S.; McGready, R.; Moo, C. L.; Al-Saai, S.; Dondorp, A. M.; Lwin, K. M.; *et al.*, Emergence of artemisinin-resistant malaria on the western border of Thailand: a longitudinal study. *Lancet* **2012,** *379*, 1960–1966. DOI: 10.1016/s0140-6736(12)60484-x
19. Trape, J. F., The public health impact of chloroquine resistance in Africa. *Am. J. Trop. Med. Hyg.* **2001,** *64*, 12–17.
20. Baird, J. K.; Rieckmann, K. H., Can primaquine therapy for vivax malaria be improved? *Trends Parasitol.* **2003,** *19*, 115–120. DOI: 10.1016/s1471-4922(03)0005-9
21. Beutler, E., The hemolytic effect of primaquine and related compounds - A review. *Blood* **1959,** *14*, 103–139.
22. Wells, T. N. C.; Burrows, J. N.; Baird, J. K., Targeting the hypnozoite reservoir of Plasmodium vivax: the hidden obstacle to malaria elimination. *Trends Parasitol.* **2010,** *26*, 145–151. DOI: 10.1016/j.pt.2009.12.005

23. The malERA Consultative Group on Drugs. A Research Agenda for Malaria Eradication: Drugs. *PLos Med.* **2011,** *8*, 9. DOI: 10.1371/journal.pmed.1000402
24. Mian-McCarthy, S.; Agnandji, S. T.; Lell, B.; Fernandes, J. F.; Abossolo, B. P.; Methogo, B.; Kabwende, A. L.; Adegnika, A. A.; Mordmuller, B.; Issifou, S. *et al.*, A phase 3 trial of RTS,S/AS01 malaria vaccine in African infants. *N. Engl. J. Med.* **2012,** *367*, 2284–2295. DOI: 10.1056/NEJMoa1208394
25. Roll Back Malaria. The GMAP. http://www.rollbackmalaria.org/rbmgmap.html (accessed 05/07/2014).
26. Roll Back Malaria Partnership. *Global Malaria Action Plan*; **2008**. http://www.rollbackmalaria.org/gmap/
27. Medicines for Malaria Venture. Interactive R&D portfolio. http://www.mmv.org/research-development/rd-portfolio (accessed 30/10/2014).
28. Olliaro, P.; Wells, T. N. C., The global portfolio of new antimalarial medicines under development. *Clin. Pharmacol. Ther.* **2009,** *85*, 584–595. DOI: 10.1038/clpt.2009.51
29. Vennerstrom, J. L.; Arbe-Barnes, S.; Brun, R.; Charman, S. A.; Chiu, F. C. K.; Chollet, J.; Dong, Y. X.; Dorn, A.; Hunziker, D.; Matile, H.; *et al.*, Identification of an antimalarial synthetic trioxolane drug development candidate. *Nature* **2004,** *430*, 900–904. DOI: 10.1038/nature02779
30. Younis, Y.; Douelle, F.; Feng, T. S.; Cabrera, D. G.; Le Manach, C.; Nchinda, A. T.; Duffy, S.; White, K. L.; Shackleford, D. M.; Morizzi, J.; *et al.*, 3,5-Diaryl-2-aminopyridines as a novel class of orally active antimalarials demonstrating single dose cure in mice and clinical candidate potential. *J. Med. Chem.* **2012,** *55*, 3479–3487. DOI: 10.1021/jm3001373
31. Ramsden, N.; Wilson, F. Aminopyridine derivates as kinase inhibitors. Google Patents: WO2008025820, **2008**.
32. White, N. J.; Pukrittayakamee, S.; Phyo, A. P.; Rueangweerayut, R.; Nosten, F.; Jittamala, P.; Jeeyapant, A.; Jain, J. P.; Lefevre, G.; Li, R. B.; Magnusson, B.; Diagana, T. T.; Leong, F. J., Spiroindolone KAE609 for falciparum and vivax malaria. *N. Engl. J. Med.* **2014,** *371*, 403–410. DOI: 10.1056/NEJMoa1315860
33. Rottmann, M.; McNamara, C.; Yeung, B. K. S.; Lee, M. C. S.; Zou, B.; Russell, B.; Seitz, P.; Plouffe, D. M.; Dharia, N. V.; Tan, J.; *et al.*, Spiroindolones, a potent

compound class for the treatment of malaria. *Science* **2010,** *329*, 1175–1180. DOI: 10.1126/science.1193225

34. Yeung, B. K. S.; Zou, B.; Rottmann, M.; Lakshminarayana, S. B.; Ang, S. H.; Leong, S. Y.; Tan, J.; Wong, J.; Keller-Maerki, S.; Fischli, C.; *et al.*, Spirotetrahydro beta-carbolines (spiroindolones): A new class of potent and orally efficacious compounds for the treatment of malaria. *J. Med. Chem.* **2010,** *53*, 5155–5164. DOI: 10.1021/jm100410f
35. Spillman, N. J.; Allen, R. J. W.; McNamara, C. W.; Yeung, B. K. S.; Winzeler, E. A.; Diagana, T. T.; Kirk, K., Na+ regulation in the malaria parasite Plasmodium falciparum involves the cation ATPase PfATP4 and is a target of the spiroindolone antimalarials. *Cell Host Microbe* **2013,** *13*, 227–237. DOI: 10.1016/j.chom.2012.12.006
36. Lehane, A. M.; Ridgway, M. C.; Baker, E.; Kirk, K., Diverse chemotypes disrupt ion homeostasis in the malaria parasite. *Molecular microbiology* **2014,** *94*, 327–39. DOI: 10.1111/mmi.12765
37. Charman, S. A.; Arbe-Barnes, S.; Bathurst, I. C.; Brun, R.; Campbell, M.; Charman, W. N.; Chiu, F. C. K.; Chollet, J.; Craft, J. C.; Creek, D. J.; *et al.*, Synthetic ozonide drug candidate OZ439 offers new hope for a single-dose cure of uncomplicated malaria. *Proc. Natl. Acad. Sci. U. S. A.* **2011,** *108*, 4400–4405. DOI: 10.1073/pnas.1015762108
38. Medicines for Malaria Venture. Potential new class of antimalarials now open source. http://www.mmv.org/newsroom/news/potential-new-class-antimalarials-now-open-source (accessed 29/10/2014).
39. Open Source Malaria. OpenSourceMalaria: Story So Far. http://openwetware.org/wiki/OpenSourceMalaria:Story_so_far (accessed 29/10/2014).
40. Inherited Contract Research Organisation (CRO) data - Final Report MMV670652 (CR302-6082-84C). Downloadable from http://malaria.ourexperiment.org/data/files/7384/FINAL REPORT MMV670652.doc
41. Woelfle, M.; Olliaro, P.; Todd, M. H., Open science is a research accelerator. *Nat. Chem.* **2011,** *3*, 745–748. DOI: 10.1038/nchem.1149

42. Robertson, M. N.; Ylioja, P. M.; Williamson, A. E.; Woelfle, M.; Robins, M.; Badiola, K. A.; Willis, P.; Olliaro, P.; Wells, T. N. C.; Todd, M. H., Open source drug discovery - A limited tutorial. *Parasitology* **2014,** *141*, 148–157.
43. Open Source Malaria. OpenSourceMalaria: Triazolopyrazine (TP) Series. http://openwetware.org/wiki/OpenSourceMalaria:Triazolopyrazine_%28TP%29_Series (accessed 24/10/2014).
44. Southan, C., Searching the triazolopyrazines for Open Source Malaria. 2014. http://cdsouthan.blogspot.com.au/2013/12/searching-triazolopyrazines-for-open.html (accessed 24/10/2014).
45. National Institute of Health Chemical Genomic Center. Compound Summary for CID 7118230. https://pubchem.ncbi.nlm.nih.gov/compound/7118230?from=summary#section=Top (accessed 29/10/2014).
46. Boros, L. G.; Decorte, B.; Gimi, R. H.; Welch, J. T.; Wu, Y.; Handschumacher, R. E., Fluoroolefin peptide isosteres - Tools for controlling peptide conformations. *Tetrahedron Lett.* **1994,** *35*, 6033–6036. DOI: 10.1016/0040-4039(94)88067-0
47. Bartlett, P. A.; Otake, A., Fluoroalkenes as peptide isosteres - Ground-state analog inhibitors of thermolysin. *Journal of Organic Chemistry* **1995,** *60*, 3107–3111. DOI: 10.1021/jo00115a028
48. Welch, J. T.; Lin, J., Fluoroolefin containing dipeptide isosteres as inhibitors of dipeptidyl peptidase IV (CD26). *Tetrahedron* **1996,** *52*, 291–304. DOI: 10.1016/0040-4020(95)00912-r
49. Couve-Bonnaire, S.; Cahard, D.; Pannecoucke, X., Chiral dipeptide mimics possessing fluoroolefin moiety: a relevant tool for conformational and medicinal studies. *Org. Biomol. Chem.* **2007,** *5*, 1151–1157. DOI: 10.1039/b701559c
50. Yang, M.-H.; Matikonda, S. S.; Altman, R. A., Preparation of fluoroalkenes via the shapiro reaction: Direct access to fluorinated peptidomimetics. *Org. Lett.* **2013,** *15*, 3894–3897. DOI: 10.1021/ol401637n
51. Chen, C.; Wilcoxen, K.; Huang, C. Q.; Strack, N.; McCarthy, J. R., New methods for the synthesis of fluoroolefins via the palladium catalyzed cross-coupling reaction of 1-fluorovinyl halides with organoboranes and organostannanes. *J. Fluor. Chem.* **2000,** *101*, 285–290. DOI: 10.1016/s0022-1139(99)00172-4

52. Urban, J. J.; Tillman, B. G.; Cronin, W. A., Fluoroolefins as peptide mimetics: A computational study of structure, charge distribution, hydration, and hydrogen bonding. *J. Phys. Chem. A* **2006,** *110*, 11120–11129. DOI: 10.1021/jp062881n
53. Medicines for Malaria Venture Expert Scientific Advisory Committee. ESAC Report 2014. **2014**. Downloadable from http://malaria.ourexperiment.org/osddmalaria_meeting_/10462/ESAC_Report_2014.html
54. Guiguemde, W. A.; Shelat, A. A.; Garcia-Bustos, J. F.; Diagana, T. T.; Gamo, F. J.; Guy, R. K., Global phenotypic screening for antimalarials. *Chem. Biol.* **2012,** *19*, 116–129. DOI: 10.1016/j.chembiol.2012.01.004
55. Flannery, E. L.; Fidock, D. A.; Winzeler, E. A., Using genetic methods to define the targets of compounds with antimalarial activity. *J. Med. Chem.* **2013,** *56*, 7761–7771. DOI: 10.1021/jm400325j
56. Bradac, J.; Furek, Z.; Janezic, D.; Molan, S.; Smerkolj, I.; Stanovnik, B.; Tisler, M.; Vercek, B., Heterocycles. 167. Telesubstitution and other transformations of imidazo[1,2-a]- and s-triazolo[4,3-a]pyrazines. *J. Org. Chem.* **1977,** *42*, 4197–4201. DOI: 10.1021/jo00862a005
57. Kumar, D.; Chandra, S. K. V. G.; Dhillon, H.; Rao, V. S.; Varma, R. S., An expeditious synthesis of 1-aryl-4-methyl-1,2,4-triazolo[4,3-a]quinoxalines under solvent-free conditions using iodobenzene diacetate. *Green Chem.* **2004,** *6*, 156–157. DOI: 10.1039/b315031c
58. El-Mottaleb M. Ramadan, A.; El-Mehasseb, I. M., Synthesis, characterization and biomimetic oxygenations of manganese(II), iron(III) and copper(II) pyridyl hydrazone complexes. *Transition Met. Chem. (London)* **1998,** *23*, 183–189.
59. Zheng, Z. S.; Ma, S. Y.; Tang, L. L.; Zhang-Negrerie, D.; Du, Y. F.; Zhao, K., PhI(OCOCF3)(2)-mediated intramolecular oxidative N-N bond formation: Metal-free synthesis of 1,2,4-triazolo 1,5-a pyridines. *Journal of Organic Chemistry* **2014,** *79*, 4687–4693. DOI: 10.1021/jo500298j
60. Ubels, J., Literature search for ether synthesis reaction conditions for model reactions. 2014. http://malaria.ourexperiment.org/uri/532

61. Yang, J.; Dudley, G. B., [1,2]-Anionic rearrangement of 2-benzyloxypyridine and related pyridyl ethers. *J. Org. Chem.* **2009,** *74*, 7998–8000. DOI: 10.1021/jo901707x
62. Lanni, E. L.; Bosscher, M. A.; Ooms, B. D.; Shandro, C. A.; Ellsworth, B. A.; Anderson, C. E., Synthesis of substituted N-benzyl pyridones via an O- to N-alkyl migration. *Journal of Organic Chemistry* **2008,** *73*, 6425–6428. DOI: 10.1021/jo800866w
63. Tao, Z. F.; Wang, L.; Stewart, K. D.; Chen, Z. H.; Gu, W.; Bui, M. H.; Merta, P.; Zhang, H. Y.; Kovar, P.; Johnson, E.; *et al.*, Structure-based design, synthesis, and biological evaluation of potent and selective macrocyclic checkpoint kinase 1 inhibitors. *Journal of Medicinal Chemistry* **2007,** *50*, 1514–1527. DOI: 10.1021/jm061247v
64. Motohashi, K.; Inaba, K.; Fuse, S.; Doi, T.; Izumikawa, M.; Khan, S. T.; Takagi, M.; Takahashi, T.; Shin-ya, K., JBIR-56 and JBIR-57, 2(1H)-pyrazinones from a marine sponge-derived streptomyces sp SpD081030SC-03. *J. Nat. Prod.* **2011,** *74*, 1630–1635. DOI: 10.1021/np200386c
65. Vandenberg, J. I.; Perry, M. D.; Perrin, M. J.; Mann, S. A.; Ke, Y.; Hill, A. P., hERG K+ channels: Structure, function, and clinical significance. **2012**, *92*, 1393–1478.
66. Debbert, S., PIDA Cyclisation #97. **2013**. https://github.com/OpenSourceMalaria/OSM_To_Do_List/issues/97
67. Thiel, O. R.; Achmatowicz, M. M.; Reichelt, A.; Larsen, R. D., Palladium-catalyzed coupling of aldehyde-derived hydrazones: Practical synthesis of triazolopyridines and related heterocycles. *Angew. Chem.-Int. Edit.* **2010,** *49*, 8395–8398. DOI: 10.1002/anie.201001999
68. Aggarwal, R.; Sumran, G., Hypervalent iodine-mediated synthesis of 1-aryl-4-methyl-1,2,4-triazolo[4,3-a]quinoxalines by oxidative cyclization of arene carbaldehyde-3-methylquinoxalin-2-yl hydrazones. *Synth. Commun.* **2006,** *36*, 1873–1878. DOI: 10.1080/00397910600602586
69. Galli, C.; Guarnieri, A.; Koch, H.; Mencarelli, P.; Rappoport, Z., Effect of substituents on the structure of the vinyl radical: Calculations and experiments. *Journal of Organic Chemistry* **1997,** *62*, 4072–4077. DOI: 10.1021/jo962373h
70. Bouillon, A.; Lancelot, J.-C.; Sopkova de Oliveira Santos, J.; Collot, V.; Bovy, P. R.; Rault, S., Synthesis of novel halopyridinylboronic acids and esters. Part 4:

Halopyridin-2-yl-boronic acids and esters are stable, crystalline partners for classical Suzuki cross-coupling. *Tetrahedron* **2003,** *59*, 10043–10049. http://dx.doi.org/10.1016/j.tet.2003.10.020

71. Leach, A. G., Synthesis of pyrazinyl boronic acids #250. **2014**. https://github.com/OpenSourceMalaria/OSM_To_Do_List/issues/250
72. Noonan, G.; Leach, A. G., Boronic acids as agents of their own destruction; experimental and computational studies of protodeboronation provide a predictive model. Personal Communication **2014**.
73. Vander Haar, R. W. J. Study of some halomethyl phosphonium salts. PhD Thesis. University of Iowa, **1973**.
74. Burton, D. J.; Yang, Z. Y.; Qiu, W. M., Fluorinated ylides and related compounds. *Chem. Rev.* **1996,** *96*, 1641–1715. DOI: 10.1021/cr941140s
75. Burton, D. J.; Flynn, R. M.; Manning, R. G.; Kessler, R. M., The hydrolysis of dibromofluoromethyltriphenylphosphonium bromide. *J. Fluor. Chem.* **1982,** *21*, 371–376. DOI: 10.1016/s0022-1139(00)81522-5
76. Mitchell, M. B.; Wallbank, P. J., Coupling of heteroaryl chlorides with arylboronic acids in the presence of [1,4-bis-(diphenylphosphine)butane]palladium(II) dichloride. *Tetrahedron Lett.* **1991,** *32*, 2273–2276. DOI: 10.1016/S0040-4039(00)79700-0
77. Du, W.; Wang, Q.; Wang, L.; Yu, Z., Ruthenium complex catalysts supported by a bis(trifluoromethyl)pyrazolyl-pyridyl-based NNN ligand for transfer hydrogenation of ketones. *Organometallics* **2014,** *33*, 974–982. DOI: 10.1021/om401144u
78. Open Source Malaria. Metabolism ID Study for Three Triazolopyrazines. 2013. http://malaria.ourexperiment.org/uri/49a
79. Badiola, K., NaBH4 mediated reduction to give 2,3-dihydrobenzob-1,4-dioxin-6-ylmethanol KAB83-2. 2013. DOI: 118.138.241.43

A. Supporting NMR for Selected Compounds

A. 1. 4-((2-(6-Chloropyrazin-2-yl)hydrazono)methyl)benzonitrile 22

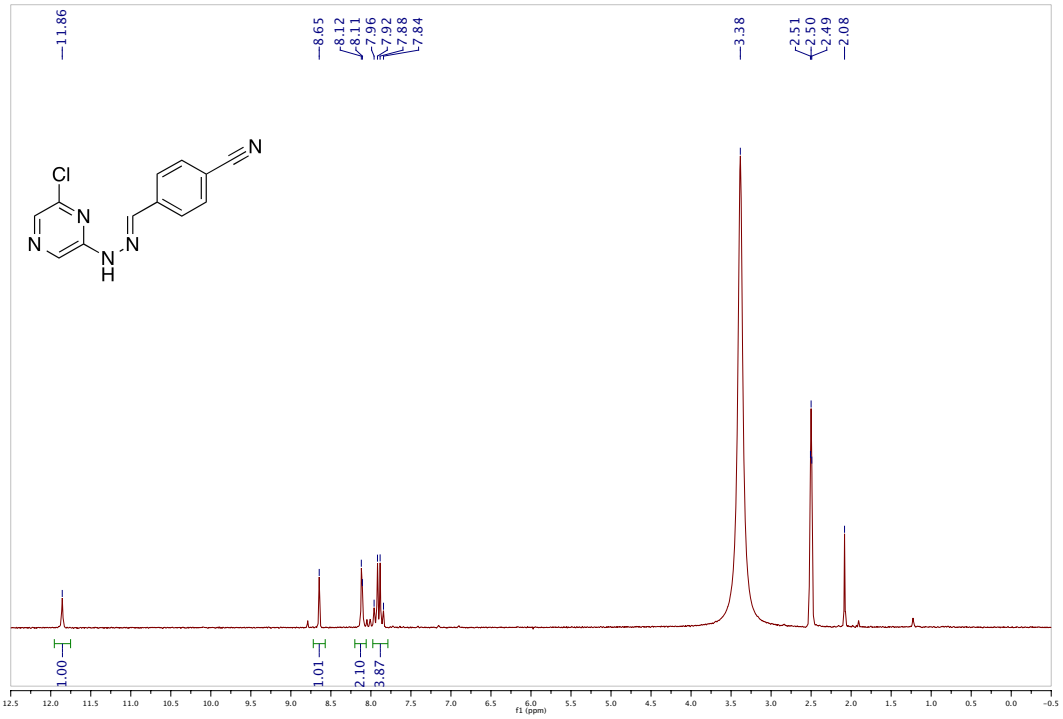

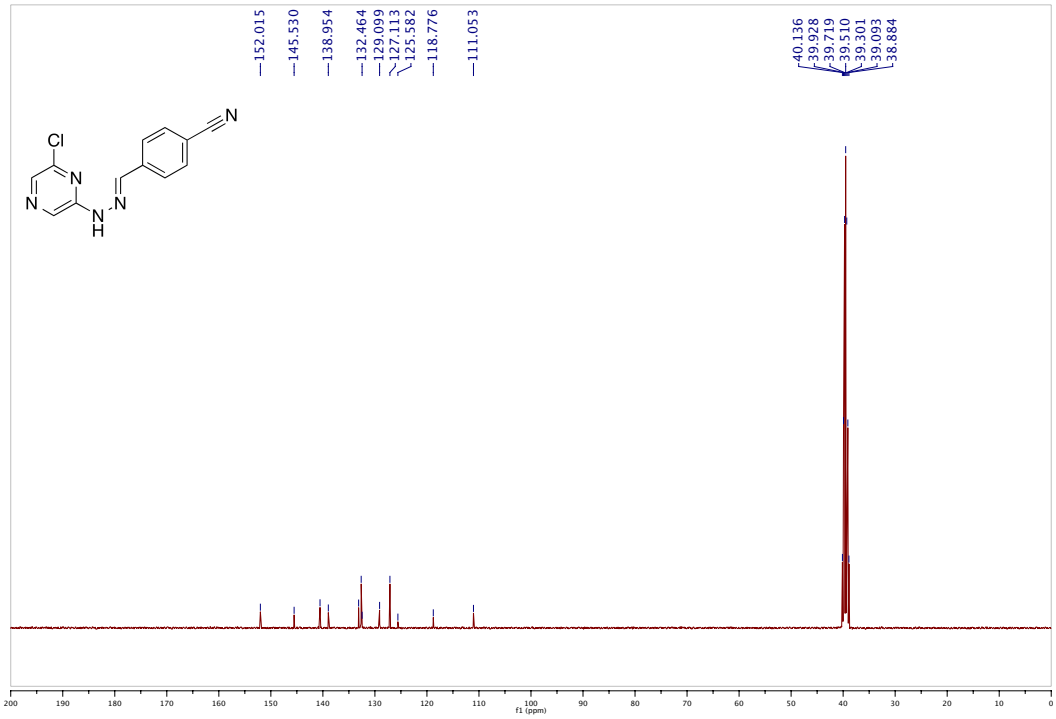

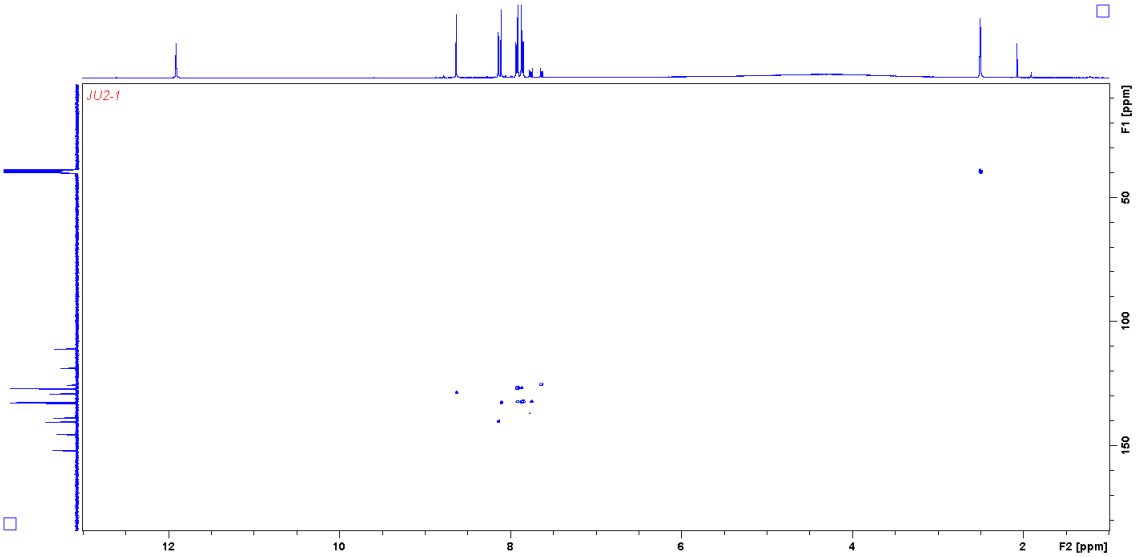
JU2-1
F1 [ppm]
50
100
150
12
10
8
6
4
2
F2 [ppm]

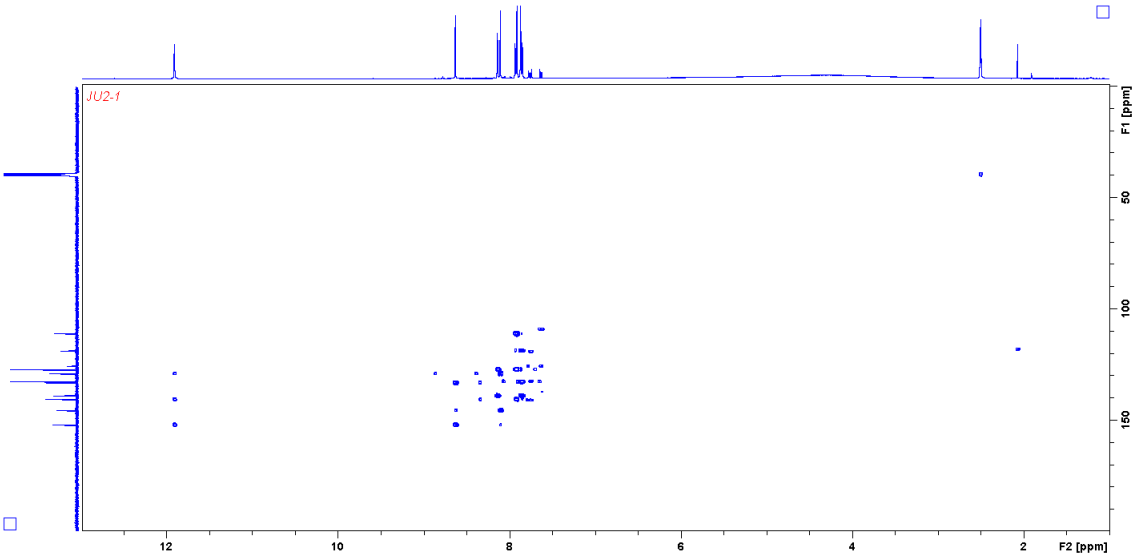
JU2-1
F1 [ppm]
50
100
150
12
10
8
6
4
2
F2 [ppm]

A. 2. 2-Chloro-6-(2-(4-chlorobenzylidene)hydrazinyl)pyrazine 25

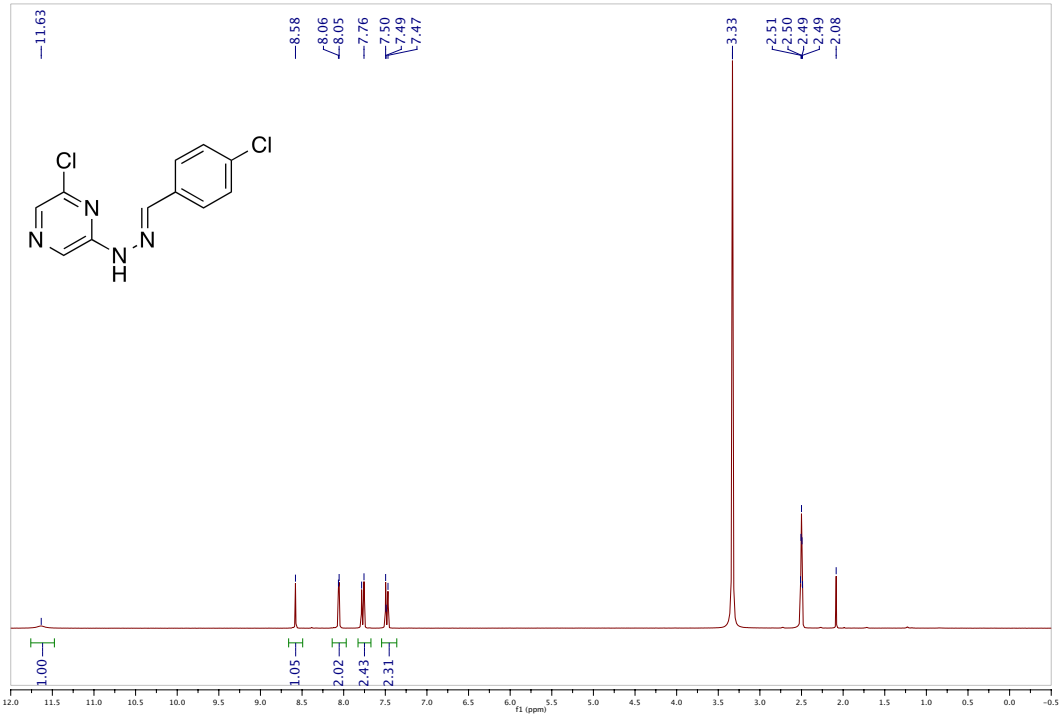

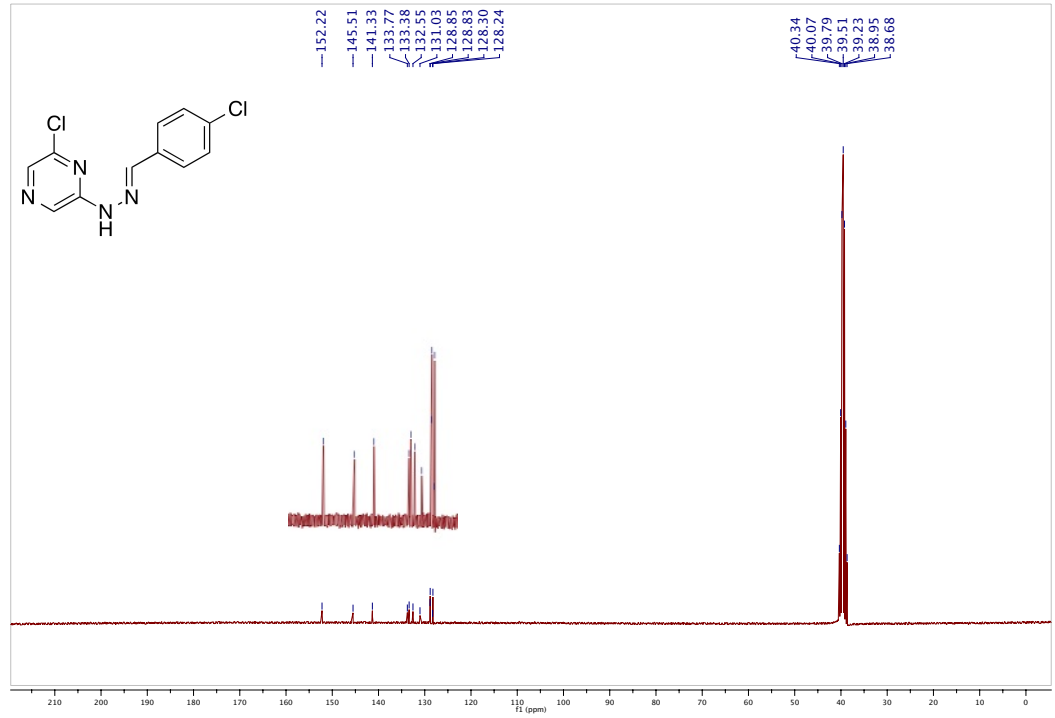

A. 3. 4-(5-Chloro-[1,2,4]triazolo[4,3-a]pyrazin-3-yl)benzonitrile 23

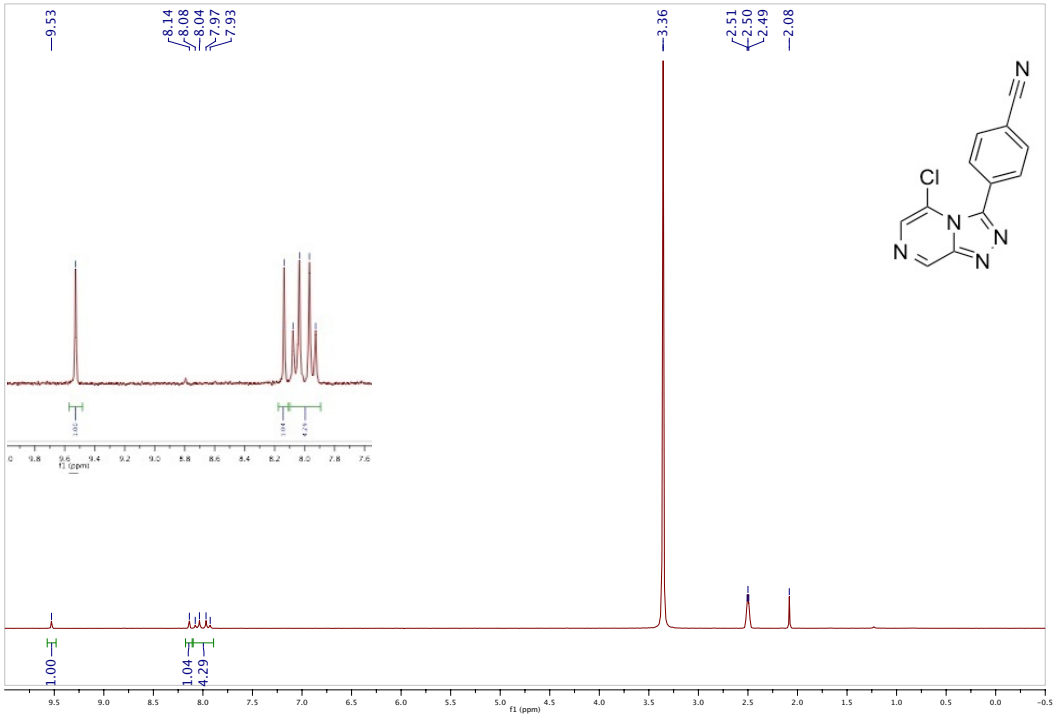

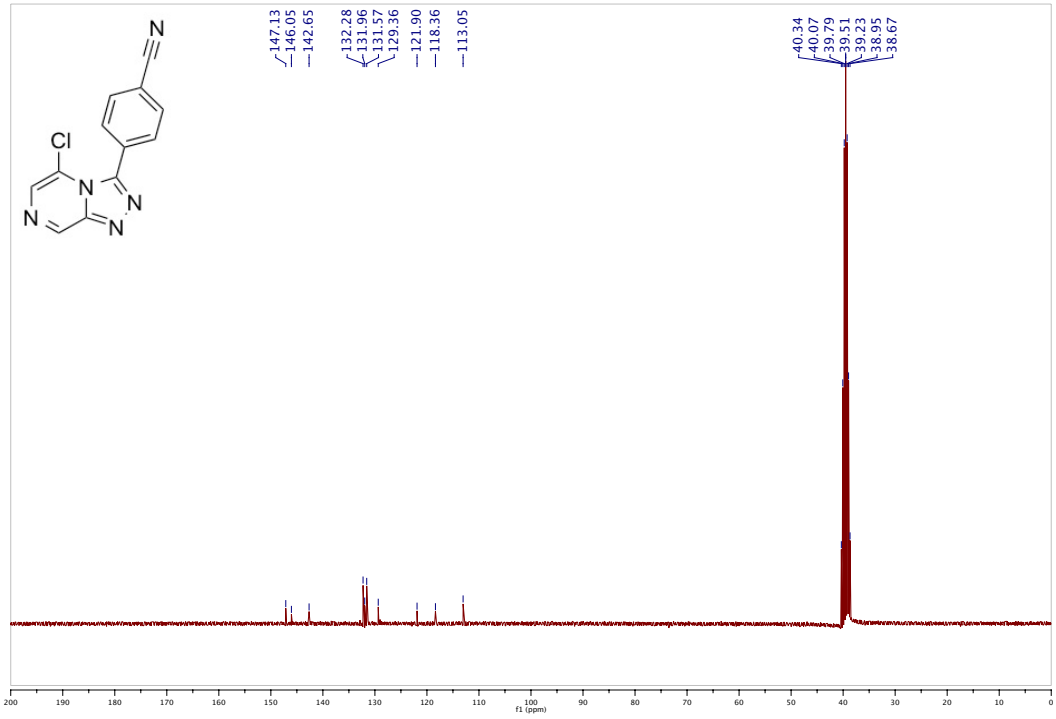

A. 4. 5-Chloro-3-(4-chlorophenyl)-[1,2,4]triazolo[4,3-a]pyrazine 26

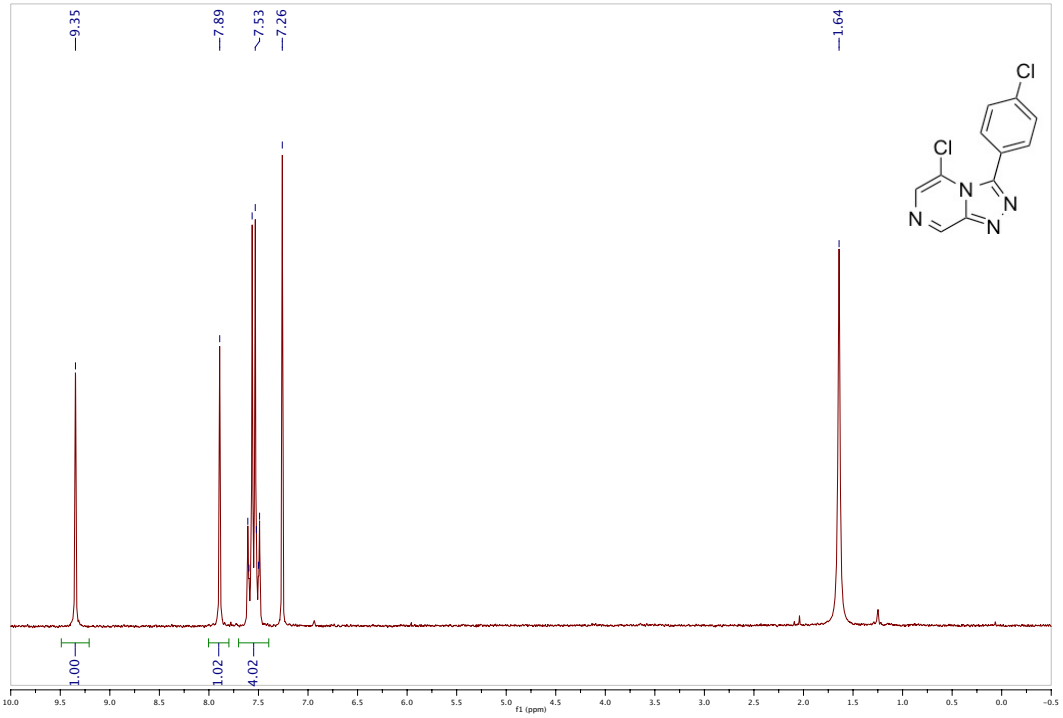

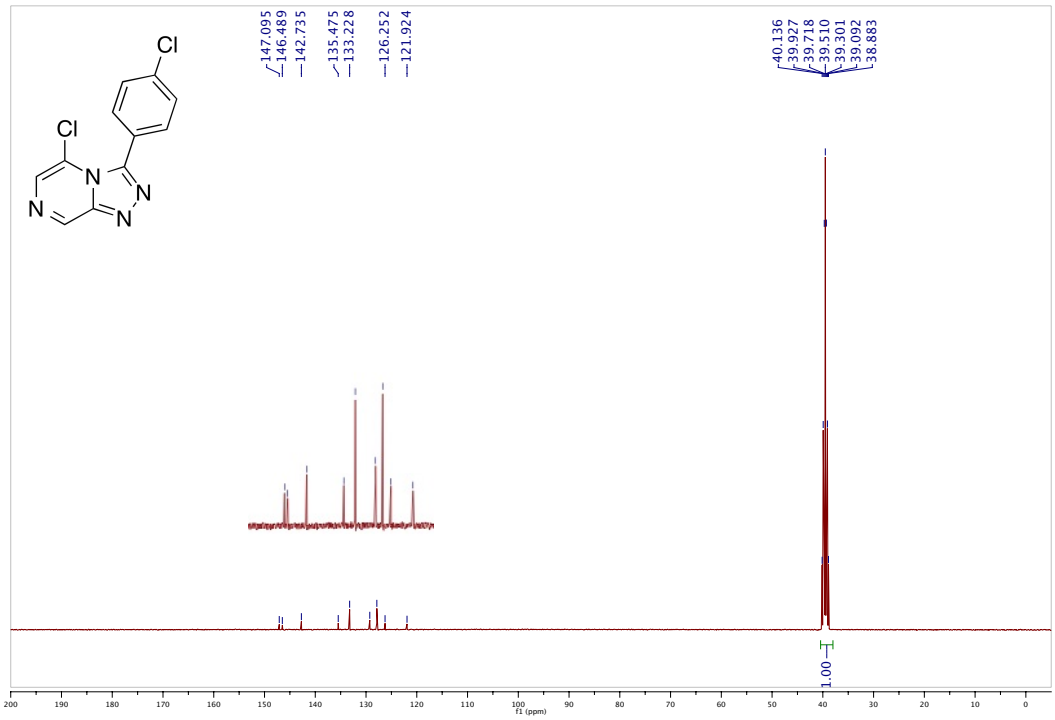

A. 5. 4-(5-Phenethoxy-[1,2,4]triazolo[4,3-a]pyrazin-3-yl)benzonitrile 28

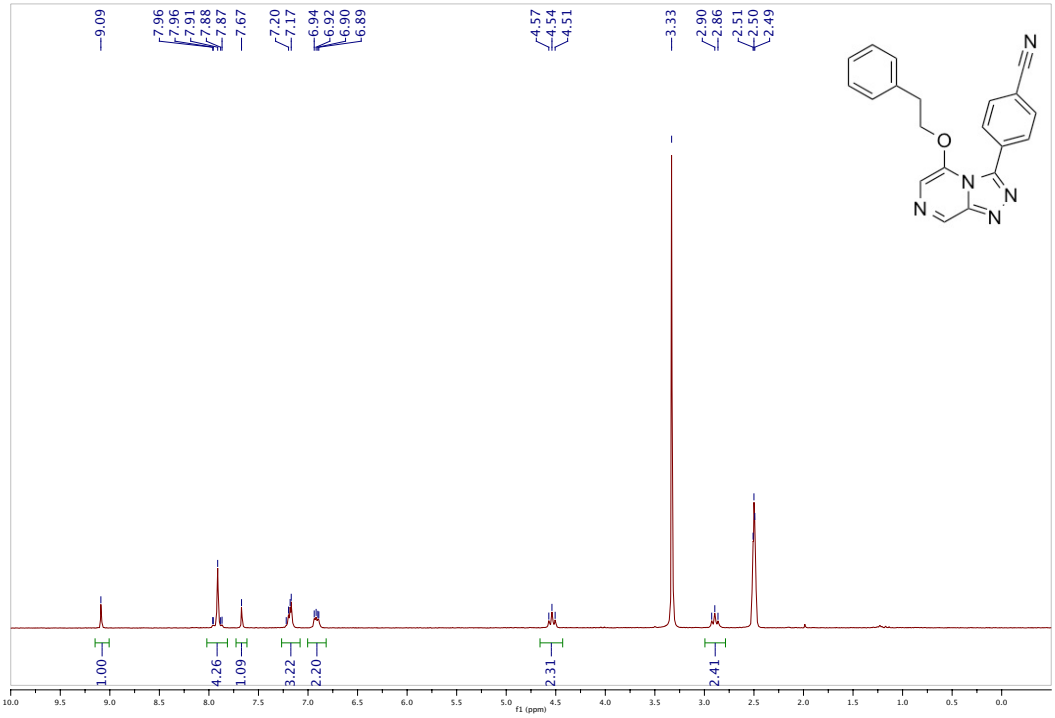

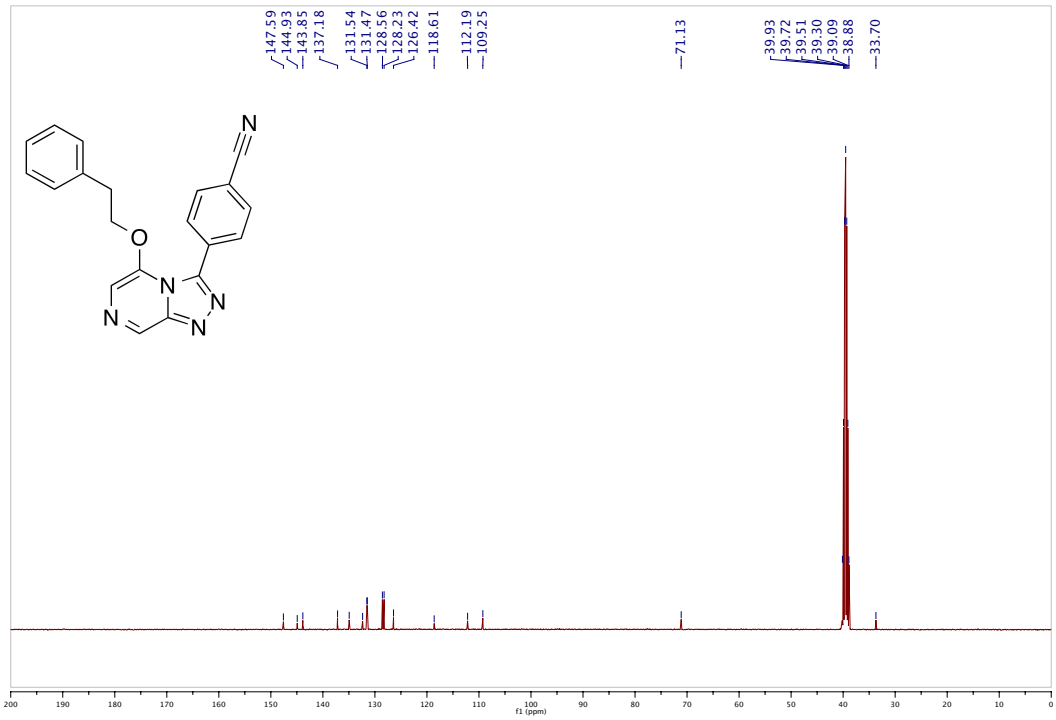

A. 6. 4-(5-(2-Chlorophenethoxy)-[1,2,4]triazolo[4,3-a]pyrazin-3yl)benzonitrile 29

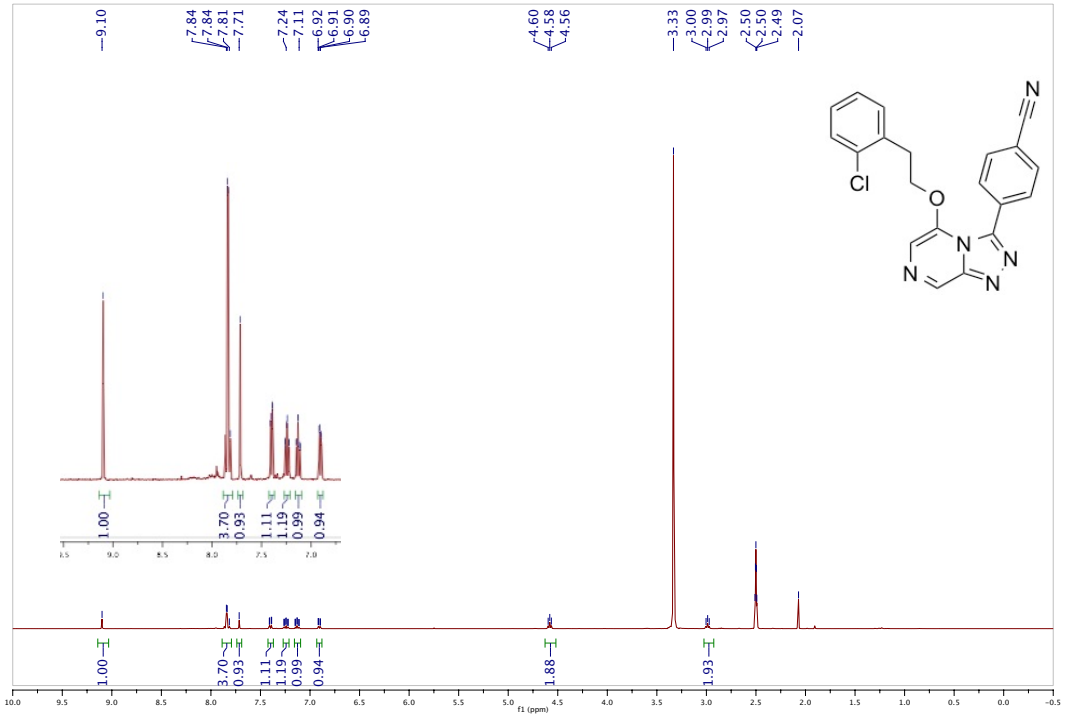

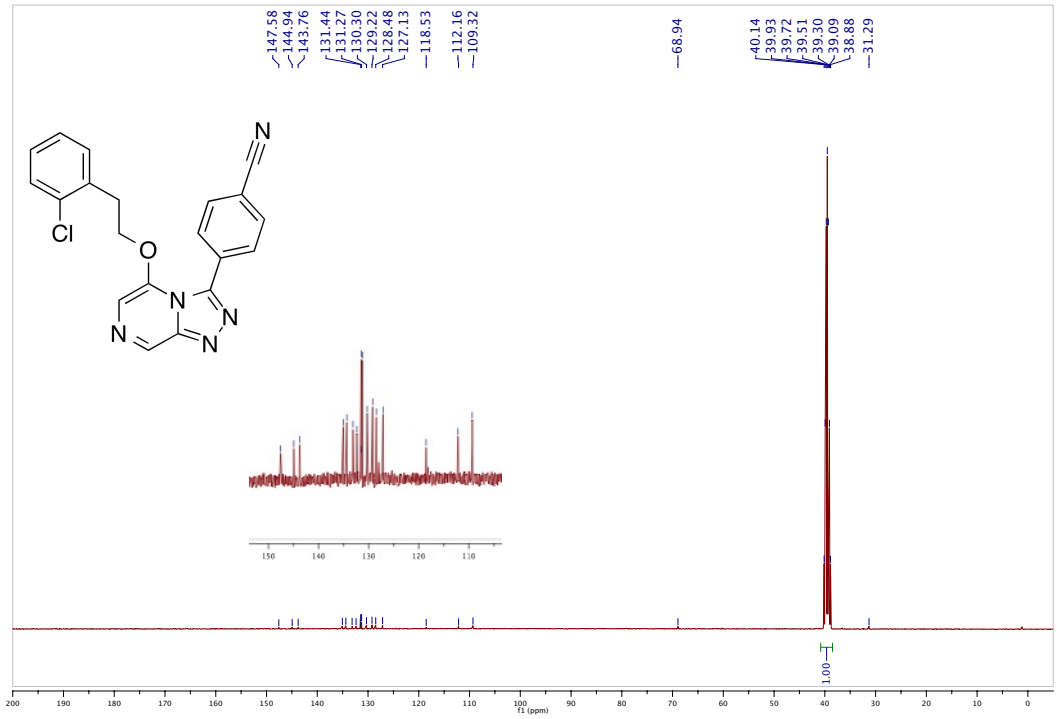

A. 7. 4-(5-(Phenethylthio)-[1,2,4]triazolo[4,3-a]pyrazin-3yl)benzonitrile 30

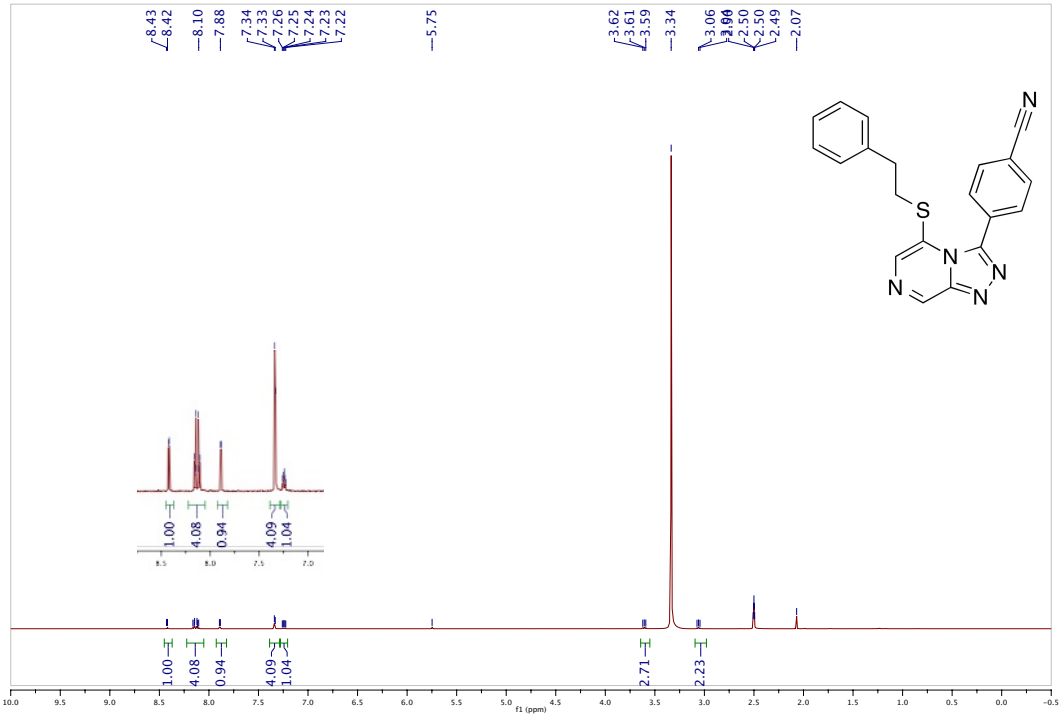

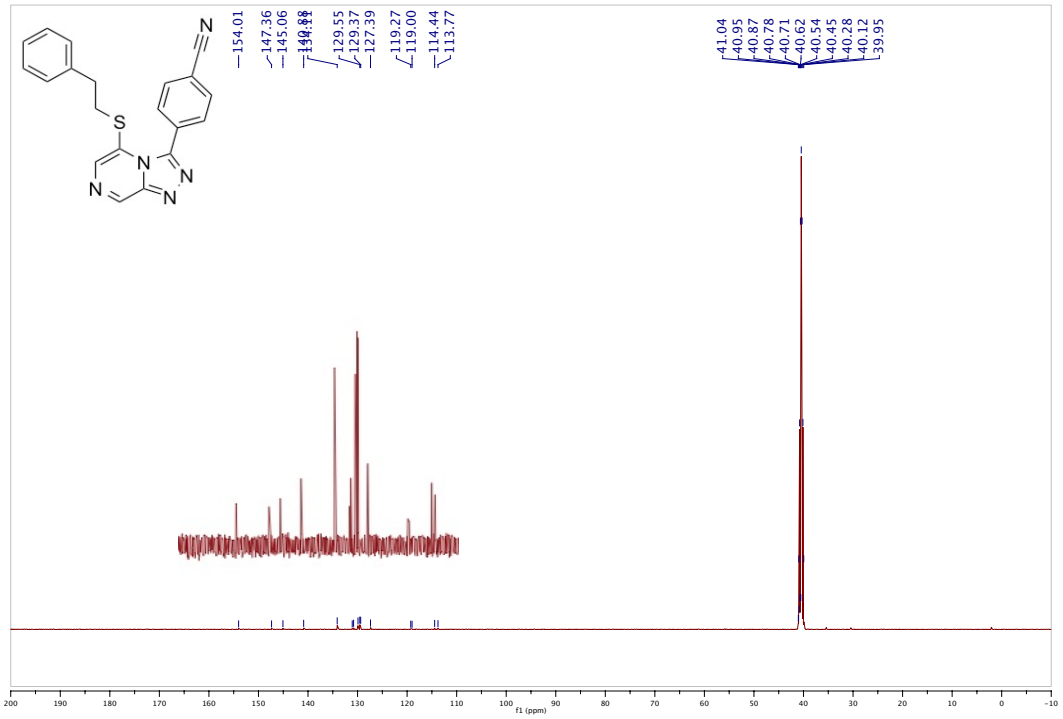

A. 8. 4-(5-((3-Chlorophenethyl)amino)-[1,2,4]triazolo[4,3-a]pyrazin-3-yl)benzonitrile 31

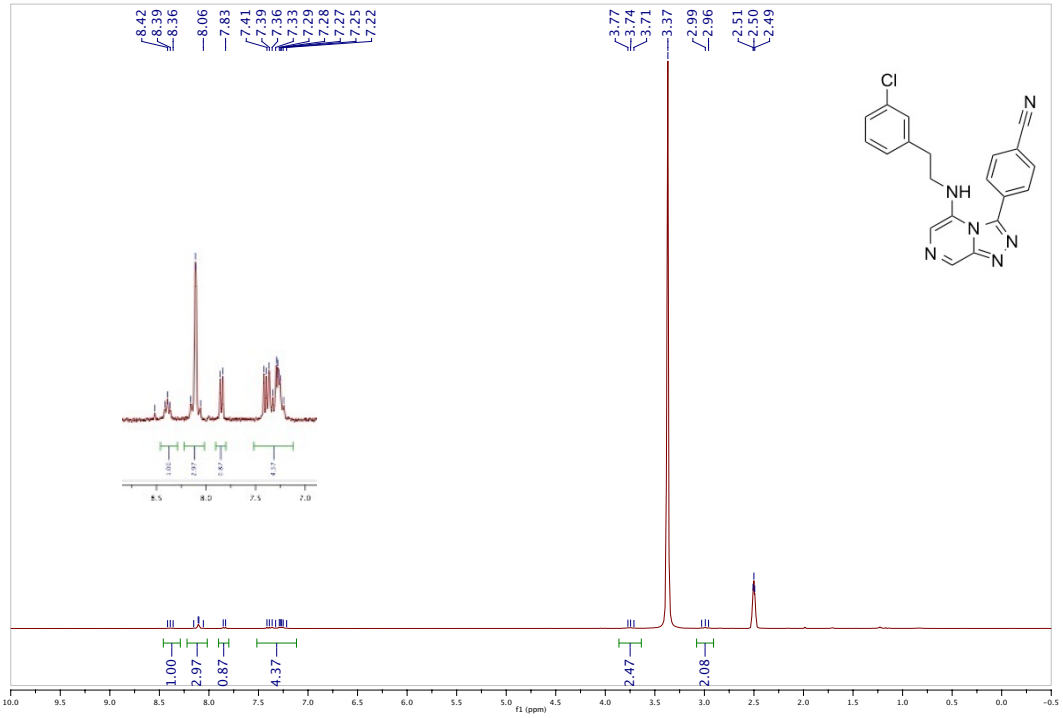

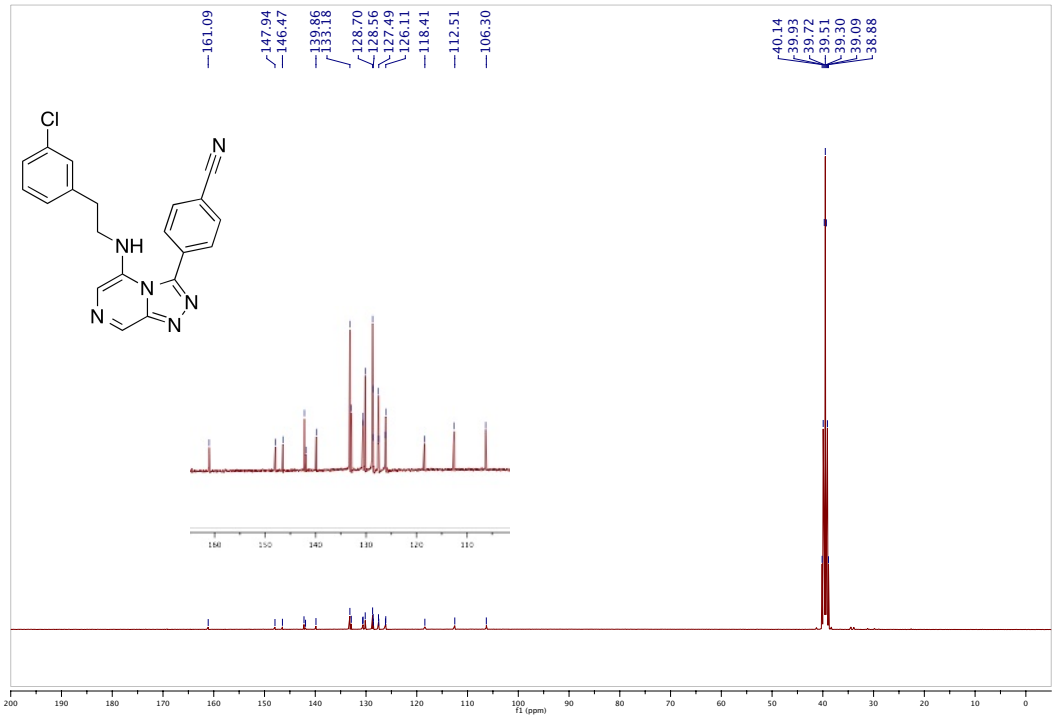

A. 9. N-(3-chlorophenethyl)-3-(4-chlorophenyl)-[1,2,4]triazolo[4,3-a]pyrazin-5-amine 32

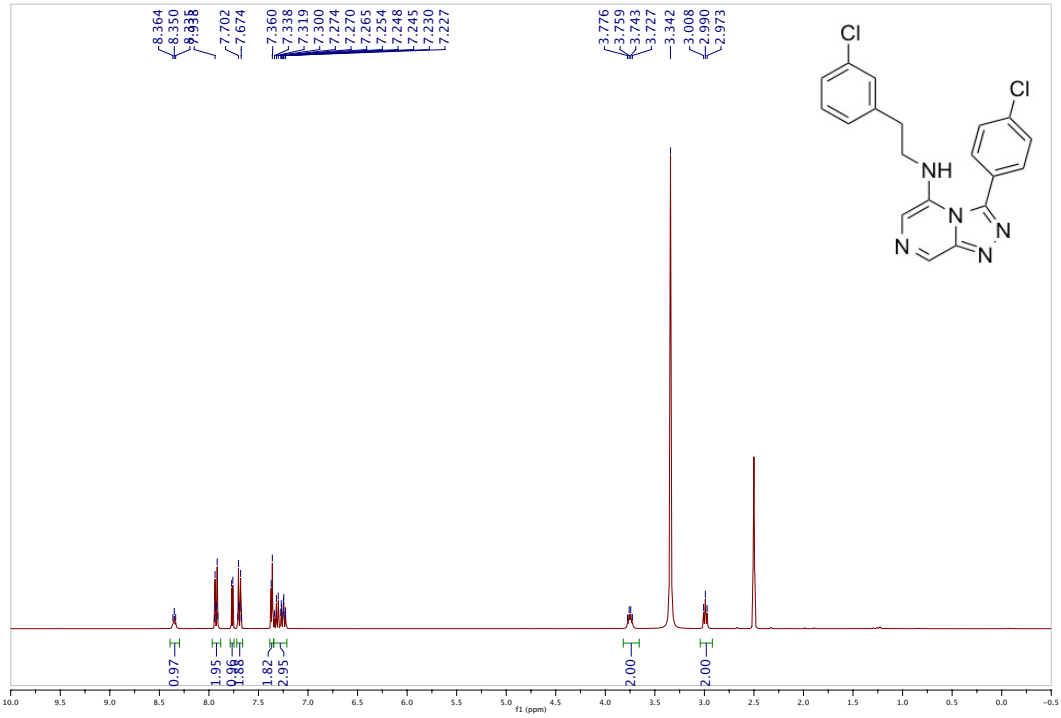

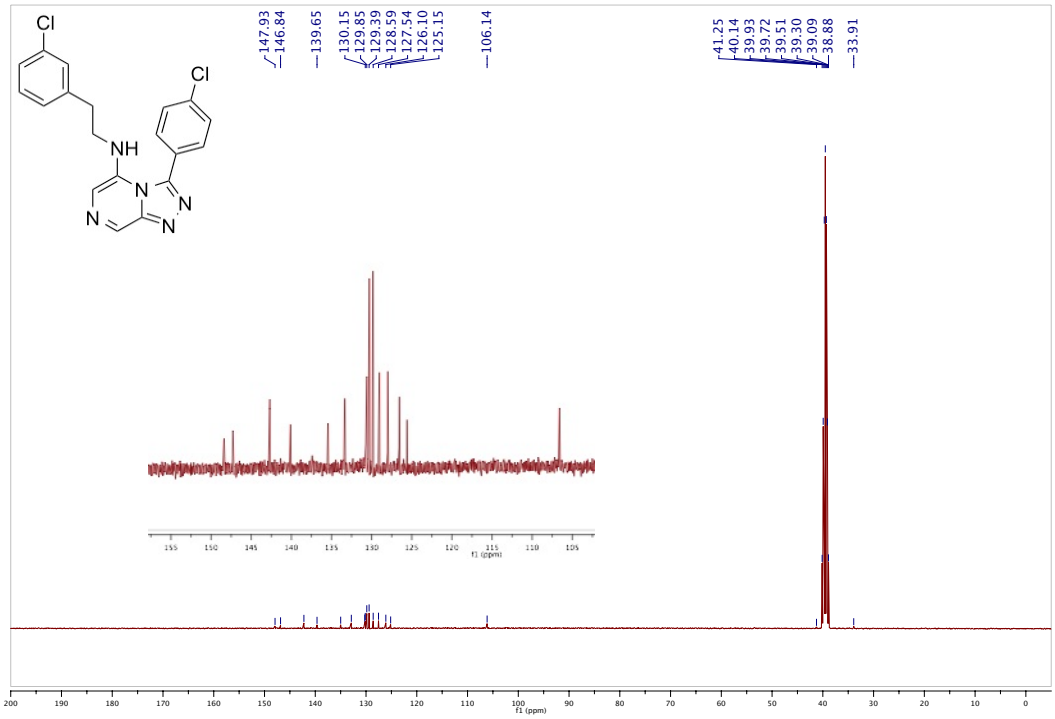

A. 10. 3-(4-Chlorophenyl)-5-((3,4-difluorobenzyl)oxy) [1,2,4]triazolo[4,3-a]pyrazine 38

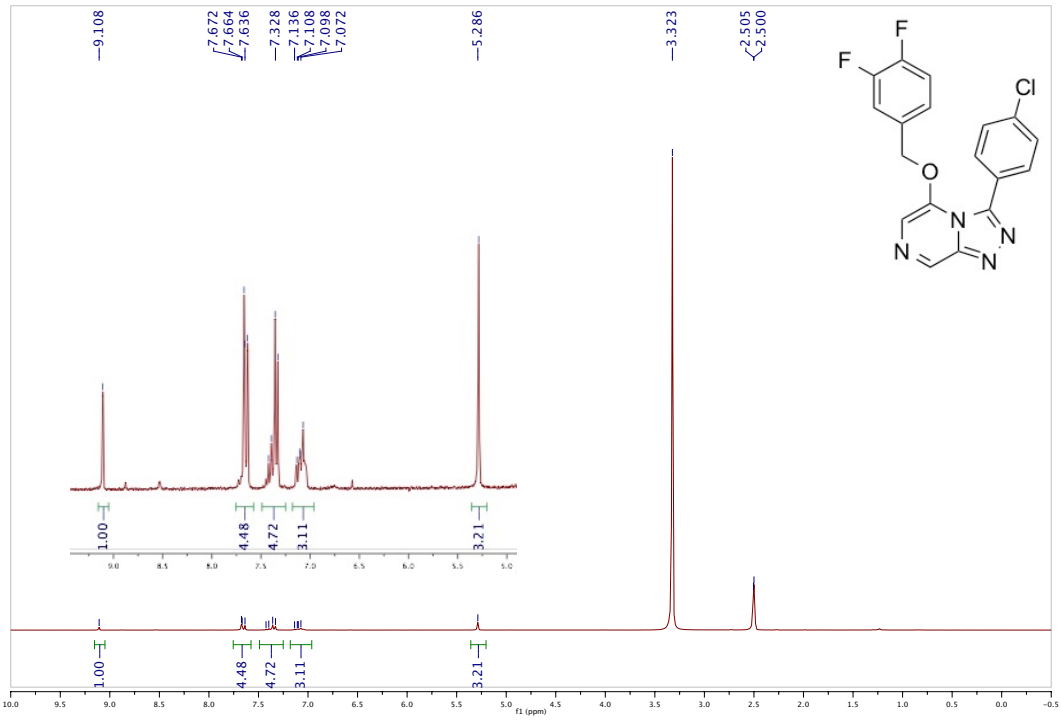

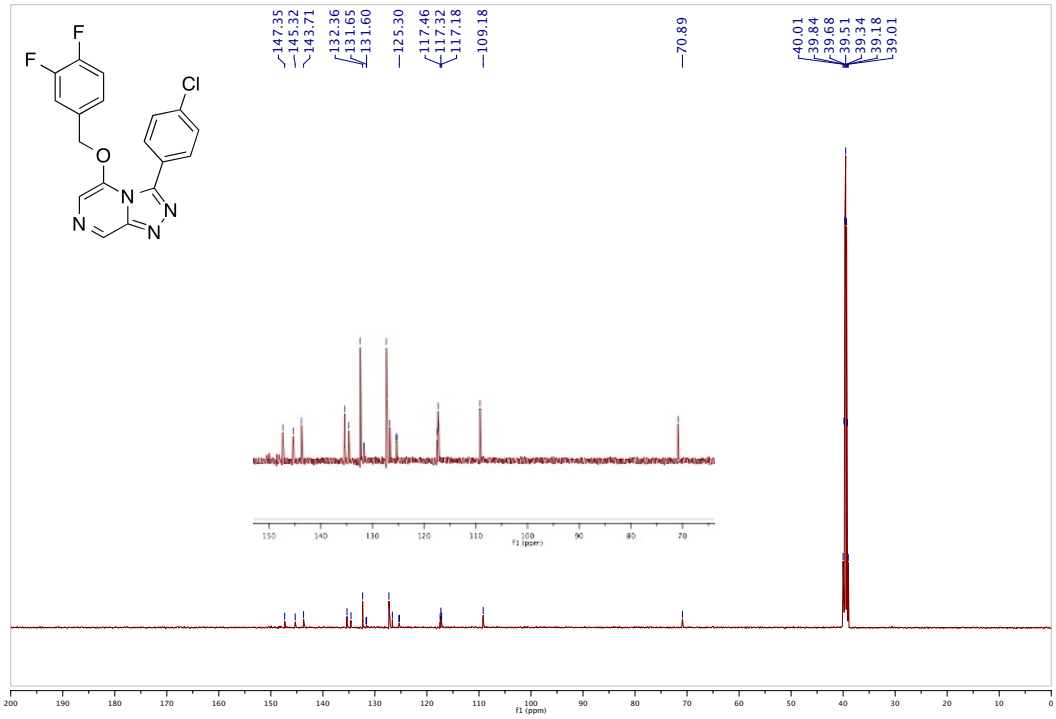

A. 11. 3-(4-(Difluoromethoxy)phenyl)-5-(3,4-difluorophenethoxy)-[1,2,4]triazolo[4,3-a]pyrazine 39

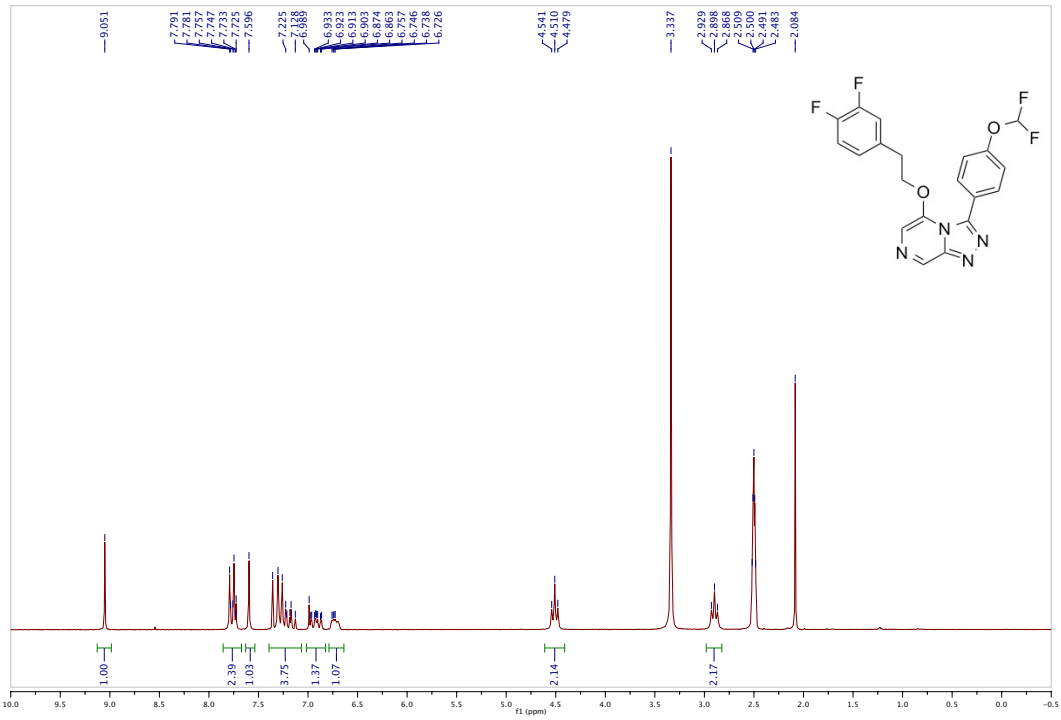

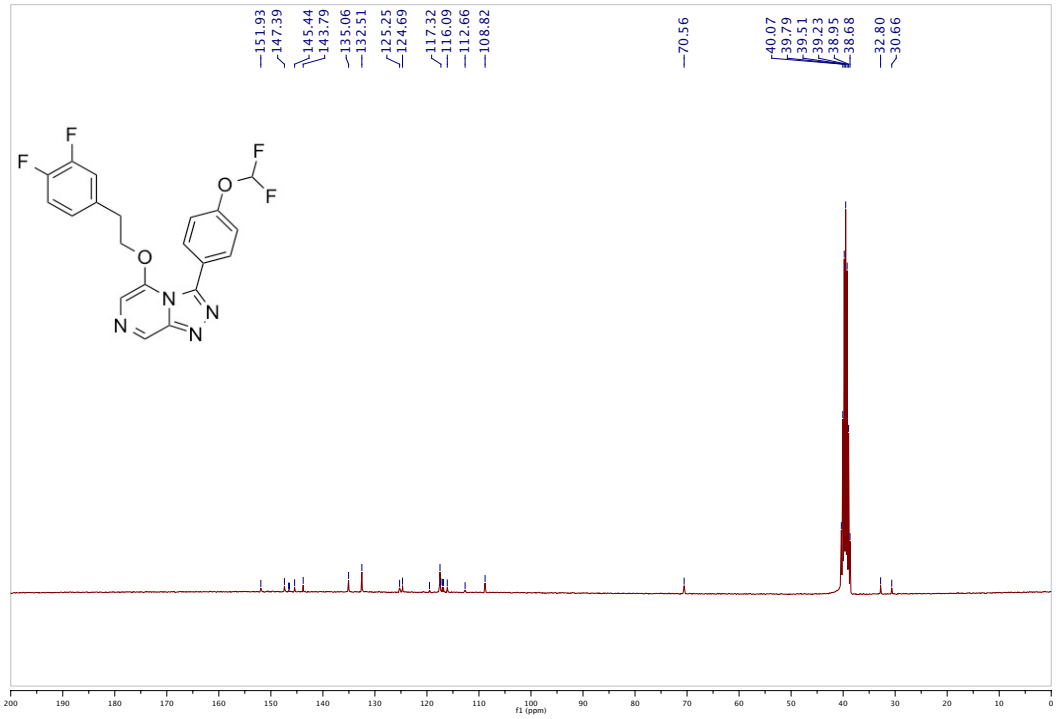

A. 12. 5-(2-chlorophenethoxy)-3-(pyridin-4-yl)-[1,2,4]triazolo[4,3-a]pyrazine 40

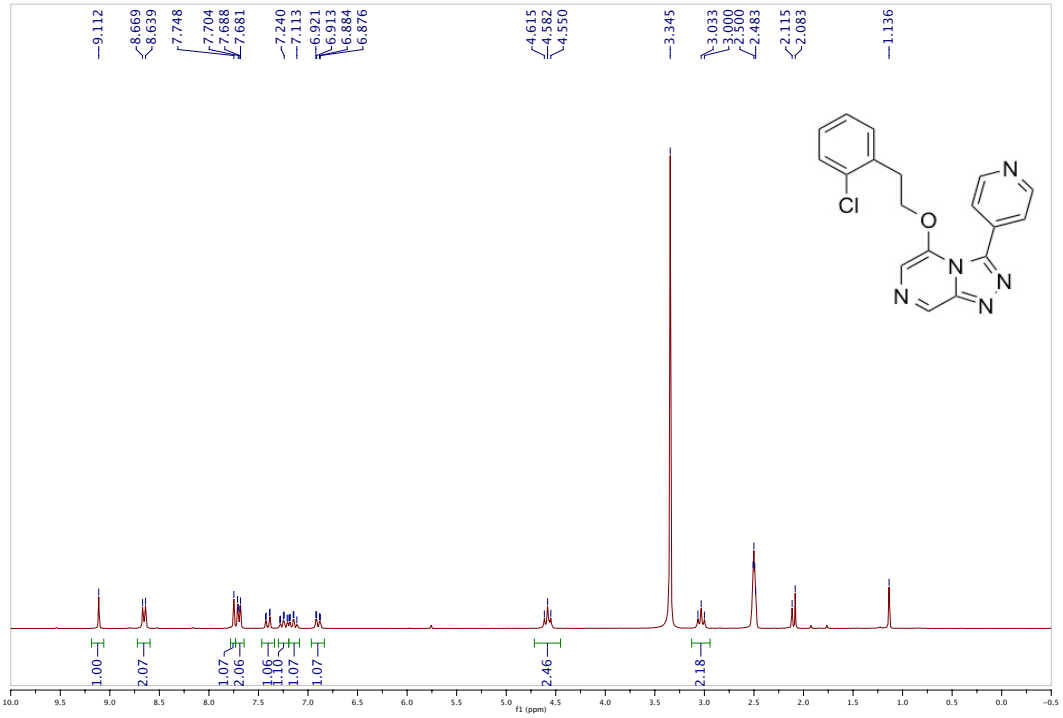

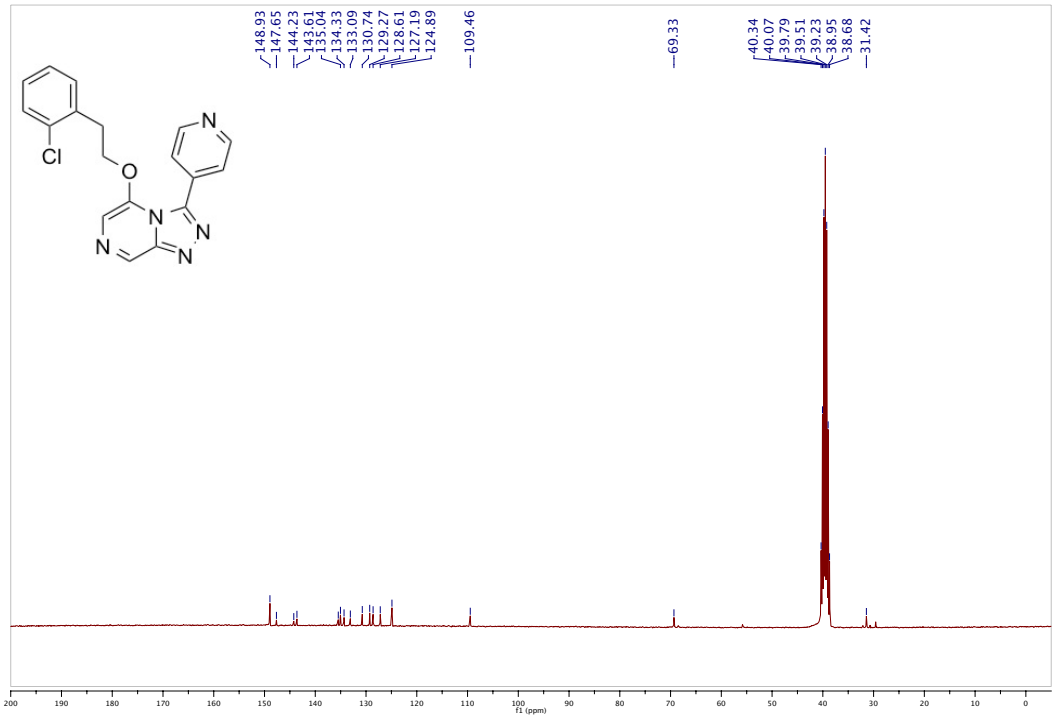

A. 13. 2-Bromo-6-(4,4,5,5-tetramethyl-1,3,2-dioxaborolan-2-yl)pyridine 50

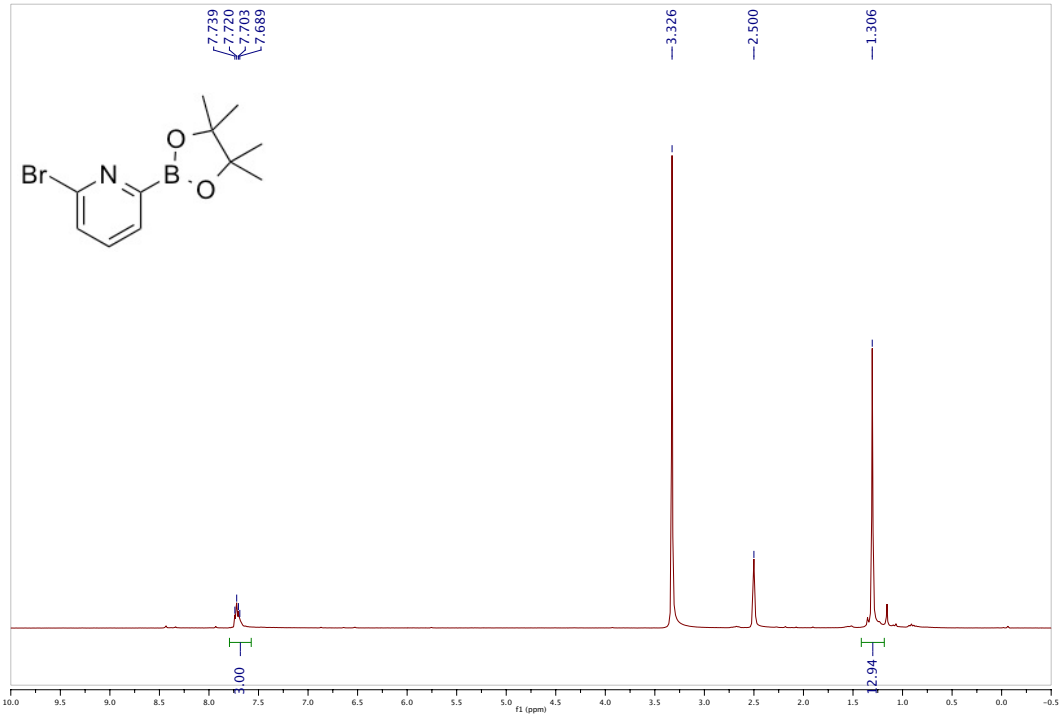

A. 14. (2-Bromo-2-fluorovinyl)benzene 51

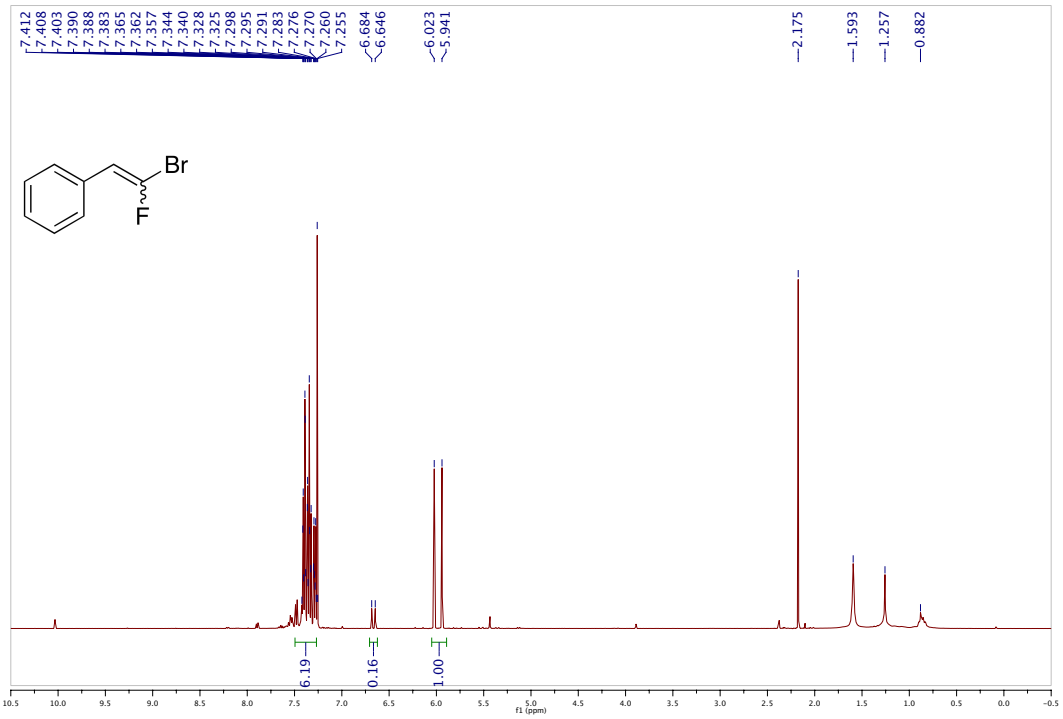

A. 15. 2-Bromo-6-styrylpyridine 53

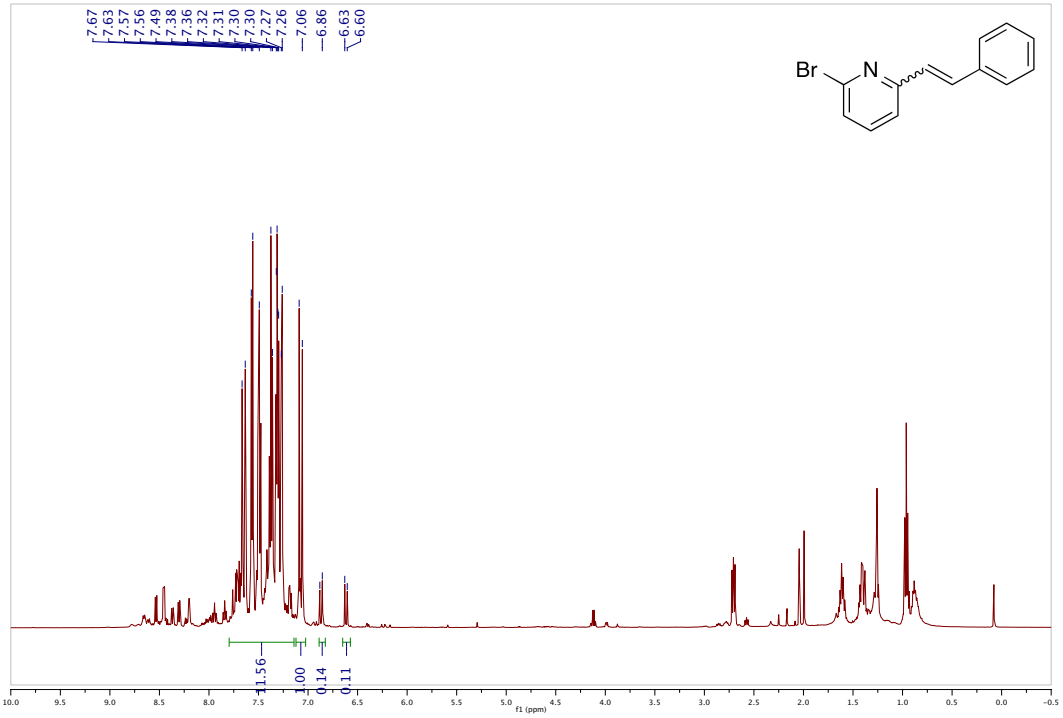

A. 16. 2-Bromo-6-(1-fluoro-2-phenylvinyl)pyridine 54

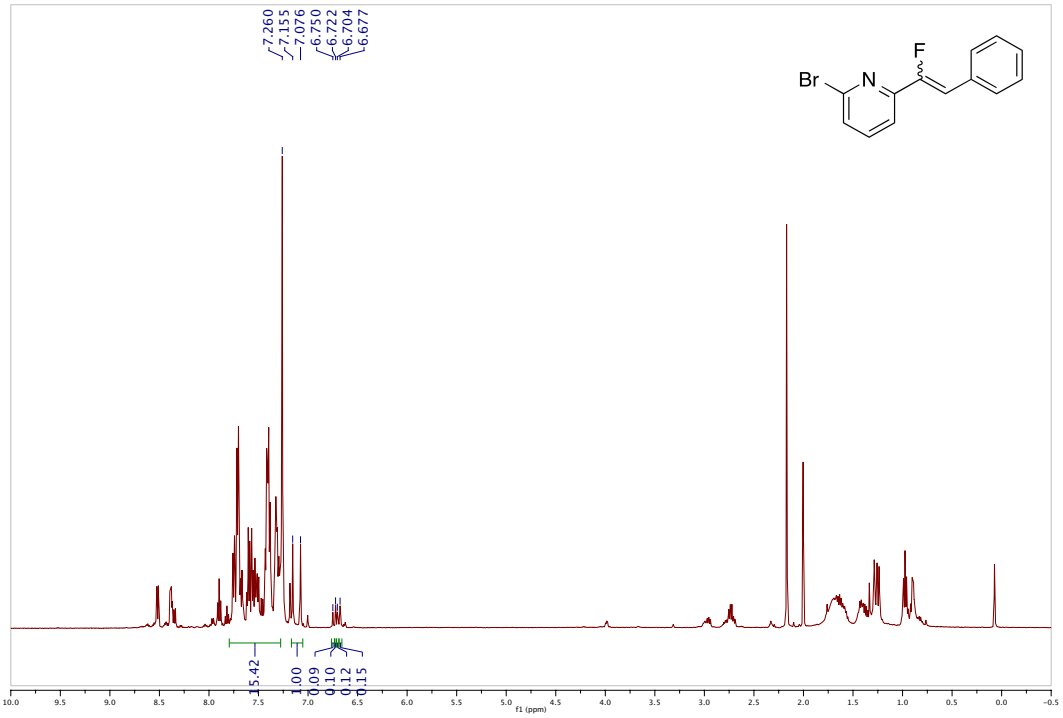

B. Example UV Biotage Isolera Purification Traces

B. 1. Biotage isolera UV trace and purification details for compound 38

Isolera™ Archive Report - JU 17-1 1.

User	Joanna		
Sample Name	JU 17-1		
Date	2014-Aug-04 15.59		
Method			
Project			
Comment			
Cartridge	SNAP 25g	**Detection Mode**	Lambda-all
Flowrate	25 ml/min	**Baseline Correction**	On
Solvent A	n-Hexane	**UV1 (Monitor)**	254 nm
Solvent B	Ethyl acetate	**UV2 (Monitor)**	280 nm
		Start Threshold	20 mAU
Rack Type	16x150 mm		
Max Fraction Volume	16 ml		
Dispense Order	S		

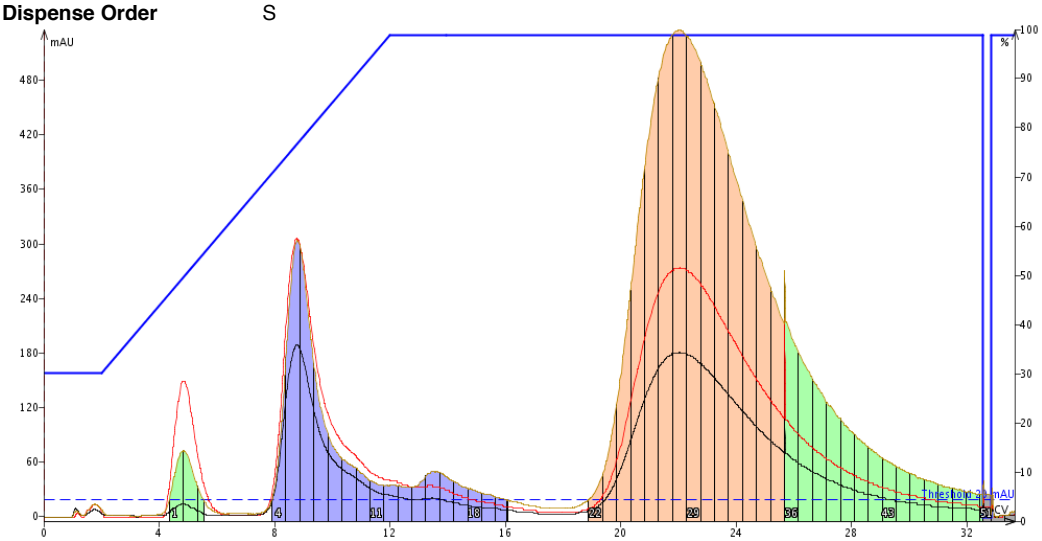

Gradient

	Solvents	Mix	Length (CV)	
Equil.	A/B	30%	3.0	flowrate 25 ml/min
1	A/B	30%	2.0	
2	A/B	30% - 100%	10.0	
3	A/B	100%	1.9	
4	A/B	100%	18.5	Isocratic Hold Enabled
5	A/B	100%	0.0	Isocratic Hold Disabled

B. 2. Biotage isolera UV trace and purification details for compound 40

Biotage

Isolera™ Archive Report - 2014-Jul-25 10.29 1.

User	Joanna		
Sample Name	2014-Jul-25 10.29		
Date	2014-Jul-25 10.29		
Method	JU15		
Project			
Comment			
Cartridge	SNAP 25g	**Detection Mode**	Lambda-all
Flowrate	25 ml/min	**Baseline Correction**	On
Solvent A	n-Hexane	**UV1 (Monitor)**	254 nm
Solvent B	Ethanol	**UV2 (Monitor)**	280 nm
		Start Threshold	12 mAU
Rack Type	16x150 mm		
Max Fraction Volume	16 ml		
Dispense Order	S		

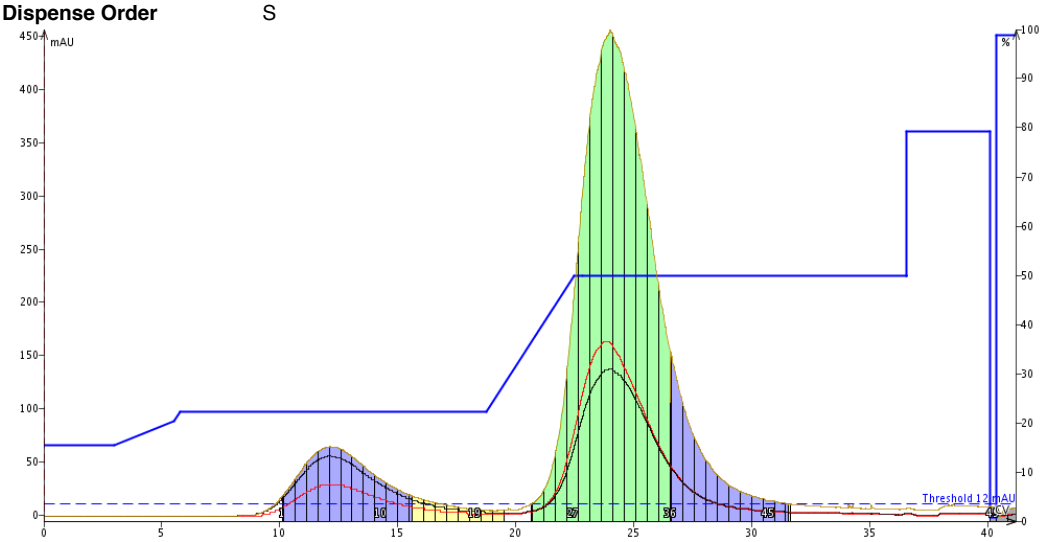

Gradient

	Solvents	Mix	Length (CV)	
1	A/B	15%	3.0	
2	A/B	15% - 20%	2.5	
3	A/B	20% - 22%	0.2	
4	A/B	22%	12.9	Isocratic Hold Enabled
5	A/B	22% - 50%	3.7	Isocratic Hold Disabled
6	A/B	50%	0.3	
7	A/B	50%	13.7	Isocratic Hold Enabled
8	A/B	50%	0.0	Isocratic Hold Disabled
9	A/B	80%	3.5	

C. Experimental Biological Procedures

C. 1. *In vitro* antiplasmodial activity as determined by GSK

Parasite growth inhibition assays, single shot assays and IC_{50} determination were carried out following standard methods using the 3H-hypoxanthine incorporation assay. This assay relies on the parasite incorporation of labeled hypoxanthine that is proportional to *P. falciparum* growth. A culture of parasitized red blood cells (RBC), a sensitive 3D7 strain was used (source MR4), (0.5% parasitemia, 2.0% haematocrite) in RMPI-1640, 0.5% Albumax and 5 μM hypoxanthine was exposed to drug serial dilutions or a single drug concentration (2 μM). Plates were incubated 24 h at 37 °C, 5% CO_2, 5% O_2, 90% N_2. After 24 h of incubation, 3H-hypoxanthine was added and plates were incubated for an additional 24 h period. After that, parasites were harvested on a glass fiber filter using a TOMTEC Cell Harvester 96. Filters were dried and melt-on scintillator sheets were used to determine the incorporation of 3H-hypoxanthine. Radioactivivity was measured using a microbeta counter. Data were normalized using the incorporation of the positive control (parasitized red blood cells without drug). IC_{50} were determined using Grafit 7 program.

Desjardins, R.E.; Canfield, C.J.; Haynes, J.D.; Chulay, J.D. Quantitative assessment of antimalarial activity in vitro by a semiautomated microdilution technique. *Antimicrob. Agents Chemother*, **1979**, 16 (6), 710-8.

C. 2. *In vitro* conditions for *P. falciparum* strain culture for biological testing by GSK

P. falciparum strains were grown in the following culture medium: RPMI 1640 (Sigma Catalog Number R5886), 25 mM HEPES and $NaHCO_3$ without L-glutamine supplemented with an albumax solution containing: Albumax II 100g/L (Gibco, Catalog Number 11021-037), D-Sucrose 40g/L (#Sigma 68720), L-glutamine 6 g/L (Merck, Catalog Number 1.00229), Hypoxanthine 0.150 mM (Fluka, Catalog Number: 5670) using red blood cells: Human blood supplied by the Spanish Red Cross. Incubation conditions: 37 °C, 5% CO_2, 5% O_2, 90% N_2

C. 3. General assay principle for determination of hERG cross-reactivity carried out by AstraZeneca

The hERG-expressing Chinese hamster ovary K1 (CHO) cells described by Persson, Carlsson, Duker, and Jacobson (2005) were grown to semi-confluence at 37 °C in a humidified environment (5% CO_2) in F-12 Ham medium containing L-glutamine, 10% foetal calf serum (FCS) and 0.6 mg/ml hygromycin (all Sigma-Aldrich). Prior to use, the monolayer was washed using a pre-warmed (37 °C) 3 ml aliquot of Versene 1:5000 (Invitrogen). After aspiration of this solution the flask was incubated at 37 °C in an incubator with a further 2 ml of Versene 1:5000 for a period of 6 min. Cells were then detached from the bottom of the flask by gentle tapping and 10 ml of Dulbecco's phosphate-buffered saline containing calcium (0.9 mM) and magnesium (0.5 mM) (PBS; Invitrogen) was then added to the flask and aspirated into a 15 ml centrifuge tube prior to centrifugation (50×g, for 4 min). The resulting supernatant was discarded and the pellet gently re-suspended in 3 ml of PBS. A 0.5 ml aliquot of cell suspension was removed and the number of viable cells (based on trypan blue exclusion) was determined in an automated reader (Cedex; Innovatis) so that the cell re-suspension volume could be adjusted with PBS to give the desired final cell concentration. It is the cell concentration at this point in the assay that is quoted when referring to this parameter. CHO-Kv1.5 cells, which were used to adjust the voltage offset on IonWorksTM HT, were maintained and prepared for use in the same way.

Bridgland-Taylor, M.H., Hargreaves, A.C., Easter, A., Orme, A., Henthorn, D.C., Ding, M., Davis, A.M., Small, B.G., Heapy, C.G., Abi-Gerges, N., Persson, F., Jacobson, I., Sullivan, M., Albertson, N., Hammond, T.G., Sullivan, E., Valentin, J-P., Pollard, C.E. Optimisation and validation of a medium-throughput electrophysiology-based hERG assay using IonWorks™HT. *Journal of Pharmacological and Toxicological Methods,* **2006**, 54: 189–199 (10.1016/j.vascn.2006.02.003)

C. 4. General assay principle for *in vitro* antiplasmodial activity as determined by Syngene

This protocol assessed compound efficacy against *P. falciparum in vitro*. This assay used [3H]-hypoxanthine incorporation or DNA labeling by SYBR Green as markers of parasite growth. This procedure was designed for use with culture adapted *P. falciparum* strains or clones only. On one 96-well plate typically 3 drugs are tested in duplicate. The standard strain used was *Plasmodium falciparum*, NF54 (sensitive to all known drugs). The assay can be performed in dose response mode (12 concentrations in duplicate, 24 data points), which allows for the determination of the IC_{50}, or in single concentration mode (one concentration in triplicate, 3 data points), which allows for the determination of the percentage of growth inhibition.

Desjardins, R.E.; Canfield, C.J.; Haynes, J.D.; Chulay, J.D. Quantitative assessment of antimalarial activity in vitro by a semiautomated microdilution technique. *Antimicrob. Agents Chemother*, **1979**, 16 (6), 710-8.